Regulation and Function of the PH domain-containing Adaptor Protein TAPP2 in B cell Signaling

by

Samuel M.S. Cheung

A Thesis submitted to the Faculty of Graduate Studies of

The University of Manitoba

in partial fulfilment of the requirements of the degree of

MASTER OF SCIENCE

Department of Immunology
University of Manitoba
Winnipeg

THE UNIVERSITY OF MANITOBA

FACULTY OF GRADUATE STUDIES

*****

COPYRIGHT PERMISSION

Regulation and Function of the PH domain-containing Adaptor Protein TAPP2 in B cell Signaling

by

Samuel M. S. Cheung

A Thesis/Practicum submitted to the Faculty of Graduate Studies of The University of Manitoba in partial fulfillment of the requirement of the degree

of

Master of Science

Acknowledgment

I would like to thank my supervisor Dr. Aaron Marshall, who provided me with exceptional mentorship and guidance throughout my years of study under his supervision.

I would also like to thank my committee members who put extra effort into the critical review of this thesis and provided me with valuable feedback.

I want to thank our resourceful technician Sen Hou who generated various TAPP2 constructs that made this thesis possible to complete.

ABSTRACT

Superoxides and hydrogen peroxide are transiently produced after activation through various cell surface receptors and play important roles in immune and inflammatory responses. I have examined the effect of peroxide on phosphoinositide 3-kinase - dependant signaling pathways in B lymphocytes using PH domain containing adaptor proteins Bam32 and TAPP2. PI3Ks generate several distinct lipid second messengers including phosphatidylinositol (3,4,5) trisphosphate (PIP3) and phosphatidylinositol (3,4) bisphosphate (PI(3,4)P2). The PH domain of Bam32 binds to both PIP3 and PI(3,4)P2 whereas TAPP2 specifically binds to PI(3,4)P2. I found that peroxide induced membrane recruitment of Bam32 and TAPP2, but not the PIP3-binding PH domain of Btk. I also found that peroxide-induced membrane recruitment is dependant on PI3K activity, with the p110δ isoform contributing much of the activity in the BJAB model. BJAB cells are devoid of PTEN and this suggesting that peroxide-induced membrane recruitment cannot be completely attributed to oxidative inactivation of PTEN. Re-expression of PTEN in these cells led to reduction of antigen receptor-induced membrane recruitment, but not peroxide-induced recruitment, suggesting that PTEN is efficiently inactivated by oxidant, but not immunoreceptor signaling. Strikingly, combined stimulation with sub-optimal concentrations of peroxide and antigen receptor ligand led to robust membrane recruitment of TAPP2, exceeding the maximum achievable with either stimulus alone. My first section results indicate that peroxide modulates the quality and quantity of the PI3K signal triggered by immunoreceptors consistent with a role for peroxide as an immune mediator. In the second section, I optimized the conditions for immunoprecipitation using anti-TAPP2 antibody. Through gel electrophoresis and mass

spectrometry analysis, I have identified several candidate proteins that appeared to be unique to TAPP2. My preliminary results suggested utrophin is associating with TAPP2 with high confident of identification. The result has shed light on the biological function of TAPP2 as PI(3,4)P2 effector in PI3K signaling.

TABLE OF CONTENTS

CHAPTER I

CHAPTER II

List of Tables

List of Figures

Abbreviations:

AP-1	activator protein-1
APAF-1	apoptotic protease-activating factor-1
ATP	Adenosine triphosphate
Bam32	B lymphocyte adaptor molecule of 32 kilodaltons
BCAP	B-cell PI3K adaptor protein
Bcl-1	B cell lymphoma 1
BCR	B cell antigen receptor
Btk	Bruton's tyrosine kinase
CAD	Glutamine dependent carbamoyl phosphate synthase; Aspartate carbamoyl transferase; Dihydroorotase
Con A	Concanavalin A
CK2	casein kinase 2
EBV	Epstein-Barr virus
EGFP	enhanced green fluorescent protein
ETC	Electron transport chain
ERK	extracellular signal-regulated kinase
FADD	Fas associated death domain
FYVE	Fab1p, YOTB, Vac1p and EEA1
Grp1	general receptor for phosphoinositides isoform-1
HIF-1α	hypoxia-inducible factor-1α
HPLC	high pressure liquid chromatography
ITIM	immunoreceptor tyrosine based inhibitory motifs
IKK	inhibitory kB kinase
IL-1β	interleukin 1β
JNK	c-Jun N-terminal kinase
LPS	lipopolysaccharide
MAPK	mitogen-activated protein kinase
MEKK1	MAPK kinase kinase 1
MOMP	mitochondrial outer membrane permeabilization
MS/MS	tandem mass spectrometry

MZ	marginal zone
NADPH	nicotinamide adenine dinucleotide phosphate reduced form
NFkB	nuclear factor kappa B
Nox	NADPH oxidase
PDZ	post-synaptic density protein PDS-95/SAP90, Drosophila septate junction protein ZO-1
PDZ-B	PDZ-binding motif (correspond to sequence SDV)
PH	pleckstrin homology
PI3K	phosphatidylinositol 3-kinase
PI4K	phosphatidylinositol 4-kinase
PKB/Akt	protein kinase B
PKC	protein kinase C
PLCγ2	phospholipase C gamma 2
PTEN	phosphatase and tensin homologue deleted on chromosome 10
PTK	protein tyrosine kinase
PTP-1B	protein tyrosine phosphatase – 1B
Prx	peroxiredoxin
PX	phox homology
ROS	reactive oxygen species
SH2	Src Homology 2
SHIP	Src Homology 2 Domain-containing Inositol-5-Phosphatase
SHP	SH2-containing tyrosine phosphatase
SOD	superoxide dismutase
Syk	spleen tyrosine kinase
TAPP	tandem-PH-domain-containing-protein
TLR4	toll like receptor 4
TNF-α	tumor necrosis factor-alpha
TRAIL	TNF-related apoptosis-inducing ligand
XIAP	X-linked inhibitor of apoptosis

BACKGROUND

a) **Source of reactive oxygen species (ROS) in B cells.** Nicotinamide adenine dinucleotide phosphate (NADPH) oxidase (Nox), leukotriene biosynthesis and mitochondria are well characterized sources of ROS in lymphocyte. NADPH oxidase is a multi-subunit enzyme which is responsible for the majority of ROS produced in immune cells. Activated oxidase is comprised of two membrane bound ($gp91^{PHOX}$ and $p22^{PHOX}$) and three cytosolic subunits ($p67^{PHOX}$, $p47^{PHOX}$ and $p40^{PHOX}$) in addition to small G protein Rac1 and Rac2. [1] Out of seven Nox family members characterized to date, B cells express Nox1, Nox2 and Nox5 depending on the subset and activation status. Nox5 is most abundantly expressed in B cells and it is thought to be responsible for majority of the ROS production. [2-4] Another source of ROS generation is suggested through leukotriene biosynthesis. [5, 6] Even though it has been shown to produce ROS in non-immune cells, this pathway apparently does not play a major role in B cells according to one study and might contribute very little to receptor-induced ROS production. [7]

Mitochondrion plays a vital role in cellular respiration and is recognized as the major site for ROS production in mammalian cells. [8, 9] The mitochondrial electron transport chain (ETC) harvests the energy of electron flow to generate an electrochemical gradient, in the form of hydrogen ion, at the intermembrane space. This electrochemical gradient powers the adenosine triphosphate (ATP) synthase to generate ATP as cellular energy. [10] Although mitochondria-derived ROS usually remain inside the mitochondrion, it has been suggested that the electron can escape ETC to contribute ROS present in cytosol. [11, 12] The extent of how much

mitochondria and NADPH oxidase contribute to receptor-induced ROS production in lymphocyte is currently unknown.

While the mitochondrion is well characterized in the literature, currently very little is known regarding to the function and location of NADPH oxidase in lymphocyte. In neutrophil phagocytosis, the cytosolic subunits translocate to the phagosome membrane where they form an active NADPH oxidase with the membrane bound subunits to produce ROS for bactericidal purpose. In B cells, one study suggested that Nox5 resided on lipid raft. [13] Whether NADPH oxidase could redistribute in endocytic vesicle of internalized immune complexes B cells is currently unknown. Although NADPH oxidase is well characterized in phagocytes, the detailed mechanism of activation and function in B cells still remain at its infancy. The current model for oxidase assembly appears to be similar in various cell types but the expression is quantitatively different and the regulation mechanism might be distinct. It was found that B cells produce much lower levels of ROS compared to neutrophils and this is correlated to the lower expression of cytosolic subunits. [14] Regardless, NADPH oxidase in B cells are fully functional and are capable of producing ROS at a rate estimated to be 1 to 5% that of phagocytes. [15]

b) **Types of ROS.** The term ROS refers to a group of reactive oxygen-containing molecules. These include superoxide anion (O_2^-), hydrogen peroxide (H_2O_2), hydroxyl radical (OH^-), nitric oxide (NO) and peroxynitrite ($ONOO^-$). O_2^- is produced by Nox during respiratory burst according to the reaction: $NADPH + 2O_2 \rightarrow 2O_2^- + NADP^+ + H^+$. [16] The majority of O_2^- produced in the cell is suggested to spontaneously or enzymatically convert to H_2O_2 by superoxide dismutase (SOD).

While proposals are plenty, the source of OH^- currently remains unclear. [17] On the other hand, NO is produced via catalytic conversion of L-arginine to citrulline by nitric oxide synthase (NOS). Three types of NOS have been identified in mammalian cells – neuronal NOS (nNOS), inducible NOS (iNOS) and endothelial NOS (eNOS). [18, 19] $ONOO^-$ is the most chemically unstable and it is produced by reaction between O_2^- and NO. [20] (Figure 1)

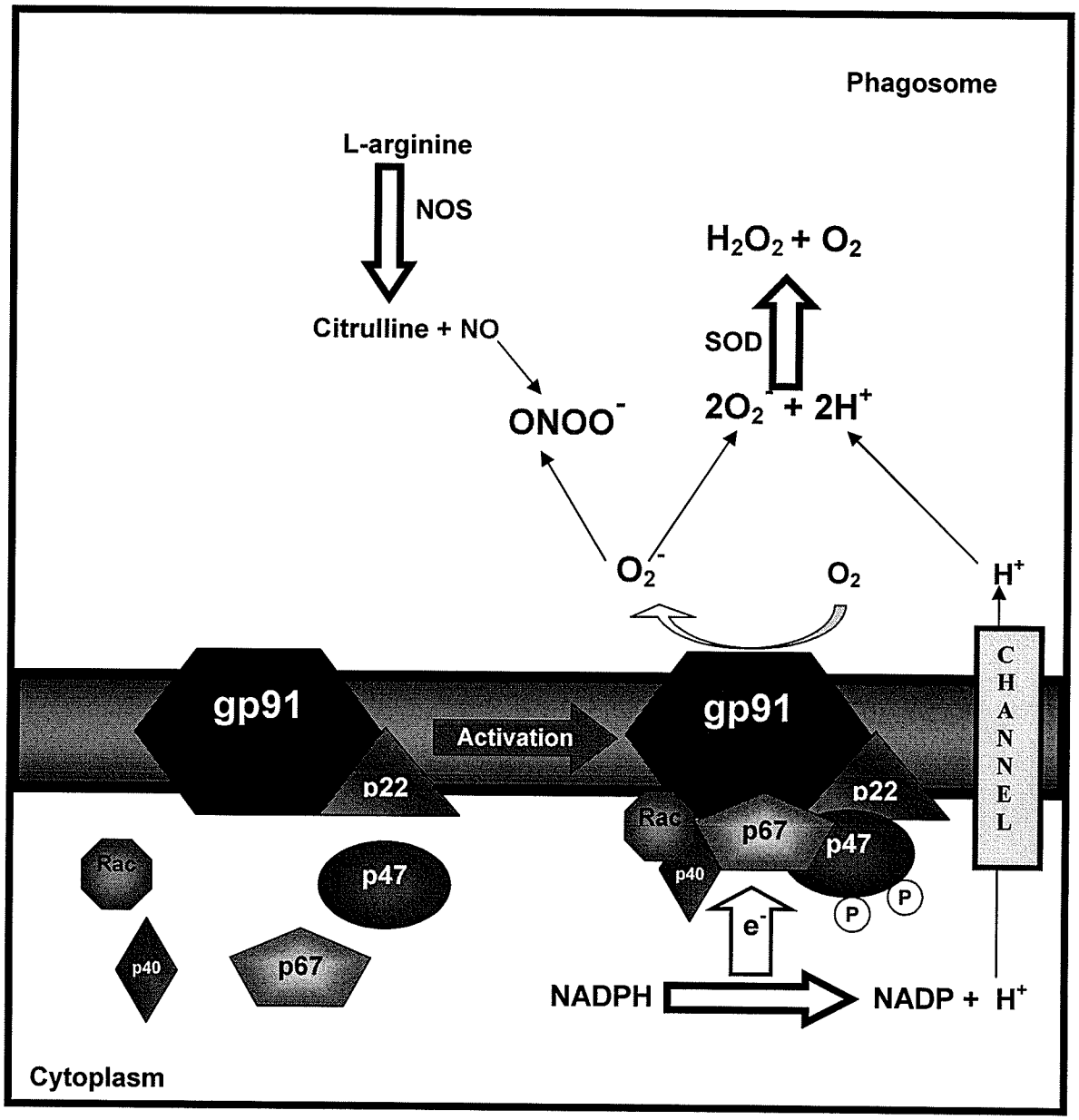

Figure 1. Activation of NADPH oxidase and ROS generation. Activation of NADPH oxidase required phosphorylation of cytosolic subunits ($p47^{phox}$) and proper assembly at the phagosome membrane of macrophage or plasma membrane of lymphocyte. Electron transfer from NADPH to O_2 is catalyzed by NADPH oxidase. The resulting O_2^- generated can be enzymatically converted to H_2O_2 by superoxide dismutase (SOD) or form $ONOO^-$ by reacting with NO. H^+ movement across the membrane is facilitated by proton channel.

c) **ROS production by B lymphocyte.** Early studies suggested that Epstein-Barr virus (EBV)-transformed B lymphocytes are capable of producing ROS following a variety of stimuli. By measuring *ex vitro* cytochrome c reduction, it is shown that tumor necrosis factor-α (TNF-α), interleukin-1β, lipopolysaccharide (LPS) and opsonized immune complexes can trigger ROS release. [21] Another study using luminol-enhanced chemiluminescence method was reported to show extracellular ROS production following anti-Fas or menadione stimulation. [22] With the advance of biotechnology, intracellular ROS production can now be measured endogenously using membrane-permeable ROS sensitive dyes. Besides the most commonly used mitogenic stimulus such as phorbol-myristyl-acetate (PMA), receptor activation such as TNF family member CD40 or B cell antigen receptor (BCR) cross-linking can also induce ROS production. [23-25] Collectively, it is now established that ROS production can be induced by engagement of various receptors involved in multiple signaling pathways. Depending on the agonist and method of measurement, ROS production kinetics can range from seconds to minutes.

d) **Control of ROS production.** Since each subunit of the NADPH oxidase is indispensable in enzyme assembly and overall function, it is not surprising that ROS production is essentially controlled by factors regulating the subunits. [1, 14] The binding domains of all three cytosolic subunits are non-catalytic and structurally well conserved between human and mouse. They appeared to function solely as adaptor proteins which interact with membrane bound subunits to form the stable enzymatic complex to generate ROS. [26] For example, the $p22^{PHOX}$ subunit is absolutely required for proper expression and overall oxidase function in both B cells and

phagocytes. [27] Both Rac1 and Rac2 are important for NADPH oxidase activity according to an antisense knock down assay. But it is unclear which isoform is more relevant since the antisense sequence employed is common to both Rac1 and Rac2 genes. [28] Currently, regulation mechanism of the subunits is unclear in B cells. However, initial studies on neutrophils showed that each cytosolic subunit undergoes site specific phosphorylation by various kinases such as protein kinase C (PKC), casein kinase 2 (CK2), extracellular signal-regulated kinase (ERK2) and mitogen-activated protein kinase (p38MAPK) upon activation. The importance of phosphorylation-induced activation is demonstrated by using specific kinase inhibitors lead to inhibition of ROS production. [29-32] Regarding the signal further upstream, recent research has shed light on the early control point and the factors influence ROS production. Singh et al. showed that BCR-induced ROS generation is largely dependent on protein tyrosine kinase (PTK), as demonstrated with the PTK inhibitor genistein, and phosphatidylinositol 3-kinase (PI3K), as showed by using PI3K inhibitor Wortmannin. [24] They also demonstrated that normal ROS production is dependent on Ca^{2+}. Such observation can be explained by the nature of Nox5, which is mainly Ca^{2+}-dependent and is the major isoform expressed in B cells. [3, 13] Nonetheless, in order to balance cellular redox state to prevent excessive damage, cells must terminate NADPH oxidase activity and clear the excess ROS produced. Deactivation of oxidase activity seems to be controlled by the availability of NADPH and phosphorylation status of the $p47^{phox}$ subunits. [33] Clearance of ROS seems to be controlled by various antioxidant enzymes.

e) **Clearance of ROS by antioxidant enzymes.** SOD, catalase, glutathione peroxidase and peroxiredoxin (Prx) are well characterized and known to regulate cellular redox balance. Incubation with or overexpressing these enzymes in lymphocyte culture impair ROS generation. [24, 34] Although these studies proved an antioxidant role for these enzymes, it has limitation and caveats in reflecting real physiological condition. For instance, SOD regulates the ratio of O_2^- and H_2O_2 rather than eliminate ROS as discussed above. Catalase is mainly found in peroxisomes whereas glutathione peroxidase is confined to mitochondria and nuclei. These two enzymes are normally not present to eliminate cytosolic ROS. On the other hand, Prx is ubiquitously expressed in variety of tissues and abundant in cytosol. [35] Therefore, Prx seems to be a prominent candidate in clearing receptor-induced ROS in the cytoplasm and to protect the cell from basal activity of NADPH oxidase. There are six isoforms of Prx characterized up-to-date. All of them contain a conserved cysteine residue as part of the redox center for catalyzing the breakdown of H_2O_2. [36] Among these isoforms, Prx II deletion mice have recently shown a defective immune phenotype. This will be discussed in more detail in a later section.

f) **Biological effect of ROS.** The biological effect of ROS and its physiological roles in lymphocytes are controversial. As discussed in the following sections, ROS, particularly O_2^- and H_2O_2, are well known to be involved in many biological processes ranging from apoptosis induction to malignant transformation. Although H_2O_2 is relatively stable compared to O_2^-, it can still oxidize all major classes of biomolecules. For instance, it can directly oxidize the bases and sugars of nucleotides *in vitro* to predispose DNA for mutation. [37] The mechanism of H_2O_2-induced DNA

damage in mammalian cells is suggested to be similar as those observed in bacteria, which involve a transition metal such as iron to produce OH^- from H_2O_2 followed by direct nucleotide modification. [38] An early study in T cells showed that H_2O_2-induced DNA damage occurred within 15 min of treatment followed by DNA damage repair within an hour. [39] The DNA damage observed is characterized by single-strand breaks and is suggested to be a Ca^{2+}-dependent process, which implies the requirement of a signaling pathway to trigger the damage. [40] The outcome drawn from two studies mentioned above was ROS-induced apoptosis. But the latter group observed that continuous presence of H_2O_2 in T cells can also induce anti-apoptotic response. This contrary anti-apoptotic response is also evident by studies which showed the requirement of H_2O_2 to phosphorylate proliferation factors such as ERK. This indicates a role of ROS plays in cell survival under oxidative stress. [41, 42]

g) **Apoptotic pathways.** Currently there are two well characterized mechanisms of apoptosis in the literature and they are mitochondrial (intrinsic) and death receptor (extrinsic) pathways. [43, 44] In intrinsic pathway, dysfunction of mitochondria lead to mitochondrial outer membrane permeabilization (MOMP) followed by release of cytochrome *c* into cytoplasm where it activates apoptotic protease-activating factor-1 (APAF-1). Activated APAF-1 undergoes oligomerization which subsequently binds to two procaspase 9 molecules. The complex involved APAF-1 and procaspase 9 dimer is called apoptosome. The apoptosome can cleave procaspase 3 and activating it. The result of caspase 3 activation is series of proteolytic cascade which lead to apoptosis. In extrinsic pathway, the formation of 'death-inducing signaling complex' involved procaspase 8 dimer is required to activate procaspase 3. Ligation of TNF

receptor family member such as Fas or TNF-related apoptosis-inducing ligand (TRAIL) recruits the adaptor molecule Fas associated death domain (FADD). FADD in turn recruits two procaspase 8 molecules. The dimerized procaspase 8 becomes activated in manner similar to procaspase 9. This death-inducing signaling complex cleaves procaspase 3 and induces the subsequent apoptosis. At the cell level, apoptosis is characterized by chromatin condensation, nuclear fragmentation, cell shrinking, membrane blebbing, mitochondria depolarization and externalization of phosphatidyl-serine.

h) **Role of ROS in apoptosis.** Early studies showed that Fas-mediated apoptosis required endogenous ROS production as demonstrated by the ability of various antioxidants to inhibit Fas-mediated apoptosis.[45-47] These studies implicated an indispensable role of ROS play in extrinsic pathway. Another study on T cells showed H_2O_2 treatment can lead to direct activation of caspase-3 without upstream caspase-8 activation which suggested a role of H_2O_2 plays in intrinsic pathway. [48] Subsequent mechanistic study showed that ROS itself can cause MOMP and plays an essential role in apoptosome formation by oxidizing APAF-1. [49] Therefore, both extrinsic and intrinsic pathways have a common converging point where ROS play an important role upstream of caspase 3. The mechanism of Fas-induced ROS production is currently unknown but it has been shown to involved activation of NADPH oxidase. [50, 51] The major Fas-induced ROS production are suggested to be H_2O_2 and hydroxyl radicals. [52] It is also unclear how H_2O_2 trigger MOMP but these studies clearly demonstrated that both endogenous and exogenous ROS are major element in mitochondria mediated apoptosis.

i) **Role of ROS in malignant transformation.** Since H_2O_2-induced DNA damage is evident *in vivo*, there may be a positive correlation between intracellular ROS level and gene mutation, which predispose the cell to malignant transformation. Indeed, two reports independently showed T cells exposed to H_2O_2 have higher mutation frequency and the effect is dose-dependent. [53, 54] Another study using non-immune cells exposed to macrophage derived ROS showed that these cells were resistance to mutation when incubated with various ROS inhibitors and/or scavengers. [55] Taken together, it is likely that endogenous ROS can contribute to malignant transformation. In fact, this is implicated in early studies involving transgene expression of NADPH oxidase component $gp91^{phox}$ which showed high incidents of tumors in mice. [56, 57] In terms of cancer progression, it has been widely accepted that ROS plays a major role in cancer development. [58, 59] For example, radiation therapy can induced ROS production and direct DNA damage and the accumulation of DNA damage predisposes the surrounding normal cells to mutation. The majority of DNA mutation was characterized by G→T transversions. [60] On the other hand, ROS also evidently affect apoptosis as discussed above. This raises a question on the effectiveness of using antioxidant for cancer treatment. Because ROS has diverse affect in multiple signaling pathways, in additional to the complexity and variation among different types of cancer, it is very difficult to selectively target apoptotic pathway to alter survival of cancer cells by use of antioxidants. Nonetheless, some agents that modulate the cellular redox system such as buthionine sulfoximine, ascorbic acid, arsenic trioxide, imexon, and motexafin gadolinium have been used in various clinical stages in effort to provide a treatment

for cancer. [61] Further mechanistic study into the role of ROS play in apoptotic and survival pathways are expected in the near future to elucidate the differential role of ROS play in normal and cancer cells.

j) **Evidence of H_2O_2 as signal messengers.** There is strong evidence for H_2O_2 to serve as a second messenger in signaling. It is rapidly produced upon variety of stimuli as mentioned above. It is more stable than O_2^- and has a longer half life. It is uncharged so it can freely diffuse across the cell membrane to exert its effect on adjacent cells. [11] Its production is highly controlled and signal-dependent. The level of H_2O_2 is controlled by antioxidant enzymes as mentioned above. Furthermore, H_2O_2 can activate various cellular components such as redox-sensitive proteins and transcription factors. Over the past few years, many phosphatases containing low-pKa sulfhydryl group with cysteine residue as catalytic centre were identified as potential ROS targets. [11, 35] Among these candidates, only few were studied *in vivo* and very little is done on lymphocytes. These included protein tyrosine phosphatase (PTP-1B), phosphatase and tensin homologue deleted on chromosome 10 (PTEN), and SH2-containing tyrosine phosphatase (SHP). [62-64] In studies regarding B cells, only SHP-1 has been shown to be regulated by endogenous ROS. [13, 24] Similar results are reported in T cell treated with H_2O_2. [65] It has been shown that SHP-1 is constitutively associated with the BCR. Upon BCR cross-linking, ROS is produced to regulate BCR signaling by transiently inhibiting SHP-1 activity. This allows the mitogenic signal to advance during the state of reduced inhibition. Although not directly demonstrated, it is likely that PTEN and PTP-1B are also the targets of H_2O_2 regulation in B cells. Emerging evidence supports a model in which H_2O_2 is being

produced as a signaling messenger to transiently inhibit phosphatase activity, which then allows kinase activation to proceed and amplify. In human B cells, this is demonstrated by a recent study which showed that treatment with H_2O_2 immediately before or within a minute after BCR signaling can enhance tyrosine kinase Syk and ERK phosphorylation. But similar effects were not found when cells were treated 1 minute before BCR cross-linking. This indicated that H_2O_2 must be present immediately or soon after BCR cross-linking to exert its effect as phosphatases inhibitor. [66] This is a strong indication for the function of H_2O_2 as signal messenger whose effect is time and space dependent.

k) **Effects of H_2O_2 on lymphocyte signaling.** As discussed so far, H_2O_2 can produce diverse effects on B cells ranging from phosphatase inactivation to apoptosis induction. In regard to signal transduction, initial reports showed that treatment of B cells with H_2O_2 can lead to signal and dose dependent activation of nuclear factor kappa B (NF-kB) and Syk as well as calcium mobilization. [67, 68] Subsequent studies by Qin et al. found that the mechanism of H_2O_2-induced calcium response was partially dependent on Syk by using Syk-deficient B cells. [69] A follow up study done by the same group reported that H_2O_2 can also activate Bruton's tyrosine kinase (Btk) which led to subsequent phosphorylation of phospholipase C gamma 2 (PLCγ2), an important upstream regulator of calcium signaling. [70, 71] In addition, they also observed H_2O_2 induced PI3K activation and protein kinase B (PKB or Akt) phosphorylation. By using PI3K inhibitor, they showed that PI3K activity was also required for H_2O_2-induced calcium mobilization. [72] In these studies, H_2O_2-induced PI3K activation is suggested to be independent of Syk tyrosine kinase, and Akt

activation seemed to be a result of H_2O_2-induced accumulation of PI(3,4,5)P3.

Other kinases further downstream of receptor signaling such as c-Jun N-terminal kinase (JNK) and ERK are also reported to be activated in response to H_2O_2 treatment. In a separate study, Syk was also found involved in H_2O_2-induced cell cycle arrest and MAPK activation. [73] Also, H_2O_2-induced NFkB activation is suggested to be dependent on MAPK kinase kinase 1 (MEKK1) signaling. [74] All these studies collectively demonstrated that H_2O_2 can act on multiple pathways and the signaling effect is dose-dependent. H_2O_2 treatment can result in activation of specific transcription factors. Among many stress responsive elements identified in many cell types, NF-kB, hypoxia-inducible factor-1α (HIF-1α) and activator protein-1 (AP-1) appeared specifically regulated by ROS. [75, 76] The detailed mechanism of how ROS signaling lead to transcription activation is currently not fully understood. But some recent studies suggested that ROS affect upstream signaling at multiple points which control the subsequent transcription activation. For example, H_2O_2 was recently showed to inhibit the inhibitory kB kinase (IKK) through regulation by redox sensitive protein glutaredoxin. [77] Similar observation was made with the p50 subunit which showed DNA-binding is regulated by oxidant. [78]

Regarding to upstream signaling affects, the observation of H_2O_2-induced PI3K activation is of particular interest. Although H_2O_2 can induce tyrosine phosphorylation of PI3K catalytic subunit, it has no affect on the enzymatic activity of PI3K. In addition, the extent and mechanism of how H_2O_2 can induce accumulation of PI3K lipid messenger is not known. Since H_2O_2 can activate various responses as described above, one would expect similar responses will be reduced or

inhibited in the absence of ROS. Indeed, B cell pre-incubated with ROS scavenger such as N-acetyl cysteine (NAC) or NADPH oxidase inhibitor diphenyleneiodonium chloride (DPI) have showed strong inhibition of CD40 or H_2O_2-induced MAPK activation. [7] Also, BCR-mediated calcium response was also attenuated in the presence of NAC or in cell overexpressing Prx 1. [24] Furthermore, T cells incubated with NAC have been showed to inhibit NF-kB activation. [79] Taken together, it is suggested that physiological level of ROS or low concentration of H_2O_2 can positively regulate receptor signaling in multiple pathways which in turn govern specific transcription factors. Yet excessive ROS or high levels of H_2O_2 will result in cell damage and eventual apoptosis that is mediated by mitochondria.

l) **Importance of ROS in lymphocyte development and function.** Given the evidence that B cells express Nox and are able to generate ROS upon activation, in addition to the specific signaling responds upon H_2O_2 stimulation, one might speculate that ROS play a role in normal lymphocyte development and function. This is implicated by various studies using Prx deficient mice. Prx II knockout mice showed higher numbers of B cell in spleen. The observed 40% increase was correlated to augment expression of B-cell-activating factor (BAFF) as a result of higher level of H_2O_2. The suggested mechanism is that H_2O_2 accumulated in Prx II knockout cells which led to increase NFkB activation. [80] The observed correlation between BAFF levels and B cell population was in agreement with studies of BAFF transgenic mice which showed an elevated number of B cells. [81] A similar increase of T cell population was reported earlier in Prx II-null mice. [82] They observed the thymus of Prx II-null mice became larger than the wild-type mice at 9 weeks of age and the condition was

more severe in older mice. This difference in thymus size was caused by higher percentage of double positive T cells found in thymus. Detailed mechanistic studies revealed that the T cells from Prx II-null mice were more resistant to apoptosis as demonstrated by increase expression of anti-apoptotic factors such as B cell lymphoma-1 (Bcl-1) and X-linked inhibitor of apoptosis (XIAP). Consistent with the role of endogenous ROS in positively regulating mitogenic signals, they also found the Prx II-null T cells exhibit higher proliferative response to concanavalin A (Con A) stimulation. Similar enhanced proliferation was also observed in Prx II knockout mice in recent study. [83] Although in this study they reported greater bone marrow derived dendritic cell differentiation and enhanced mixed lymphocyte reaction (MLR) in Prx II knockout mice, the underlying mechanism was not explored.

Interestingly, Bleesing et al. are the first group to identify an abnormality in B cell development among patients with chronic granulomatous disease (CDG), a genetic defect caused by mutation in one the NADPH oxidase subunits. [84] They reported that these patients have an altered B cell compartment, characterized by expansion of $CD5^+$ cells and a significant reduction in CD27 expressing memory B cells in peripheral blood. The defects are B cell restricted since it does not effect T cell population. This implicated that endogenous ROS generation can influence memory B cell development. In the past, majority of study on NADPH oxidase has been focused on neutrophil because of the obvious defects in bacterial clearance found in CDG patients. Furthermore, although various phox knockout mice have been generated, no functional characterization is being done on lymphocytes. Up until now, accumulated studies clearly established the critical role of ROS in lymphocyte

signaling and function. Further works are expected in the near future to elucidate the mechanism of ROS regulate lymphocyte response and development.

m) **Introduction to PI3K.** PI3K is a family of enzymes that catalyze the phosphorylation of phosphoinositides at the D3 position of the inositol ring. PI3K signaling is essential to many biological processes including cell survival, proliferation, migration, and adhesion. There are three classes of PI3K (I, II and III) according to their structure and substrate specificity. Class I PI3K phosphorylate phosphatidylinositol phosphate (PI), PI(4)-phosphate and PI(4,5)-bisphosphate. Class II prefer to phosphorylate PI and PI(4)P and class III can only phosphorylate PI *in vitro*. [85] Only class I PI3K can produce the well characterized lipid second messenger phosphatidylinositol-3,4,5-trisphosphate (PI(3,4,5)P3 or PIP3) *in vivo*. (Table 1) All class I PI3K consist of a catalytic subunit and a regulatory subunit. In class IA, there are three catalytic isoforms (p110α, p110β and p110δ) and five regulatory isoforms (p85α, p55α, p50α, p85β or p55γ). The catalytic isoforms p110α and p110β are widely expressed, whereas p110δ is restricted to leukocytes. [86, 87] All catalytic subunits of class IA can bind interchangeably to any regulatory subunits. Class IB PI3K has only a single catalytic subunit (p110γ) and one regulatory subunit (p101). Class II PI3K has three isoforms; PI3K-C2α, PI3K-C2β and PI3K-C2γ. The class II is less characterized compared to class I. Class III PI3K only has a single isoform and it is the least studied among the three. [88] Currently only class I PI3K is the most widely studied in the context of lymphocytes.

Table 1. The substrates and products of PI3K and the identified domains which recognize the specific phosphoinositides.

Substrate	PI3K	Product	Binding Domain
PI PI(4)P PI(4,5)P2	Class I	PI(3)P PI(3,4)P2 PI(3,4,5)P3 or PIP3	FYVE, PX PH, PX PH
PI PI(4)P	Class II	PI(3)P PI(3,4)P2	
PI	Class III	PI(3)P	

n) **Mechanism of PI3K activation in B cell.** In regard to class IA PI3K, the precise molecular mechanisms are not entirely understood but a working model has been established. It has been shown that receptor engagement such as BCR, CD40, toll-like receptor 4 (TLR4) and IL-4R can induce PI3K activation. [89] Upon BCR activation, cross-linking of antigen receptor activates tyrosine kinase Syk, which subsequently phosphorylate tyrosine residue of CD19 and B-cell PI3K adaptor (BCAP) at the YXXM sequence (where X is any amino acid). The Src homology 2 (SH2) domain of regulatory subunits along with the constitutively associated catalytic subunit then binds to the tyrosine phosphorylated CD19 or BCAP near the membrane where lipid substrates are located. CD40L-induced PI3K activation was suggested to be mediated by c-Cbl protein. [90] In that particular study they showed CD40L-induced Akt activation, a well accepted surrogate marker for PI3K activity, in B cells was severely impaired in c-Cbl knockout mice. The suggested mechanism of CD40L induced PI3K activation is achieved through direct interaction of PI3K with c-Cbl, which resulted in translocation to the plasma membrane. [91, 92] Although the involvement of CD19

and BCAP was not mentioned, it has been reported that PI3K can also form complexes with c-Cbl and CD19 together in a BCR activated lymphoma cell line. [93] On the other hand, the mechanism of LPS or IL-4 mediated PI3K activation in B cell remains unclear. As for class IB PI3K activation, it is generally promoted by G protein-coupled receptor signaling and is involved in chemotaxis and homing. [85, 94] However, it has been shown that p110γ did not play a major role in B cell chemotactic response to the same chemokines compared to T cells. [95] This indicated that each PI3K isoform and subtype is differentially regulated in different cell types. Although the mechanism of class II and class III PI3K activation in B cells remain unexplored, one study suggested that class II PI3K might play a selective role in more differentiated lymphocytes. [96]

o) **Generation of distinct phosphoinositides.** The hallmark of PI3K activation is immediate generation of distinct lipid second messengers on the plasma membrane (Table 1 and Figure 2). The extent of how each PI3K class contributes to each of the 3-phosphoinositides in response to a given agonist is poorly defined in lymphocyte. In a study of BCR-induced PI3K activation, PIP3 was shown to increase 50% transiently within the first minute followed by sustained increase of PI(3,4)P2 up to 5 fold. Meanwhile, PI(3)P levels increased slowly and were quantitatively the lowest among the three PI3K products. [97] The differences in production levels and kinetics of each of the 3-phosphoinositide might reflect diverse cellular responses generated by PI3K signaling. Upon production of PI3K products, specific protein modules can bind and form signaling complex at the site where PI3K is activated. Although many molecular motifs have been identified to have phosphoinositide binding property,

only pleckstrin homology (PH) domain, phox homology (PX) domain and FYVE (domain identified in Fab1p, YOTB, Vacip and EEA1) domain showed recognition to PI3K products. [98] In lymphocyte, PIP3-dependent signaling is most widely studied but only a limited amount of data is available for PI(3,4)P2-dependent signaling. Currently very little is known about the signaling role of PI(3)P in lymphocyte but it has been implicated in endocytic pathway in other cell types under the regulation of class III PI3K. [88]

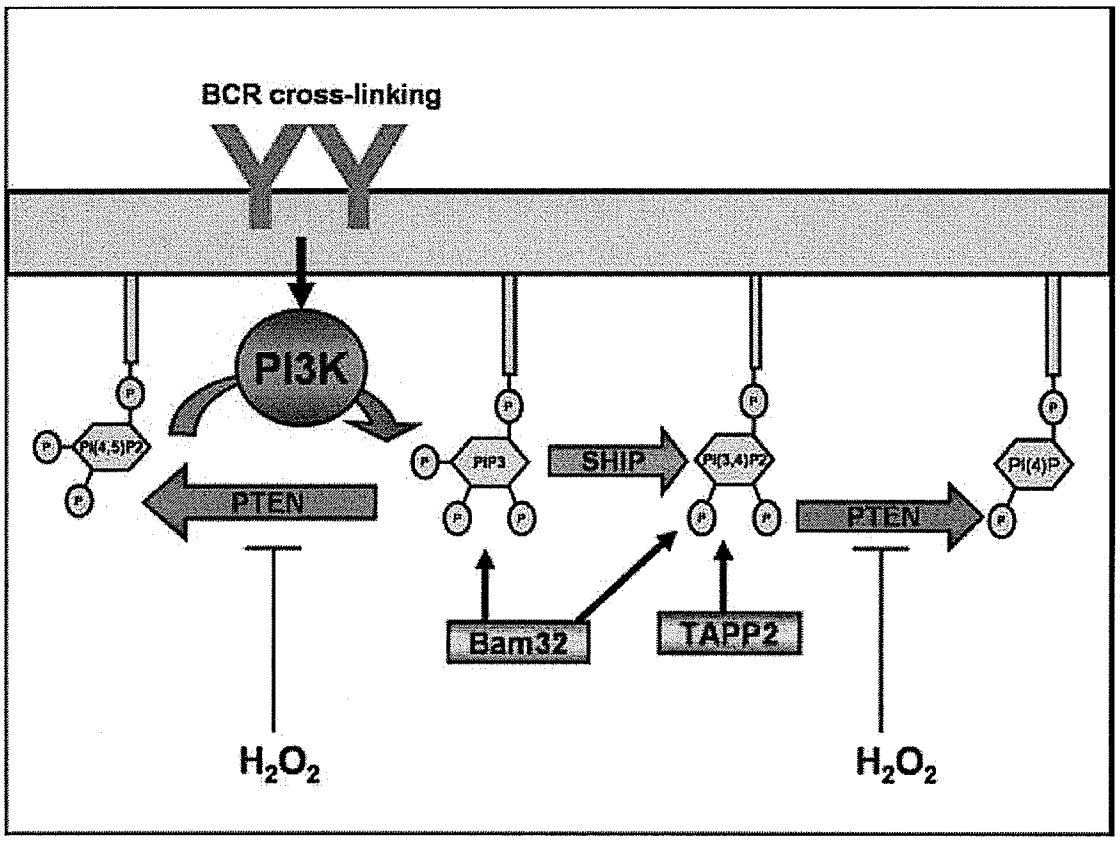

Figure 2. Regulation of PI3K signaling and distinct generation of lipid second messenger. The diagram shows BCR-induced PI3K activation will lead to sequential generation of PIP3 and PI(3,4)P2. PTEN and SHIP antagonize and modulate PI3K products respectively and H_2O_2 can inhibit PTEN activity but not SHIP. Bam32 can binds to both PIP3 and PI(3,4)P2 whereas TAPP2 specifically binds to PI(3,4)P2.

p) **Structure and function of PH domain.** PH domain consists of a core seven-strand β-sandwich structure with one corner capped off by a C-terminal α-helix and another corner by three inter-stranded loops. [99] The three inter-stranded loops are the most variable in length and amino acid sequence and are involved in interaction with the phosphate group of the phosphoinositol to confer the lipid binding specificity. [100, 101] Alignment of amino acid sequence of these loops among various PH domains revealed six conserved residues that are involved in PIP3 binding: Lys-Xaa-Sma-$Xaa_{(6\text{-}11)}$-Arg/Lys-Xaa-Arg-Hyd-Hyd where 'Xaa' is any amino acid, 'Sma' is small amino acid and 'Hyd' is hydrophobic amino acid. [102] Out of all the PH domain identified up to date, only 33% have phosphoinositide binding property but some reports showed that small G-proteins were also targeted by PH domain. [103-106] Nonetheless, recognition of phosphoinositides by PH domain enables translocation of the protein to the site where it can exert its function in a spatial and temporal manner to propagate PI3K signaling. The function of PH domain containing proteins is very diverse and depends on the presence of other molecular motifs.

q) **PIP3 and PI(3,4)P2 effector molecules.** Various proteins have been identified which contain a PH domain with high affinity for PIP3 *in vitro*. These include Btk, Grp1, PKB (or Akt), PDK1, Gab1, Bam32 and centaurin-α1. [102] In the case of PDK1, Akt and Bam32, their PH domain can also recognize PI(3,4)P2 with comparable affinity. [107-109] Currently, the only known proteins which possess high specificity for PI(3,4)P2 is the PH domain of tandem-PH-domain-containing-protein (TAPP1/2) and the PX domain of $p47^{phox}$. [102, 110, 111] Targeting of these proteins to the membrane does not always correspond to the presence of specific lipid because it is

also influenced by the protein's biological function and molecular regulation. For example, Btk is known to be involved in activation of PLCγ to trigger calcium response. [112] In response to BCR cross-linking, Btk transiently translocates to the plasma membrane in PI3K-dependent manner. [113, 114] The membrane recruitment pattern of Btk is consistent with the kinetic profile of PIP3 generation as discussed above. On the other hand, Akt membrane recruitment is another scenario. Akt is a well characterized surrogate marker for PI3K activation and it is involved in lymphocyte survival and proliferation downstream of PI3K signaling. [115] Activation of Akt required phosphorylation at Ser-473 and Thr-308. Although the PH domain of Akt also recognize PI(3,4)P2, activation of BCR only induces transient membrane recruitment. [116, 117] Even though the recruitment patterns of Akt do not correlate with PI(3,4)P2 signal, one study suggested that PI(3,4)P2 is required for Ser-473 phosphorylation. [118] The purposed mechanism is that phosphorylation of Thr-308 by PDK1 is dependent on PIP3 but Ser-473 phosphorylation is done by an unidentified kinase which dependent on PI(3,4)P2 signal. Currently Bam32 and TAPP2 are the only proteins that show sustained membrane recruitment which correspond to PI(3,4)P2 generation upon PI3K activation by BCR cross-linking. [113] In PI3K signaling, very little is know about the regulation and function of PI(3,4)P2 in contrast to PIP3 which is more widely studied. Since TAPP2 is specific for PI(3,4)P2 and PI(3,4)P2 is quantitatively the most abundant in B cells, the function of TAPP2 potentially represents a critical component of BCR-induced PI3K signaling.

r) **PH domain containing adaptor protein.** Unlike the PH domain containing kinases described above, Bam32 and TAPP2 do not have catalytic domain and they serve

PI3K effector function by forming signalsome with other proteins. Bam32 is highly expressed in hematopoietic cells whereas TAPP2 is more widely expressed. [113, 119] Bam32 has a tyrosine phosphorylation site between the N-terminal SH2 domain and the C-terminal PH domain (Figure 3). Although the C-terminal PH domain binds to both PIP3 and PI(3,4)P2, crystal structure analysis showed that the 5-phosphate of the inositol ring was largely expose to solvent and may contribute very little to overall binding affinity. [100, 102] On the other hand, the C-terminal PH domain of TAPP2 do not bind to PIP3 because the protein secondary structure in the inter-strand loop sterically prevent fitting of the 5-phosphate of PIP3. The role of Bam32 in PI3K signaling has been extensively reviewed. [120] Briefly, Bam32 was shown to regulate multiple signaling pathways include calcium signaling, MAPK pathway, acting reorganization and antigen internalization. The SH2 domain of Bam32 was shown to interact with PLCγ2. [121] In knockout model, Bam32 was shown to play a critical role in T cell-independent type II antigen responses. [122] As I will discuss in Chapter II, although some proteins have been identified to interact with TAPP2 through the PDZ-B motif, very little data is available to define its role in PI3K signaling and biological function. The data presented in this thesis addresses the regulation of TAPP2 membrane recruitment and identifies its interacting proteins shedding light on the role of TAPP2 in PI3K signaling.

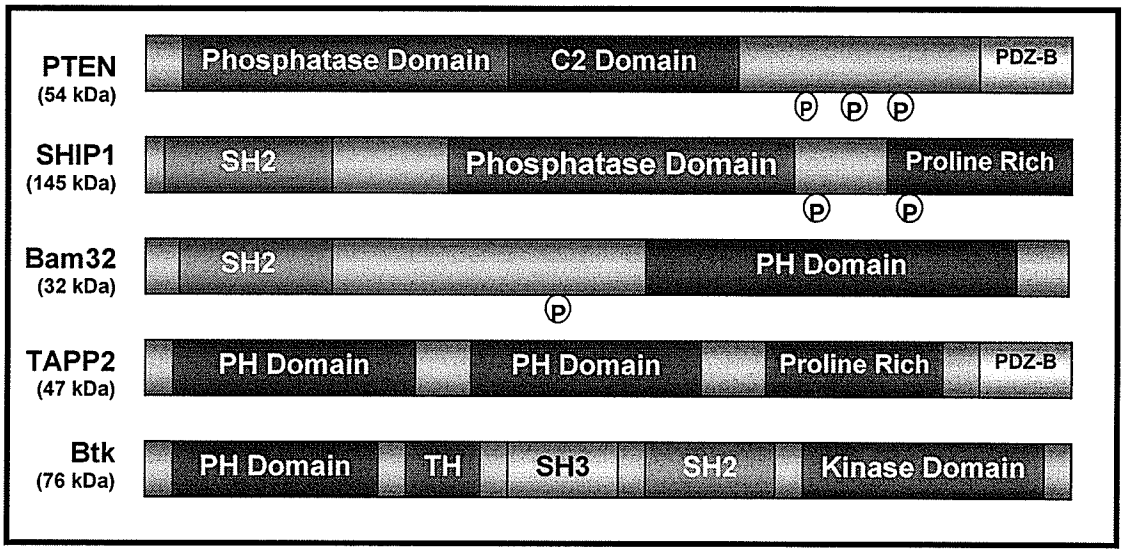

Figure 3. Molecules involved in this study and their domain structure. The drawings do not reflect upon their actual size but the molecular weight is shown. Note that the PDZ-B domain is only consisted of few amino acids.

s) **Regulation of PI3K signaling.** PI3K signaling is antagonized by PTEN and/or regulated by Src Homology 2 domain-containing inositol-5-phosphatase (SHIP). (Figure 2 and 3) *In vivo* studies have demonstrated that PTEN dephosphorylates both PIP3 and PI(3,4)P2 back to PI(4,5)P2 and PI(4)P respectively, whereas SHIP dephosphorylates PIP3 at the D5 position to generate PI(3,4)P2 (Figure 2). [123, 124] PTEN is ubiquitously expressed and its tumor suppressor property is well documented. Although it is well known to antagonize PI3K activity, the mechanism of how PTEN translocate to the membrane and exert its effect is not well defined. One study suggested that binding at the membrane involved protein interaction through the PDZ-binding domain. [125] Another study indicated that both the phosphatase domain and the C2 domain are necessary for membrane targeting, while

phosphorylation at the C-terminus disrupts membrane binding. [126] On the other hand, SHIP associates with various molecules upon activation through binding to its SH2 domain. [127] Among the three forms (sSHIP, SHIP1 and SHIP2), SHIP1 is hematopoietic-restricted and is more characterized in B cells. Upon activation, SHIP1 is tyrosine phosphorylated and recruited to the plasma membrane where it binds to immunoreceptor tyrosine based inhibitory motifs (ITIM) of the FcγRIIB receptor through its SH2 domain to negatively regulate BCR-dependent signals in both human and mouse. [128, 129]

The importance of PTEN and SHIP in B cell development and function is evident from early genetic studies. Whereas $PTEN^{-/-}$ null mutation is embryonic lethal, $PTEN^{+/-}$ null mutation shows dramatic increase in both marginal zone (MZ) and B1 populations. The B cells from mice with B cell-specific PTEN mutation were hyperproliferative and resistant to apoptosis. Also, BCR-induced Akt activation is enhanced and immunoglobulin class switch recombination is defective. Furthermore, these mice have increased serum autoantibodies as well as increase in MZ and B1a cells. [130-132] On the other hand, SHIP knockout mice have a reduced number of immature B cells in bone marrow. B cells from these mice are resistant to cell death, enhanced proliferation, increased phosphorylation of Akt and MAPK. [124, 128, 133]

t) **Importance of PI3K pathway in B cell development and function.** With multiple isoforms and regulatory factors among the class IA PI3K, it presents a challenge to dissect the role that each isoform plays in B cells. The identification of leukocyte restricted p110δ isoform opens up a new window to study the selective role of this particular PI3K in immune responses. Three separate groups utilized different genetic

approaches, and they collectively found that p110δ is indispensable to B cell development and function. In these studies, mice lacking functional p110δ have reduced number of follicular (FO) and MZ B cells as well as B1 subset. These mice respond poorly to both T-dependent and T-independent antigens. Also, proliferation of B cells is impaired and germinal centre formation is apparently defective. Furthermore, BCR-induced PIP3 production is decreased substantially and PI3K effector signaling such as Akt and Btk activation is significantly impaired. [134-136] These findings were in agreement with early studies using p85 knockout mice which showed similar B cells defect. [89] All these studies clearly showed that PI3K is critical component of B cells function and signaling.

CHAPTER I

Superoxides synergize with BCR signaling in recruitment of PH domain-containing adaptor proteins to the plasma membrane of B cells

Rationale

a) **Role of PI3K in ROS production.** Although ROS generation in B cells is a common response to variety of stimuli, several independent studies showed that PI3K signaling have a significant involvement in ROS production. This was demonstrated by using PI3K inhibitors such as Wortmannin and Ly294002 which showed substantial inhibition of receptor-induced ROS production. [7, 24] Consistent with this observation, various PI3K signaling components have been shown to regulate ROS generation in other cell types. [137] Recent mechanistic studies suggested that ROS production is induced through GTPases acting downstream of PI3K activation. [138, 139] Collectively, these data implicate ROS production is downstream of PI3K activation and they can be considered as potential effectors of PI3K signaling. The molecular mechanism of how PI3K activation leads to ROS generation in B cell is currently unknown.

b) **Evidence of ROS regulating PI3K signaling.** Given the importance of PI3K in B cells development and functions, I sought evidence of how ROS, in particular H_2O_2, might regulate PI3K signaling in B cells. One early study showed that H_2O_2 can activate PI3K and the state of activation correlates to PIP3 production. [70] Subsequent reports showed that H_2O_2 treatment triggers PI3K phosphorylation, but it has no effect on its intrinsic enzymatic activity. [72] Although these studies on B cells were contradictory and the methods of measurements were limited *in vitro*, accumulated evidence on other cell types suggested that H_2O_2 treatment can increase PI3K products *in vivo*. For examples, H_2O_2 can induce PI(3,4)P2 and PIP3 in Swiss 3T3 and cos-7 cells respectively, whereas it induces both PI(3,4)P2 and PIP3 in

glioblastoma cells. [63, 140, 141] In 293T cells, H_2O_2 triggers significant PI(3,4)P2 production while the PIP3 level was only marginally increased. [142] The study with glioblastoma cells is of particular interest because in the absence of functional PTEN, which is a common feature in many tumor cell lines, H_2O_2 treatment selectively elevates PI(3,4)P2 while there is no apparent PIP3 increase. Collectively, this suggests the possibility that ROS may activate a positive feedback loop specifically amplifying PI3K signaling in PI(3,4)P2 responses in tumor cells.

In the first part of this study, I investigated how H_2O_2 might influence PI3K signaling in regulating recruitment of PH domain containing molecules to the plasma membrane in B cells. The molecules involved in this study are described in Figure 2. Bam32 has a PH domain specific for PIP3 and PI(3,4)P2. The C-terminal PH domain of TAPP2 is specific for PI(3,4)P2 and the PH domain of Btk is specific for PIP3 binding. [102, 143] By using these specific 3-phosphoinositide binding molecules, I will define the membrane recruitment pattern of PI3K effectors upon H_2O_2 treatment in B cells. Specifically, I will understand how TAPP2 membrane recruitment is regulated upon PI3K activation. Currently very little is known about PI(3,4)P2-dependent effector signaling in overall PI3K pathway and the function of TAPP2 in B cells is unknown.

HYPOTHESIS: ***Reactive oxygen species (H_2O_2) modulate PI3K signaling by altering recruitment of PH-domain containing proteins to the plasma membrane.***

Methodology

a) Reagents and constructs. The constructs used in this study are listed on Figure 4. Plasmids encoding full length Bam32, full length TAPP2, or the C-terminal PH domain of TAPP2 fused to EGFP vector were generated as described in previous publications [113, 119]. Constructs encoding the Btk PH domain fused to the red fluorescent protein DsRed2 was generated by subcloning the PH domain from Btk PH-EGFP-C1 vector [113] into pDsRed2-C1 (Clontech, Franklin Lakes, NJ). FLAG-PTEN (gift of Dr. J. Dixon, University of California, San Diego) was subcloned into the KpnI and BamHI sites of pcDNA3.1 vector (Invitrogen). Goat anti-human IgM $F(ab')_2$ and rabbit anti-mouse IgG $F(ab')_2$ stimulating antibodies (Jackson ImmunoResearch, West Grove, PA) were used at a final concentration of 10 μg/ml unless otherwise indicated. Hydrogen peroxide (Sigma-Aldrich, St. Louis, MO) was used at the indicated concentrations. The inhibitors used are as follows: wortmannin (50 ng/ml; Sigma), LY294002 (50 μM; Biomol, Plymouth Meeting, Pa), IC87114 (10-90 μM; ICOS, Bothell, WA), diphenyleneiodonium (15 μM; Sigma), apocynin (acetovanillone; Sigma). Cells were pre-treated with the indicated inhibitors or vehicle (DMSO) for 30-60 minutes at 37°C prior to stimulation.

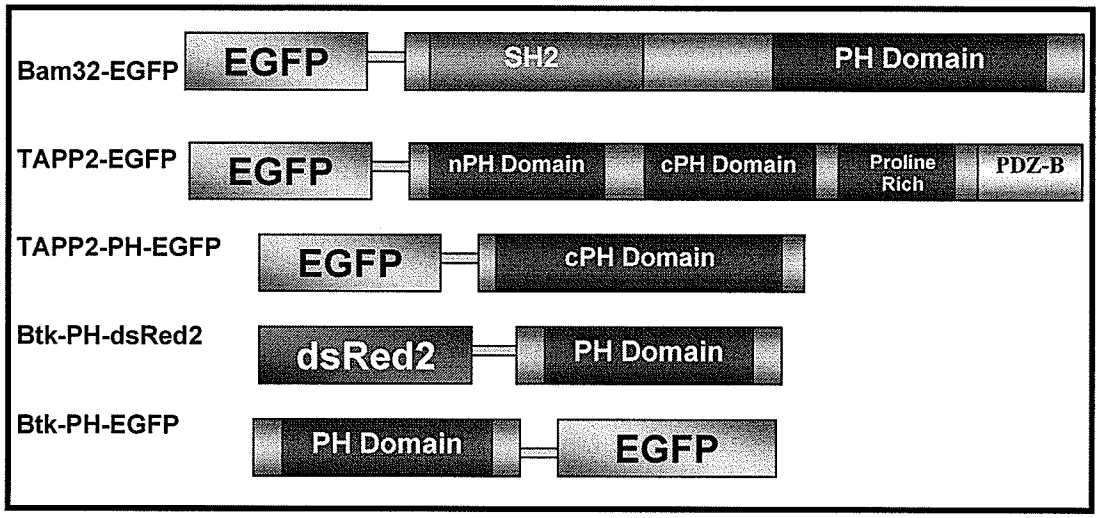

Figure 4. Fluorescent constructs used in this study.

b) Cell counting. Viability of the cells was determined by using Guava Cytometer (Hayward, CA). Briefly, cells were grown in complete medium and stimulated with the indicated H_2O_2 concentration at time 0. At each time point, a small portion of cells was withdrawn from the culture and incubated with Guava ViaCount Reagent. Cell viability and total cell number were determined by using Guava Cytometer. The Guava ViaCount assay distinguishes between viable and non-viable cells based on the differential permeability of DNA-binding dyes in the reagent. Therefore, the readout will not discriminate between apoptosis, necrosis or other forms of cell death.

c) Cell cultures and transfections. BJAB (IgM-expressing, Epstein-Barr virus-negative Burkitt's lymphoma) and A20 (IgG-expressing, mouse B cell lymphoma) were cultured in RPMI 1640 medium (Invitrogen, Burlington, ON) containing 10% FCS and Penicillin-Streptomycin (50 units and 50 ug per ml respectively). Transfection was carried out with

ElectroSquarePorator ECM 830 (BTX, San Diego, LA). Cells were resuspended at 2.5 X 10^7 cells/ml in cold RPMI medium and 0.4 ml and 15 ug plasmid construct were added to a GenePulser Cuvette (Bio-Rad, Hercules, CA) with 0.4 cm electrode gap. For BJAB cells, transfection voltage was set at 310V using a single 10 msec pulse. For A20 cells, transfection voltage was set at 300V using five 3 msec pulses with a 1 sec pulse interval. The curettes were then placed on ice for 10 minutes before transferring to RPMI 1640 medium containing 1% FCS and culturing overnight. For PTEN and PTEN phosphatase-dead stable transfections, 20 μg of linearized vector was electroporated as above. Cells were then selected with 2 mg/ml G418 and cloned to generate stable transfectants.

d) Confocal microscopy and image analysis. For live cell imaging, cells were plated in 8 well glass-bottomed LabTek ChamberSlides (Nalge Nunc Inc, Rochester, NY) and examined on an Olympus IX71 inverted microscope equipped with stage and objective heaters set at 37°C. Stimuli were added directly to the well and live-cell time courses were visualized using a high-speed confocal imaging system (Ultraview LCI, Perkin-Elmer Bioscience). For image analysis of fixed cells, cells were resuspended in pre-warmed RPMI medium containing 1% FCS, stimulated as specified and fixed by addition of an equal volume of ice-cold 4% paraformaldehyde for 30 minutes. Quantitative analysis of membrane recruitment was performed using a modification of our previous method [114]. In each individual cell, the threshold function of the Ultraview analysis software was used to obtain the peak pixel intensity on the cell periphery, while cytoplasmic fluorescence intensity was determined by pixel averaging over a defined area of cytoplasm. The data represents the average membrane:cytoplasmic fluorescence ratio from 20-40 cells per condition. This modified "maximal method" of analysis provides a

more sensitive measure of fluorescence accumulation at the cell periphery compared to pixel averaging within arbitrary areas approximating the plasma membrane (Figure 8).

e) Western blotting. Various whole cells lysates were separated with 10% acrylamide gel electrophoresis followed by protein transfer to nitrocellulose membranes. Membranes were washed with TBST three times and then incubated in TBST with 5% skim milk overnight. The next day the membrane was blotted with 1 mg/mL mouse anti-PTEN mAb (Santa Cruz Biotechnology) antibody for two hours, followed by incubation with a 1/5000 dilution of HRP-conjugated anti-mouse IgG antibody (Jackson ImmunoResearch) for one hour. Blots were then incubated with ECL chemiluminescence substrate (Amersham, Biosciences) and signals were detected with a Fluorchem 8800 chemiluminescence imager (Alpha Innotech).

Results

a) Effects of H_2O_2 on cell growth and viability. Since the toxicity of H_2O_2 is well documented in the literature, I want to determine how H_2O_2 effects cell growth and viability in our B cell models. My aim was to find a dose of H_2O_2 in which our B cell lines tolerated without effecting their overall growth and survival. It estimated that professional phagocytes can generate 1-5 mM per second of ROS inside the phagosome and B cells have approximately 1 to 5% of that efficiency by comparison. [15, 144] I treated BJAB and A20 with various concentrations of H_2O_2. As shown in Figure 5 top panel, I found that treatment of BJAB cells with 0.1 mM H_2O_2 induced growth arrest, as observed by no significant increase in total cell number during the course of the experiment. Also, the viability of the cells changed significantly from initially 92% to only 60% after 48 hours of treatment and the trend seemed to continue to decrease. Under optimal condition, the doubling time for BJAB cells is between 18 to 20 hours as seen in the control which showed no sign of cell death or growth arrest. Treatment with 0.05 mM H_2O_2 only reduced viability by a few percentages (from 90% to 82%) throughout the experiment and growth was significantly delayed compared to the control. On the other hand, A20 cells tolerated higher doses of H_2O_2 compared to BJAB cells. Treatment with 0.2 mM H_2O_2 reduced cell viability by 35% overall but cell division continued after 27 hours.

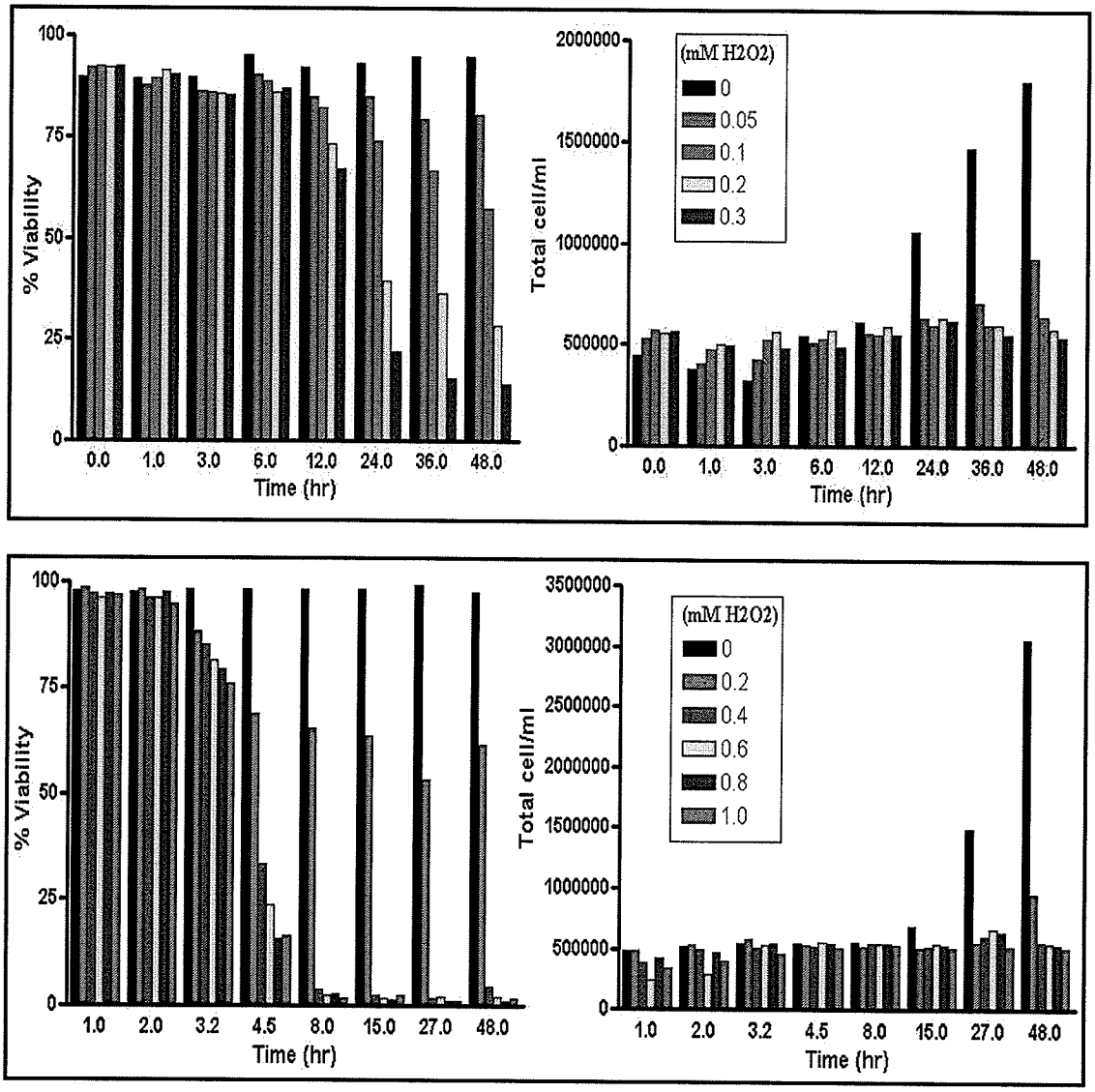

Figure 5. H_2O_2-induced growth arrest and cell viability. (top) BJAB and (bottom) A20 cells were cultured in the presence of various concentration of H_2O_2 added at time 0. Each group of columns represents a single time point with lowest dose beginning on the left side. At each time point, total cell number and viability were assessed by Guava cell counting. Experiments were performed in duplicate and representative data is shown.

b) Hydrogen peroxide can trigger Bam32 and TAPP2 membrane recruitment in B cells. To determine whether hydrogen peroxide stimulation can trigger mobilization of PH domain proteins in lymphocytes, I transiently transfected BJAB with vectors encoding Bam32-EGFP or TAPP2-EGFP. Transfected cells were stimulated with H_2O_2 and live-cell confocal imaging was performed. As shown in Figure 6, both Bam32-EGFP and TAPP2-EGFP are initially evenly distributed, but visible membrane accumulation becomes apparent at 1-2 minutes after peroxide addition. Similar results were obtained with A20. Control EGFP protein expressed in BJAB or A20 cells did not show any change in distribution after stimulation. In titration experiments I found that 3.0 mM H_2O_2 stimulation results in membrane recruitment kinetics similar to BCR stimulation using 10 ug/ml of anti-IgM. With either 3.0 mM H_2O_2 or 10 ug/ml anti-IgM stimulation, detectable recruitment occurs within 2 minutes in over 90% of cells imaged (Figure 7). In order to determine the magnitude of fluorescence redistribution from the cytosol to the membrane under different stimulation conditions, I employed a modification of our previous analysis method [113, 114] which provides improved quantitative discrimination (Figure 8 top). Such analysis averaged over 20 cells or more revealed that recruitment can be observed at doses as low as 0.3 mM (Figure 8 bottom). We used 3.0 mM H_2O_2 as optimal dose because it triggered robust membrane recruitment similar to using optimal anti-IgM stimulation. These data demonstrate that peroxide stimulation of B lymphocytes triggers membrane recruitment of PI(3,4)P2-binding PH domain adaptor proteins.

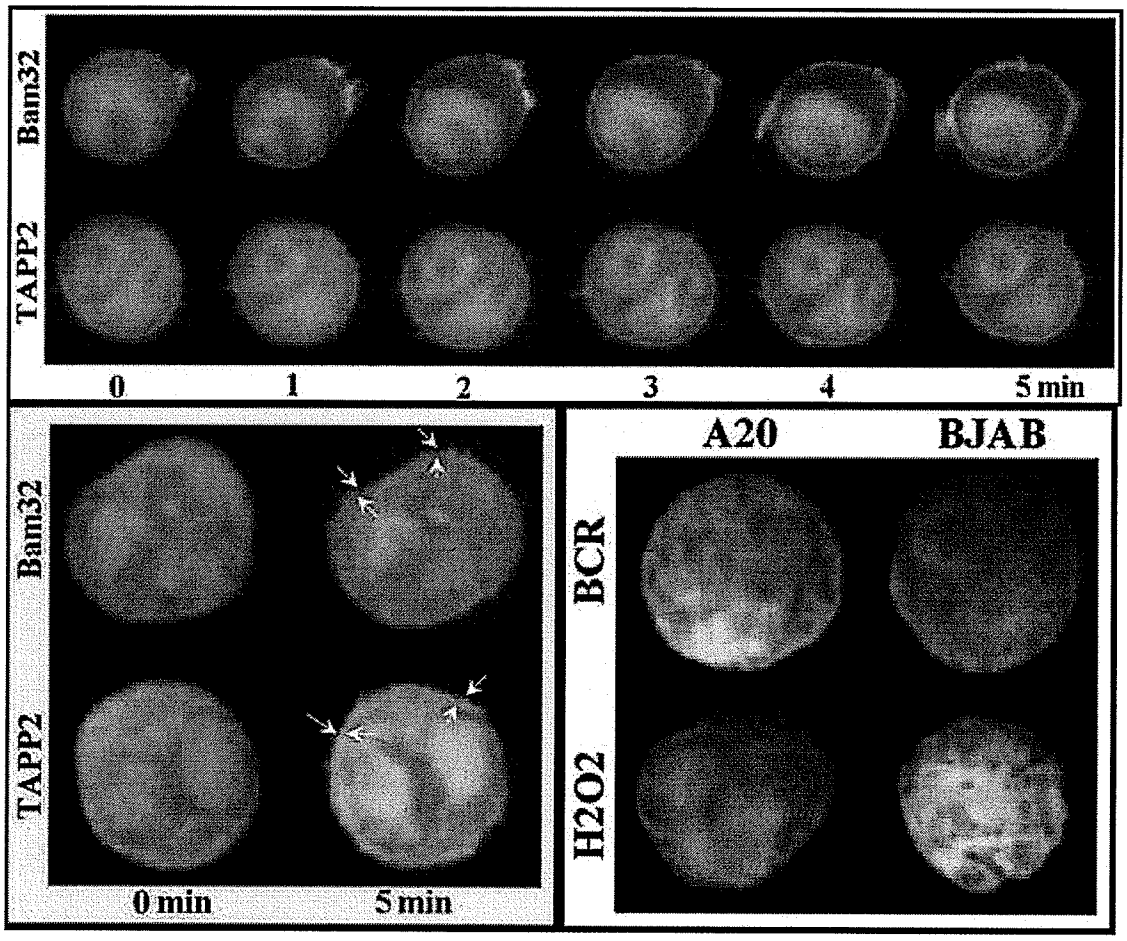

Figure 6. Peroxide triggers membrane recruitment of Bam32 and TAPP2. (Top) BJAB cells were transiently transfected with either Bam32-EGFP or TAPP2-EGFP. Transfected cells were stimulated with 3.0 mM H_2O_2 and confocal images were obtained at 1 minute intervals post stimulation up to 5 minutes. Images are representative of at least 3 independent experiments for each construct. (Bottom left) Similar results were obtained with A20 cells. Since recruitment is not apparent on figure, arrows are used to indicate where Bam32/TAPP2-EGFP accumulated on the membrane. (Bottom right) Control GFP vector transfected BJAB or A20 cells stimulated with either anti-BCR or H_2O_2 for 15 min shows no membrane recruitment.

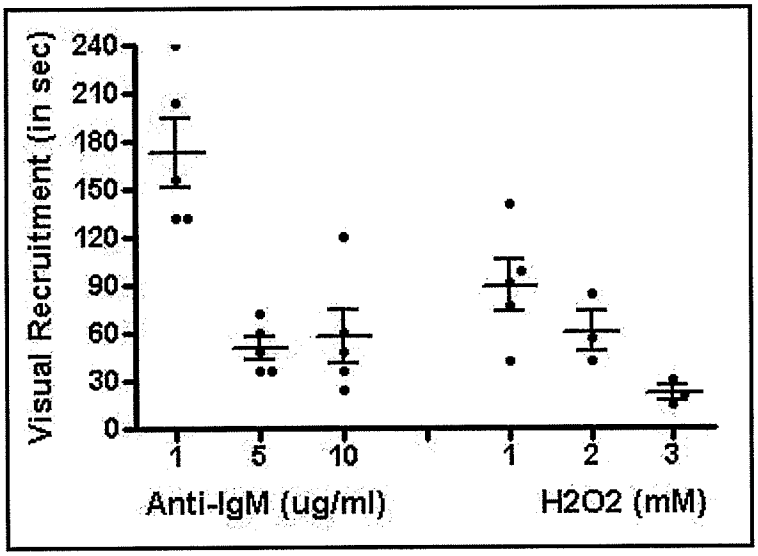

Figure 7. Visual scoring of Bam32-EGFP membrane recruitment. For each condition, a group of cells were viewed under the fluorescent microscope. Indicated stimuli were added at time 0 and recruitment was scored by the first cell that showed recruitment visible among the same group of cells. Membrane recruitment was determined by accumulation of fluorescent on membrane accompanied with fluorescent fading in the cytoplasm.

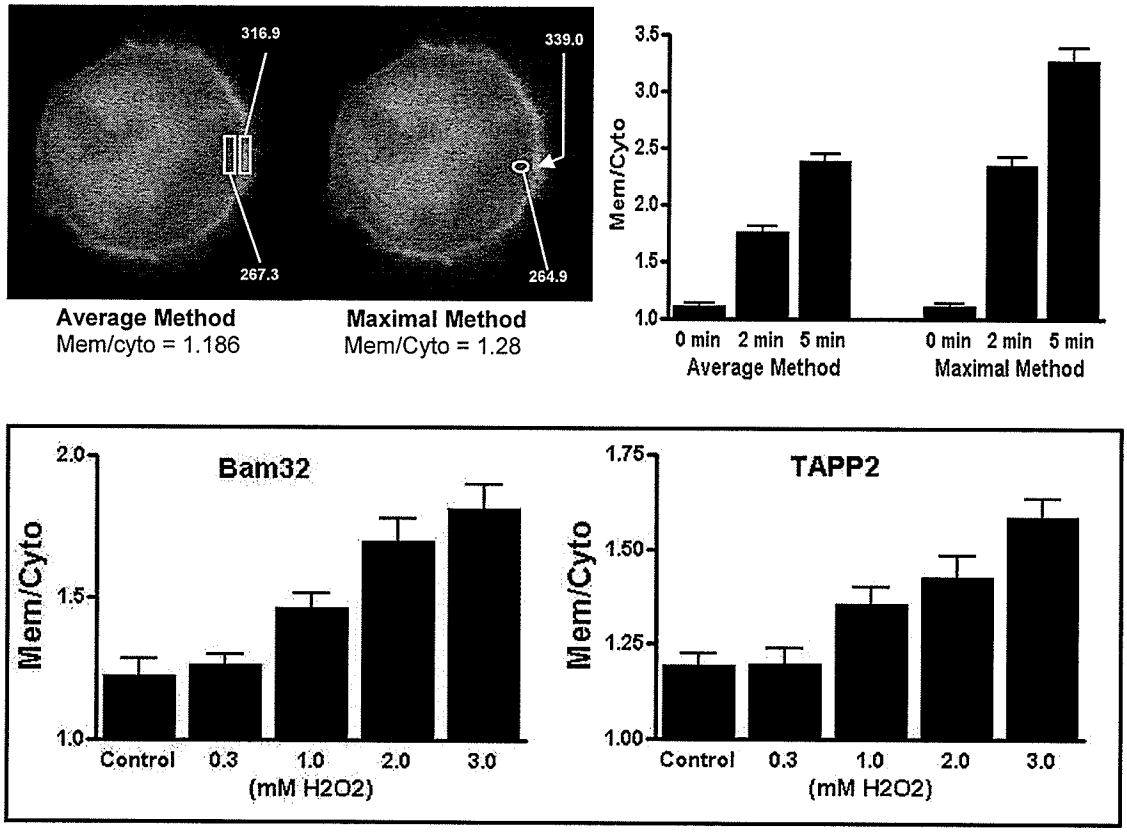

Figure 8. Dose response of H_2O_2-induced Bam32 and TAPP2 membrane recruitment. (Top left) Images illustrating two different analysis methods for quantifying intensity of membrane recruitment. The maximal method using thresholding to determine the peak fluorescence value on the membrane while the average method uses pixel averaging to determine the mean fluorescence over a selected area approximating the membrane. (Top Right) Quantitation of the same set of images (Bam32-EGFP at the indicated times after anti-IgM stimulation) using either the average or the maximal method. Note the maximal method results in greater differentials between time points and is less subjective (need to manually draw a region corresponding to membrane is avoided). (Bottom) Cells were transfected with Bam32-EGFP or TAPP2-EGFP followed by stimulation of indicated stimuli. All cells were fixed with paraformaldehyde at two minutes after stimulation. Note that recruitment of both Bam32 and TAPP2 can be measured at doses as low as 0.3 mM. Each condition represents at least 20 cells analysis. Experiment was performed in duplicate and representative result is shown.

c) Peroxide-induced membrane recruitment is PI3K dependent. Since BCR-induced recruitment of Bam32 and TAPP2 is PI3K-dependant, I tested whether peroxide-induced membrane recruitment of these molecules requires PI3K activity. Bam32-EGFP or TAPP2-EGFP transfected cells were pre-treated with the PI3K inhibitors wortmannin or LY294002 prior to stimulation with 3.0 mM H_2O_2 or 10 ug/ml anti-IgM. I found that membrane recruitment of Bam32-EGFP or TAPP2-EGFP was inhibited in cells pretreated with wortmannin or LY294002 (Figure 9). In addition, since p110δ isoform was critical for BCR signaling, I utilized the p110δ-selective PI3K inhibitor IC87114 to examine whether peroxide-induced recruitment in our human B cell model is similarly dependent on p110δ activity. Under microscopic observation, I found that pretreatment with IC87114 significantly reduced the amount of peroxide-induced membrane recruitment in both Bam32-EGFP and TAPP2-EGFP transfected cells at dose as high as 90μM.

We further quantify the membrane recruitment which averaged over 30 or more cells. Such analysis revealed that wortmannin or LY294002 pretreatment abolished peroxide-induced membrane recruitment of Bam32 or TAPP2, as well as the spontaneous low-level membrane recruitment present in BJAB cultures. On the other hand, IC87114 treated cells showed at least two fold reduction in either Bam32 or TAPP2 recruitment upon either H_2O_2 or anti-IgM stimulation. (Figure 10) By comparing the membrane/cytoplasm fluorescent ratios, the data revealed that IC87114 reduced Bam32 membrane fluorescent by 2.9 and 2.4 fold in H_2O_2 and anti-IgM stimulated cells respectively. Whereas it reduced TAPP2 membrane fluorescent by 6.5 and 3.8 fold in H_2O_2 and anti-IgM stimulated cells respectively. These results indicated that PI3K

activity is critical for peroxide-induced membrane recruitment and peroxide-induced recruitment is more dependant upon the p110δ isoform compared to immunoreceptor-induced recruitment.

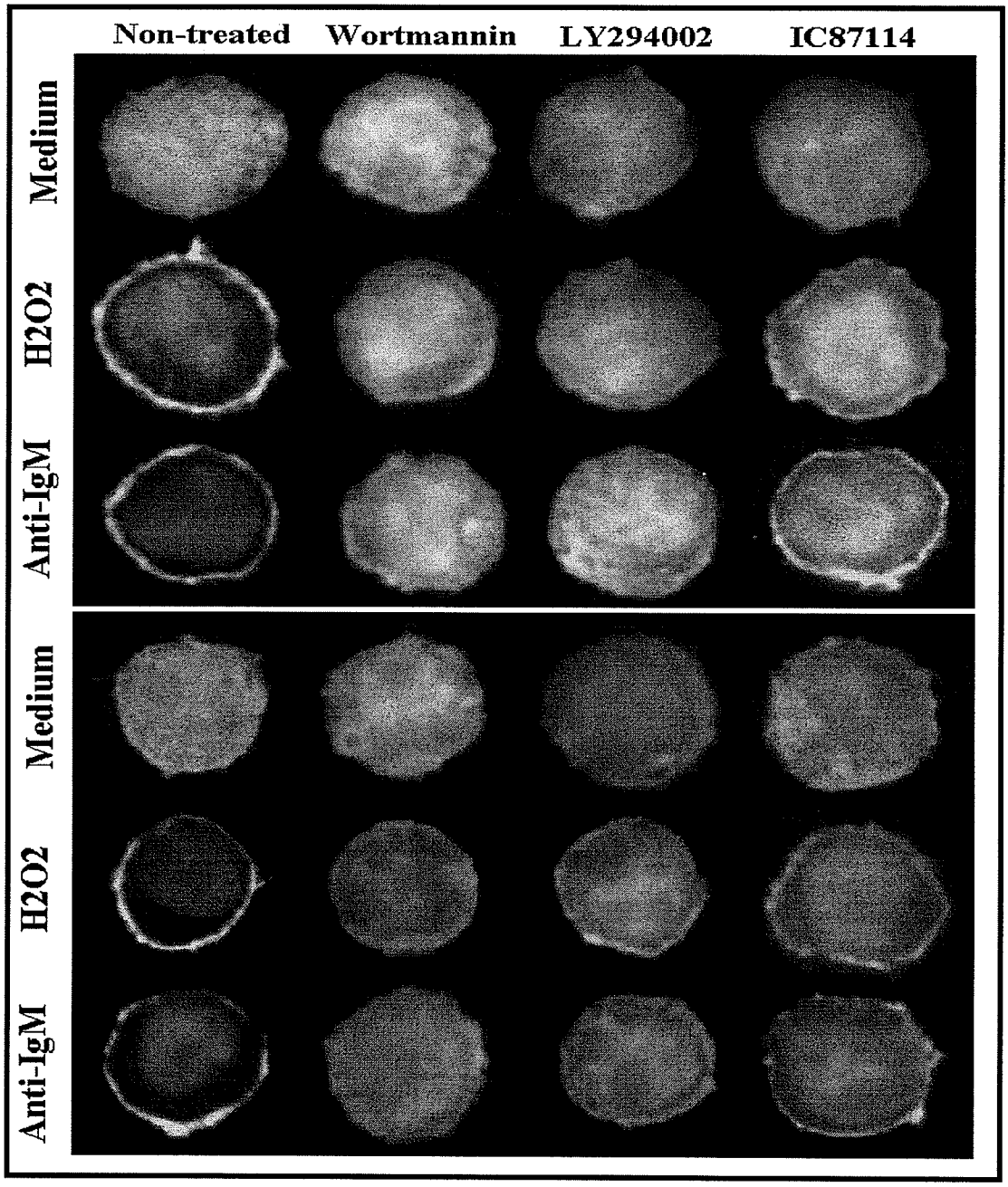

Figure 9. Peroxide-triggered recruitment of Bam32 and TAPP2 is PI3K dependent. Bam32-EGFP (top) or TAPP2-EGFP (bottom) transfected cells were pre-incubated for 30 minutes with 50 ng/ml wortmannin, 50 μM LY294002, or 50 μM IC87114 prior to stimulation. Bam32-EGFP transfected cells were fixed at 5 minutes and TAPP2-EGFP transfected cells were fixed at 10 minutes post stimulation. Representative images are shown from one of 3 independent experiments.

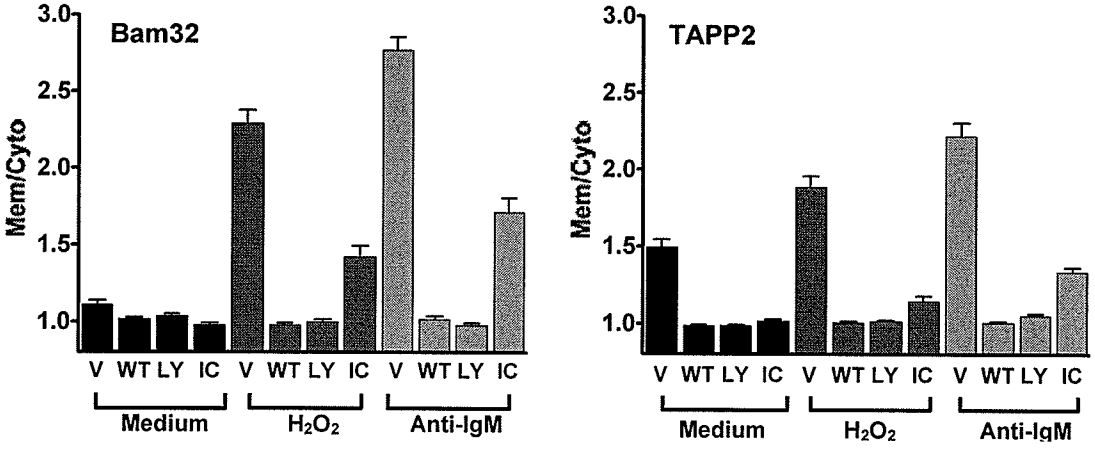

Figure 10. Quantitation of anti-IgM and peroxide-induced membrane recruitment in the presence of various PI3K inhibitors. (Bottom) Transfected cells pre-treated with various PI3K inhibitors or vehicle (DMSO) were quantified using the maximal method. V = vehicle, WT = wortmannin, LY = LY294002, IC = IC87114. At least 30 cells per condition were analyzed. The results are presented as average with SEM.

d) Peroxide induces preferential membrane recruitment of PI(3,4)P2 effector proteins. To determine whether peroxide can also trigger recruitment of a PIP3-specific PH domain in B cells, I examined recruitment of the Btk PH domain, known to bind to PIP3, but not PI(3,4)P2 [143, 145]. BJAB cells were co-transfected with TAPP2 PH-EGFP and Btk PH-dsRed2 vectors (Figure 11). Consistent with our previous results [113], anti-IgM stimulation triggered transient recruitment of Btk PH-dsRed2 to the membrane followed by sustained TAPP2 PH-EGFP recruitment (Figure 11 top). In contrast, peroxide stimulation induced only TAPP2 PH-EGFP domain recruitment but no detectable Btk PH-dsRed2 recruitment up to 5 minutes post-stimulation. A similar lack of recruitment was observed in peroxide-stimulated Btk PH-EGFP transfectants (Figure 11 middle). Quantitative analyses over many cells did not reveal detectable recruitment of Btk PH-GFP after peroxide stimulation, while TAPP2 cPH-EGFP showed significant recruitment (Figure 11 bottom). These results indicate that peroxide stimulation of B cells preferentially triggers membrane recruitment of PI(3,4)P2-binding PH domain proteins.

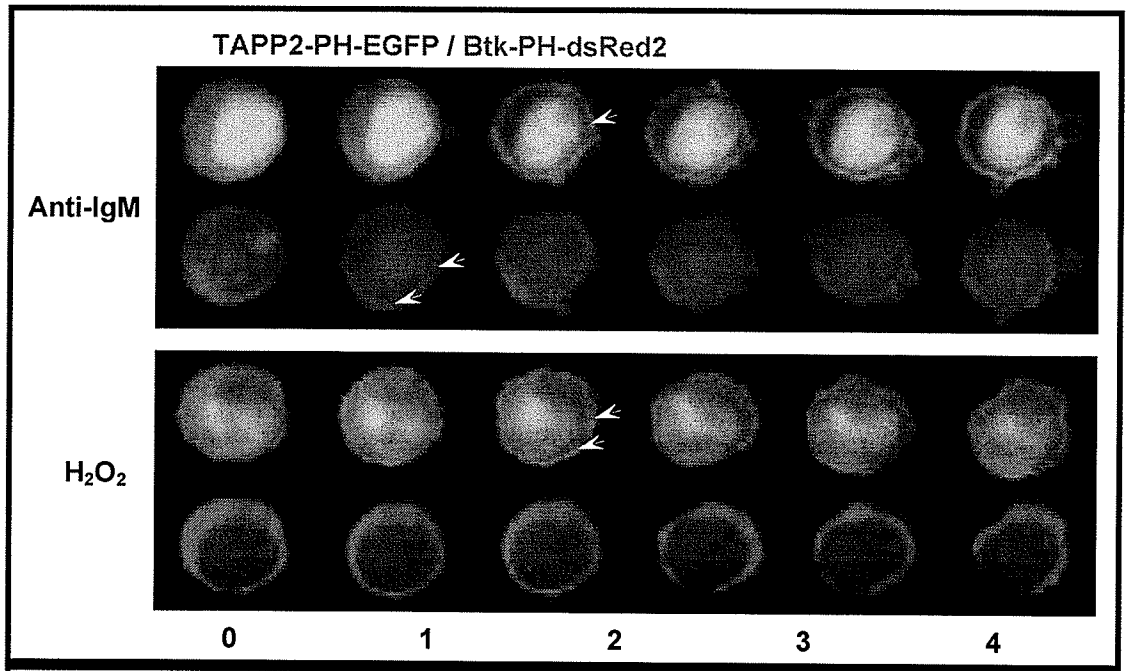
TAPP2-PH-EGFP / Btk-PH-dsRed2
Anti-IgM
H_2O_2
0
1
2
3
4

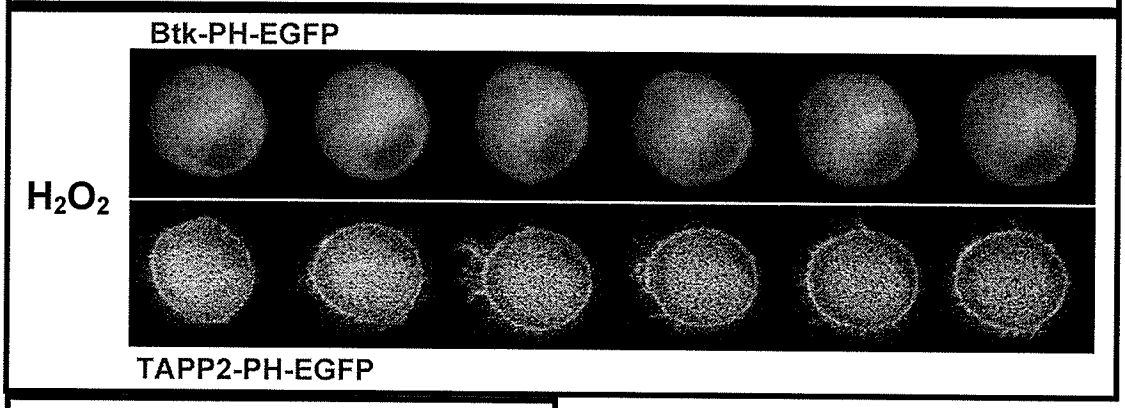
Btk-PH-EGFP
H_2O_2
TAPP2-PH-EGFP

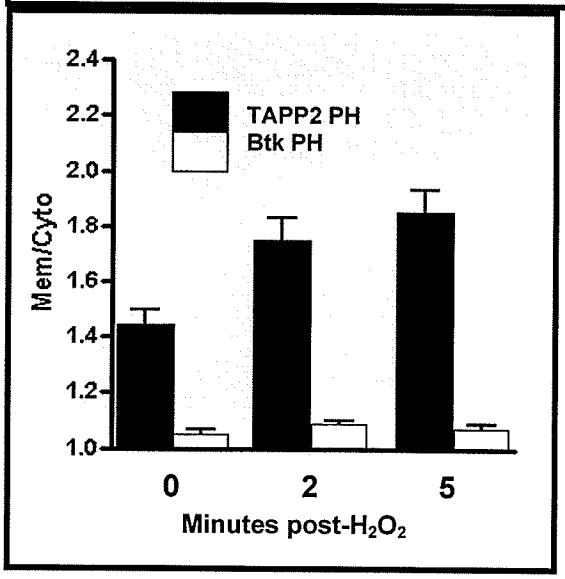
TAPP2 PH
Btk PH
Mem/Cyto
2.4
2.2
2.0
1.8
1.6
1.4
1.2
1.0
0
2
5
Minutes post-H_2O_2

Figure 11. Peroxide induces membrane recruitment of PI(3,4)P2-binding PH domains, but not PIP3-binding PH domains. (Top) BJAB cells were co-transfected with TAPP2 cPH-EGFP and Btk PH-dsRed2 vectors. Transfected cells were stimulated with either 10 μg/ml anti-IgM to crosslink BCR or 3.0 mM H_2O_2. Images were taken at 1 min intervals post-stimulation. Arrows indicate accumulations of fluorescence at the plasma membrane. (Middle) Live cell imaging of BJAB singly transfected with either Btk-PH-EGFP or TAPP2-cPH-EGFP. After treatment with 3.0 mM H_2O_2, membrane recruitment is observed only for TAPP2-cPH-GFP. Results are representative of three independent experiments. (Bottom) Quantitation of TAPP2-cPH-EGFP or Btk-PH-EGFP membrane recruitment kinetics after H_2O_2 stimulation. At least 30 cells per condition were analyzed.

e) Synergistic recruitment by antigen receptor and peroxide stimulation. To examine whether peroxide can influence BCR-induced PI3K signaling via PI(3,4)P2 effectors, I performed co-stimulation experiments using low levels of peroxide together with anti-IgM antibodies. While 0.3 mM peroxide stimulation did not induce significant recruitment on its own (in contrast to 3.0 mM used in previous figures), it markedly enhanced recruitment of Bam32 or TAPP2 when used in combination with anti-IgM antibodies (Figure 12). In contrast, recruitment of Btk PH was not enhanced under these conditions. I examined the kinetics of peroxide-enhanced recruitment of Bam32 or TAPP2 compared to those induced individually by optimal doses of peroxide or anti-IgM antibodies. Strikingly, co-stimulation with peroxide and anti-IgM results in more intense membrane recruitment of Bam32-EGFP and TAPP2-EGFP than can be achieved with either stimulus alone (Figure 13). Although it is not as apparent compared to BJAB cells, similar synergistic recruitment was observed in the murine B lymphoma A20 co-stimulated with peroxide and anti-IgG (Figure 13 bottom). We consistently observed that Bam32 and TAPP2 membrane recruitment are much weaker in A20 cells compared to BJAB cells. Although individual recruitment kinetic and intensity might vary from one experiment to another, synergistic recruitment was consistently observed in all cases.

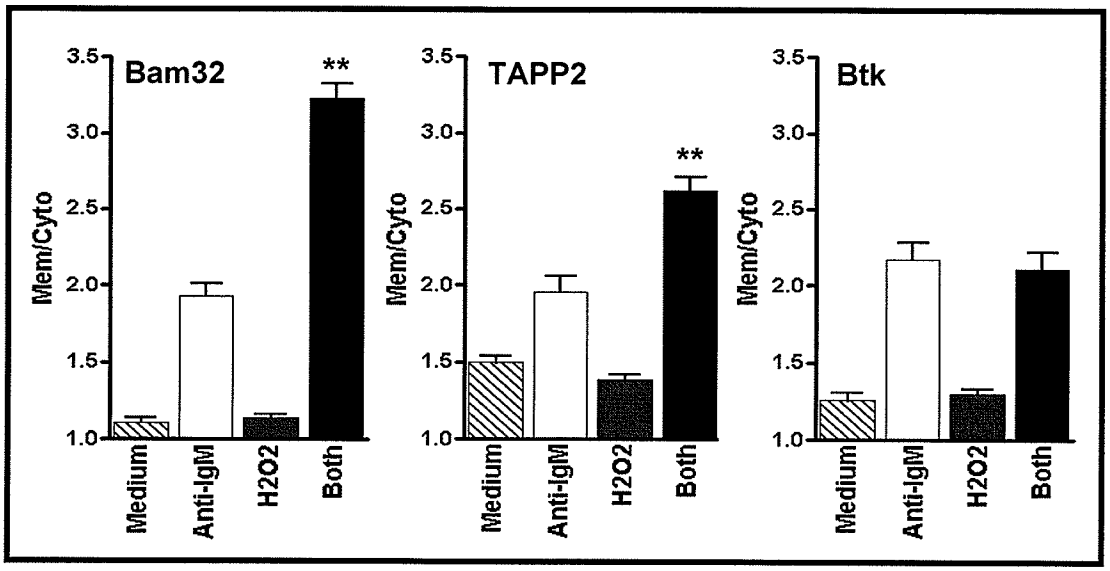

Figure 12. Enhanced recruitment of Bam32 and TAPP2 by costimulation with peroxide and anti-IgM. (A) Bam32-EGFP, TAPP2-EGFP, or Btk PH-EGFP transfected BJAB cells were untreated (medium) or stimulated (1 ug/mL anti-IgM or 0.3 mM H_2O_2 or both together). Cells were fixed for analysis at 5 minutes (Bam32 and TAPP2) or 2 minutes (Btk). ** indicates significantly increased versus anti-IgM alone ($p<0.005$). At least 30 cells were analyzed for each condition.

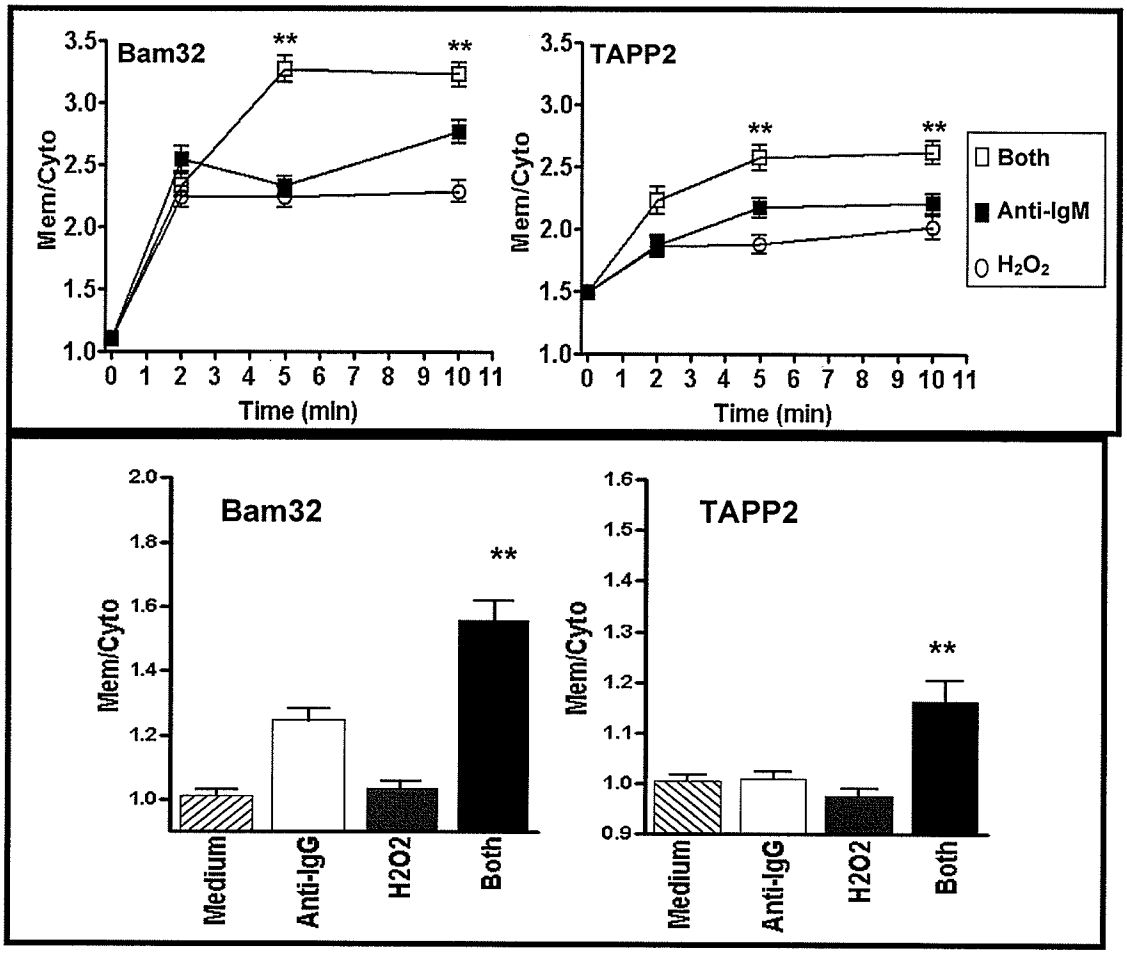

Figure 13. Kinetics of Bam32 or TAPP2 membrane recruitment induced by co-stimulation with peroxide. (Top) Cells were stimulated with either optimal dose of anti-IgM or H_2O_2 (10 μg/mL or 3.0 mM respectively) and suboptimal doses of both stimuli together (1 μg/mL and 0.3 mM respectively). At least 60 cells were analyzed for each condition. (Bottom) Peroxide-enhanced recruitment of Bam32 and TAPP2 was also observed in A20 mouse B cells. Cells were stimulated with 10 μg/ml anti-mouse IgG or 3.0 mM peroxide or both (1μg/mL and 0.3 mM) together, and fixed at 10 min post-stimulation. Note that membrane recruitment in A20 cells is considerably weaker than in BJAB cells. ** indicates significantly increased versus anti-IgM alone ($p<0.005$).

f) PTEN regulates TAPP2 membrane recruitment. The lipid phosphatase PTEN can dephosphorylate PI(3,4)P2 in vitro [146] and is susceptible to inactivation by oxidants such as hydrogen peroxide [63, 65]. Thus it is possible that oxidative inactivation of PTEN could partially account for the peroxide-induced membrane recruitment observed in our B cell system. However, western blotting indicated that BJAB cells, like many human tumor lines, are devoid of PTEN protein (Figure 14), indicating that PTEN inactivation cannot account for the membrane recruitment observed in BJAB model. It is likely that the weaker recruitment observed in A20 cells is due to the presence of PTEN. Expression of PTEN in BJAB cells with transfection confirmed that this phosphatase can indeed regulate membrane recruitment of PI(3,4)P2-specific PH domain proteins (Figure 14 bottom). Interestingly, the low-level spontaneous membrane recruitment observed in these cells is markedly inhibited by catalytically active, but not inactive PTEN, and BJAB*PTEN cells also show significantly reduced TAPP2 membrane recruitment triggered by anti-IgM. However, this inhibition could be largely overcome in the presence of peroxide, as BJAB*PTEN cells showed a similar response to co-stimulation with peroxide and anti-IgM. These results show that PTEN can regulate recruitment of TAPP2 in an oxidant-sensitive manner, but also implicate additional oxidant-sensitive selective regulators of the PI(3,4)P2 pathway.

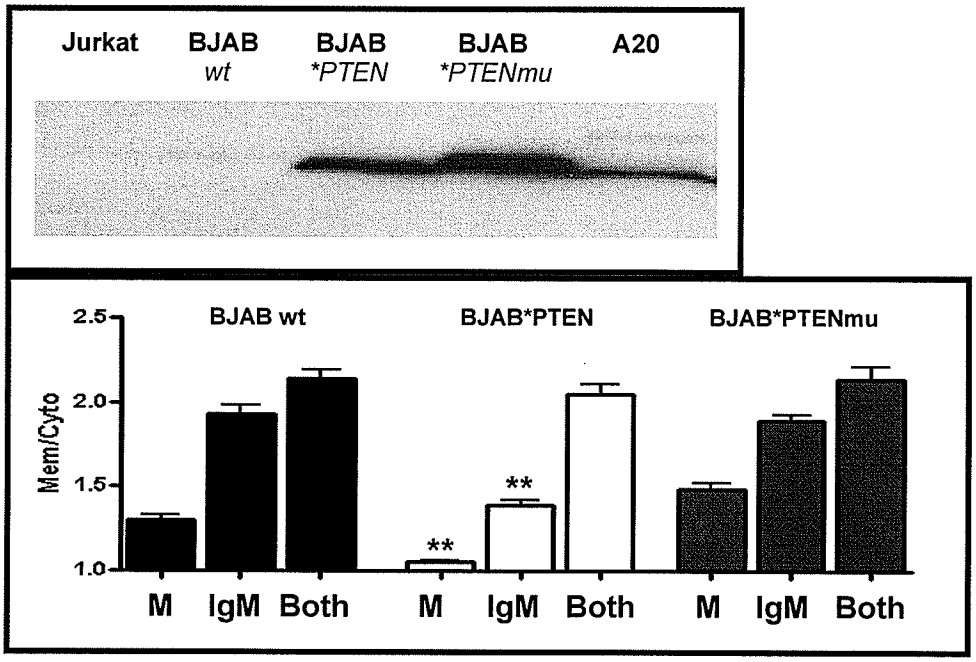

Figure 14. BJAB cells are PTEN deficient, and PTEN re-expression inhibits TAPP2 membrane recruitment. (Top) Western blotting showing PTEN expression in various cell lysates. BJAB*PTEN = wild-type PTEN transfectants, BJAB*PTENmu = phosphatase-dead PTEN transfectants. The blot is representative of 4 experiments. (Bottom) Quantitative analysis of TAPP2 membrane recruitment in BJAB*PTEN and control cells. M = medium treated, IgM = 10 ug/mL anti-IgM, Both = 1 ug/mL anti-IgM and 3.0 mM H_2O_2. All cells were fixed in 5 minutes post stimulation with the indicated stimuli. At least 30 cells per condition were analyzed and averaged. ** indicates significantly decreased ($p<0.005$) versus either parental BJAB or BJAB*PTENmu.

g) Endogenous superoxide production via NADPH oxidase enhances TAPP2 membrane recruitment. To determine whether endogenous production of superoxides through this pathway may contribute to BCR-induced TAPP2 recruitment, BJAB cells were pre-treated NADPH oxidase inhibitors prior to BCR stimulation. Pre-treatment with either diphenyleneiodonium (DPI) or apocynin led to a significant reduction in spontaneous membrane recruitment compared to control pre-treated cells (Figure 15). BCR-induced recruitment of TAPP2 was also measurably reduced, with the effect of the inhibitors particularly evident at early time points post-stimulation. These results are consistent with the hypothesis that endogenous superoxides produced by activated B cells contribute significantly to intracellular propagation of signaling via PI(3,4)P2.

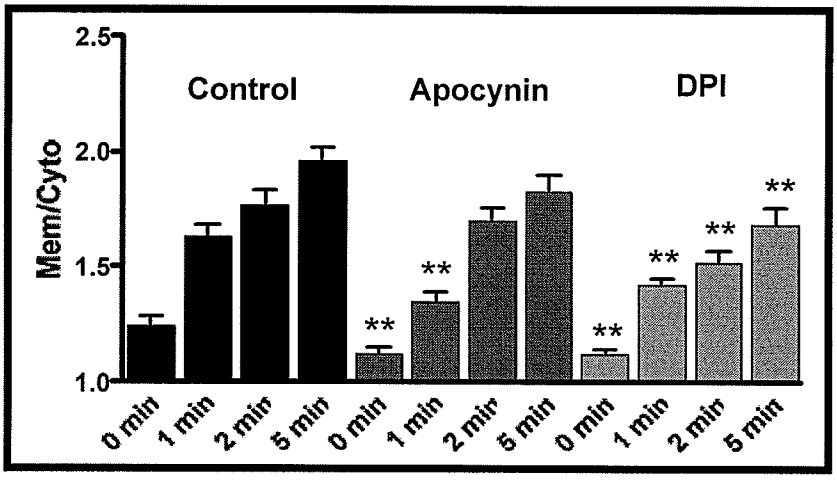

Figure 15. Inhibition of endogenous superoxide production via NADPH oxidase reduces TAPP2 membrane recruitment. BJAB cells were transfected with TAPP2-EGFP, pretreated with the NADPH oxidase inhibitors apocynin or DPI, or vehicle (DMSO as control), and stimulated with 10 ug/mL anti-IgM for the indicated times before fixation followed by image analysis. At least 30 cells per condition were analyzed and averaged. ** indicates significantly decreased ($p<0.005$) versus the control group.

Chapter Discussion

In this section I show that Bam32 and TAPP2 are recruited to the plasma membrane in response to peroxide stimulation in a manner similar to and synergistic with antigen receptor stimulation. Peroxide-induced mobilization is clearly PI3K dependent, consistent with our previous study on BCR-induced PI(3,4)P2 production and recruitment of PI(3,4)P2-binding adaptors [113]. In addition, I find that the P110δ isoform contributes the majority of PI3K activity responsible for both BCR- and peroxide-induced recruitment of these PI(3,4)P2-binding adaptors. This is the first demonstration of the importance of p110δ signaling in a human lymphocyte model (BJAB) and is consistent with the importance of this isoform in murine B cell development and activation [134-136]. My data supports the model that peroxide-induced recruitment of Bam32 and TAPP2 depends on the predominant PI3K signaling module in these cells rather than acting through a minor pathway that is particularly susceptible to the action of oxidants.

My two-color live cell imaging results demonstrate that peroxide selectively recruits the TAPP2 PH domain to the plasma membrane with no detectable Btk PH domain recruitment, suggesting that peroxide preferentially triggers recruitment of PI(3,4)P2-binding PI3K effector proteins. My result is consistent with data showing that fibroblast cells treated with hydrogen peroxide produce PI(3,4)P2, but very little PI(3,4,5)P3 [141]. My results on Bam32 and TAPP2 recruitment in B cells are generally consistent with findings on peroxide-induced recruitment of the related PI(3,4)P2-binding adaptor TAPP1 in fibroblast and epithelial cell lines [147]. TAPP1 is nearly 80% identical to TAPP2, but is generally expressed in lymphocytes at lower levels than

TAPP2 [113, 120]. Together, the available data support a generalizable pathway in which this group of related PH domain adaptors is coordinately recruited to the plasma membrane in response to oxidant stimulation.

The preferential effect of peroxide on PI(3,4)P2 responses appears to be unique, since receptor-mediated activation of PI3Ks almost invariably leads to significant levels of both PI(3,4,5)P3 and PI(3,4)P2. PI(3,4)P2 can be produced both through dephosphorylation of PI(3,4,5)P3 by SHIP phosphatases, phosphorylation of PI(3)P by phosphoinositide 4-kinase or through phosphorylation of PI(4)P by PI3Ks [148]. While the relative contributions of these pathways and their regulation are poorly understood, it is nonetheless clear that there can be large variations in the ratio of PIP3 versus PI(3,4)P2 produced depending on the receptors engaged and the cell type. The relative levels of PIP3 versus PI(3,4)P2 vary tremendously among T cell lines, with increased levels of PI(3,4)P2 correlating with expression of SHIP [149]. It is tempting to speculate that exogenous and/or endogenous peroxide may be an additional important regulator of the balance of PIP3 versus PI(3,4)P2 signaling elicited by immunoreceptor signaling.

Although PTEN is a well-recognized antagonist of PI3K signaling and can metabolize both PIP3 and PI(3,4)P2 in vitro [146], its role in regulating PI(3,4)P2-specific effector proteins in vivo has not been established. My data showed that BJAB cells re-expressing PTEN significantly reduce basal and BCR-induced TAPP2 recruitment, consistent with a function of PTEN in restraining PI(3,4)P2-dependant signaling. There is strong evidence that peroxide can reversibly inactivate PTEN by oxidizing cysteine residues within the phosphatase catalytic site [63, 150]. However, peroxide clearly must have additional targets in activating the PI(3,4)P2 pathway, since it

can induce membrane recruitment of TAPP2 in parental BJAB cells, which are devoid of PTEN protein. These additional targets may include other lipid phosphatases such as type Iα inositol polyphosphate 4-phosphatase, which specifically dephosphorylates PI(3,4)P2 and may be involved in regulating PI(3,4)P2-dependant responses in vivo [151, 152]. Interestingly, the inositol polyphosphate 5-phosphatase SHIP-2 was reported to be relatively resistant to oxidative inactivation by peroxide [63]. Thus, SHIP activity, if present, could provide one means of suppressing PI(3,4,5)P3 accumulation and boosting PI(3,4)P2 levels in cells stimulated in the presence of oxidants. Like most immune cells, BJAB cells express SHIP-1, but very little SHIP-2, so it will be important to determine the effect of peroxide or other oxidants on SHIP-1 5-phosphatase activity.

My data provides clear evidence that costimulation with peroxide and BCR can enhance Bam32 and TAPP2 recruitment to levels beyond those achievable with either stimulus alone. This readily observable synergy is consistent with the idea that peroxide can impinge upon a specific rate-limiting step in signaling to the PI(3,4)P2 pathway, such as PTEN and/or other lipid phosphatases, but cannot duplicate the entire range of BCR signaling inputs to this pathway. It is intriguing to speculate that that exogenous oxidants produced during inflammatory reactions could have specific co-stimulatory signaling function on lymphocytes or other immune cells within the inflammatory milieu. In addition, a recent elegant study has suggested that endogenously-produced hydrogen peroxide forms part of a positive feedback loop enhancing lymphocyte activation [24], strongly suggesting that peroxide-induced signaling mechanisms are an important component of signaling. My results indicate that BCR-induced activation of NADPH

oxidase contributes to generation of PI(3,4)P2 responses, consistent with a role for endogenously produced superoxides in regulating this pathway.

Although PTEN deregulation is commonly associated with many human cancers, accumulated evidences suggested that mutation of PTEN gene is just one contributing factor to carcinogenesis. [153] For tumor development, cells must undergo changes in multiple signaling pathways in favor of survival. Deregulation of PTEN affects PI3K signaling and downstream targets, but ROS can exert its effects in multiple signaling pathways. Therefore, in addition to the well characterized affects of ROS in cancer progression and development, my result implicates that increase signaling through the PI3K pathway in the presence of peroxide might amplify cell survival and proliferation of B cell derived cancers.

In regard to differences in recruitment intensity, I consistently observed Bam32 membrane recruitment is more intense compared to TAPP2 in either H_2O_2 or anti-BCR treatment. Since the full length Bam32- and TAPP2-EGFP construct was used in this study, membrane recruitment may be affected by the presence of protein motifs such as SH2 domain of Bam32 or PDZ-B domain of TAPP2. Although the associating proteins of Bam32 and TAPP2 have not been identified, the SH2 and PDZ-B motifs are common for protein-proteins interactions.

Chapter Summary

The results presented here show that exogenous and endogenous superoxides activate a PI3K-dependant signaling pathway leading to mobilization of PI(3,4)P2 effector proteins in lymphocytes. Together with immunoreceptor signaling, peroxide can specifically enhance PI(3,4)P2-dependant responses, suggesting that the quality of the PI3K signal generated in lymphocytes can be modulated by oxidants.

CHAPTER II

Identification of TAPP2 associated protein(s) in B cells

Rationale

a) **TAPP associated molecules.** TAPP2 has no catalytic domain and likely functions as an adaptor molecule which recruits to the plasma membrane in response to PI(3,4)P2 generation. TAPP1 and TAPP2 are 58% identical over the first 300 amino acid which includes both PH domains (Figure 16). [120] In contrast, there is little sequence identity in the region between the C-terminal PH domains and the PDZ-binding sequence SDV. The C-terminal PDZ-B motif apparently plays an important role on protein-protein interaction. Kimber et al. were the first to demonstrate that TAPP1/2 interact with multi-PDZ-domain-containing protein (MUPP1) and protein tyrosine phosphatase (PTPL1) through the PDZ-B. [147, 154] These interactions are highly dependent on PDZ-B since deletion of the sequence SDV abrogated interaction. However, ectopic expression of TAPP1/2 and subsequent confirmation of interaction in these studies does not prove physiological importance of these interactions. A recent *in vivo* study showed that endogenous TAPP1 co-localized with multiple syntrophin isoforms in regulating actin remodeling, and the association with syntrophins was also dependent on PDZ-B. [155] These data collectively implicate the PDZ-B is important for TAPP1/2 function in binding to their associate partners and regulating downstream signaling but it remains possible that additional protein interactions may occur via other TAPP domains. To dissect TAPP2 associating proteins in B cells, I generated BJAB clones expressing various forms of TAPP2 mutant to identify its potential associated partner(s) *in vivo* through immunoprecipitation. By deletion of PDZ-B or blocking this motif by fusion with myc epitope, one may be able to identify the protein(s) specifically associated with

TAPP2 through the c-terminal PDZ-B or other regions in B cells. Furthermore, these TAPP2 mutants can also serve as dominant negative model to study the biological roles of TAPP2 in BCR-dependent signaling.

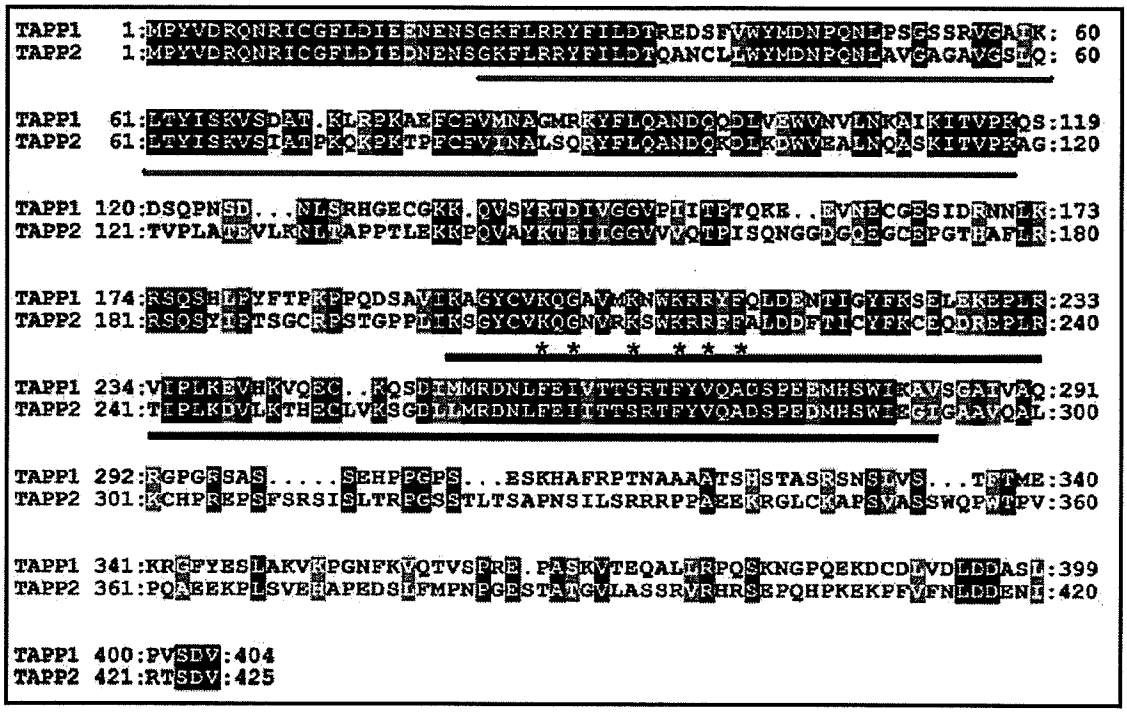

Figure 16. Amino acid sequence of TAPP1 and TAPP2. Grey underlined indicate the N-terminal PH domain and the black underlined indicate the C-terminal PH domain. Stars indicate residues within the PH domain which are conserved for 3-phosphoinositide binding. The c-terminal SDV sequence corresponds to the PDZ-B. (Modified from Marshall et. al. 2002)

HYPOTHESIS: ***TAPP2 mediates its functions by forming signaling complexes with other proteins at the plasma membrane.***

Methodology

a) **Reagents and constructs.** Anti-TAPP2 antibody was generated by immunizing rabbits with a synthetic peptide corresponding to the unique TAPP2 protein sequence CKAPSVASSWQPWTPVPQ (Affinity Bioreagents, Golden, CO). Anti-myc tag antibody was purchased from Upstate, Lake Placid, NY. N-hydroxysuccinimidobiotin (NHS-biotin) was purchased from Sigma-Aldrich, St Louis, MO. Full length TAPP2 and mutant TAPP2 lacking the c-terminal SDV sequences (TAPP2-mPDZ) were cloned into pcDNA3.0 vector. My-tagged TAPP2 was generated by cloning the full length TAPP2 into pcDNA3.1 vector. (Invitrogen) The representative constructs were shown in Figure 17. Protein G Sepharose beads was purchased from Amersham Pharmacia, Sweden. Laemmli sample buffer for sample loading was purchased from Sigma (St. Louis, MO).

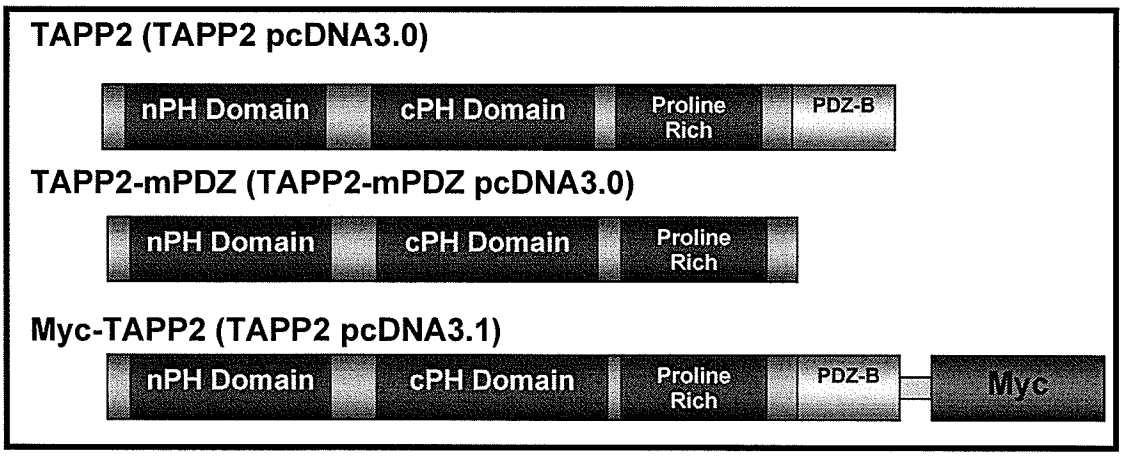

Figure 17. TAPP2 constructs used for generation of stable transfectants.

b) **Cell line and generation of stable transfectants.** Vector encoding TAPP2, TAPP2-mPDZ or myc-TAPP2 was linearized and individually transfected into BJAB by electroporation as described in Chapter I. Transfected cells were grown in complete medium overnight followed by G418 selection in culture for two weeks. Once a selected and exponentially growing population was obtained, individual cells were cloned into 96 well plates until colonies were visible. Quantitative expression of TAPP2 in these clones was determined by western blotting using anti-TAPP2 antibody (Appendix I, Figure 22 & 23). Ramos (human Burkitt's lymphoma and IgM positive) was purchased from ATCC.

c) **Immunoprecipitation and TAPP2 elution.** Cells were washed once with serum free RPMI medium followed by stimulation with 10 μg/mL anti-IgM for 10 minutes at 37°C. Stimulated cells were lysed in cold NP40 buffer containing 1% NP40, 50 mM Tris, 150 mM NaCl and 5 mM EDTA in the presence of protease inhibitor purchased from Roche (Mannheim, Germany) for 1 hour with continuous rocking. Insoluble fractions were removed by centrifuging for 10 minutes at 14, 000 RPM. Supernatant was incubated with protein G beads for 1 hour to remove non-specific binding and then centrifuged. Antibody (anti-TAPP2 or anti-myc) was added into the supernatant and incubated two hours followed by addition of protein G beads for 1 hour. The immunoprecipitates were collected by centrifuge and washed twice with NP40 lysis buffer and once with PBS. All immunoprecipitation steps were done at 4°C. To elute TAPP2 complex from specific antibody, immunoprecipitate was incubated at room temperature for 1 hour with indicated amount of epitope peptide dissolved in PBS at a final volume of 300 ul. Samples were concentrated by using Microcon filtration units

purchased from Millipore (Bedford, MA) with 10000 molecular weight cut off. Laemmli sample buffer was added into the final concentrates at 1:1 volume before loading onto the gel.

d) **Antibody biotinylation and western blotting.** NHS-biotin was dissolved in DMSO and incubated with anti-TAPP2 antibody at room temperature. After 4 hours of incubation, it was dialyzed against PBS solution overnight with several changes of buffer. Western blotting was performed as indicated in Chapter I. TAPP2 and myc-TAPP2 detection was done by using 5 μg/ml anti-TAPP2 Ab and 0.1 μg/ml anti-myc Ab respectively. The secondary HRP-conjugated goat anti-mouse (for anti-myc) or anti-rabbit (for anti-TAPP2) IgG were used at 1:5000 diluation followed by ECL detection by chemiluminescence. The biotinylated-anti-TAPP2 antibody was visualized by incubating with HRP-conjugated streptavidin.

e) **Polyacrylamide gel electrophoresis.** Various immunoprecipitated samples were boiled in sample buffer for 5 min before loading onto 7% polyacrylamide gel. The medium gel was run at 4°C for 3 to 4 hours at 250V with constant stirring. After electrophoresis is completed, gel is washed in de-ionized water followed by staining with Coomassie Blue R-250 stain purchased from Bio-Rad Laboratories Inc (Hercules, CA), GelCode Blue or silver snap stain from Pierce (Rockford, IL).

f) **In gel digestion and protein identification.** Candidate protein bands were excised from polyacrylamide gel and repeatedly washed with following cycle for at least three times. 100mM NH_4HCO_3 was added into the gel and rock for 10 min, followed by exchange of buffer with 1:1 volume of ACN:100 mM NH_4HCO_3 for another 10 min, and finally with pure acetonitrile (ACN) for additional 5 min. All steps were done at

room temperature. After the gel swelled, reduction of protein was done by adding 10 mM dithiothreitol and incubated for 45 min at 57°C. Alkylation was done by adding 55mM iodoacetamide into the mixture and incubating at room temperature for additional 45 min. Both dithiothreitol and iodoacetamide were dissolved in 100 mM NH_4HCO_3. Gel pieces were subjected to the wash cycle once and allowed to shrink with ACN. 5 ng/ul of trypsin dissolved in 50 mM NH_4HCO_3 was added into the gel to digest the peptide overnight at 37°C. After addition of 0.01% trifluoroacetic acid (TFA) to stop the digestion, peptides extraction was done by sonicating in 0.01% TFA:50% ACN solution for 10 min in cold water. ACN was added to shrink the gel for additional 5 min. Samples collected after digestion step were subjected to speed-vacuum to concentrate the volume before analysis using HPLC-MS/MS. The resulting data was submitted into The Global Proteome Machine Organization database (http://human.thegpm.org/tandem/thegpm_tandem.html) for protein identification.

Results

a) **Selection of TAPP2 stable transfectants**. I generated BJAB clones expressing various forms of TAPP2 for this study. (Appendix I, Figure 22 & 23) To optimize the condition for TAPP2 immunoprecipitation as discuss in the following section, I first used BJAB cells expressing myc-TAPP2 (BTFM) clone #3 because it has similar BCR expression as parental BJAB cells. (Figure 24).

b) **Immunoprecipitation of endogenous TAPP2 with anti-TAPP2 antibody.** Although I can immunoprecipitate myc-TAPP2 using anti-myc Ab, the myc epitope located at the TAPP2 c-terminal may interfere with PDZ-B binding to potential candidate protein. However, myc-TAPP2 can serve as tool to validate the TAPP2 antibody immunoprecipitation and blotting ability. First I tested whether anti-TAPP2 Ab can immunoprecipitate endogenous TAPP2 in BJAB cells. As shown in Figure 18, the anti-TAPP2 Ab immunoprecipitated both endogenous TAPP2 and myc-TAPP2 (lane 3 and 5), whereas the anti-myc Ab can only immunoprecipitate myc-TAPP2 but not endogenous TAPP2 as expected (lane 4 and 6). Close examination of Figure 18 revealed that there is an additional band between the endogenous TAPP2 and the myc-TAPP2 (lane 3 and 5). I speculated that it was the heavy chain of anti-TAPP2 Ab, which is about 50 kDa compared to the 47 kDa TAPP2. To confirm this, I biotinylated the anti-TAPP2 Ab then use it on western blotting. By using biotinylated-anti-TAPP2 Ab as the primary antibody followed by detection using HRP-conjugated streptavidin, I can avoid detecting the presence of anti-TAPP2 Ab used for immunoprecipitation. As shown in Figure 19, biotinylated-anti-TAPP2 Ab specifically detects the presence of endogenous TAPP2 and myc-TAPP2 but not the

immunoglobulin chain seen in Figure 19. These results showed that the anti-TAPP2 Ab has comparable ability to immunoprecipitate endogenous TAPP2 compared to the commonly used anti-myc Ab under my assay conditions (lane 3 and lane 6 in Figure 19).

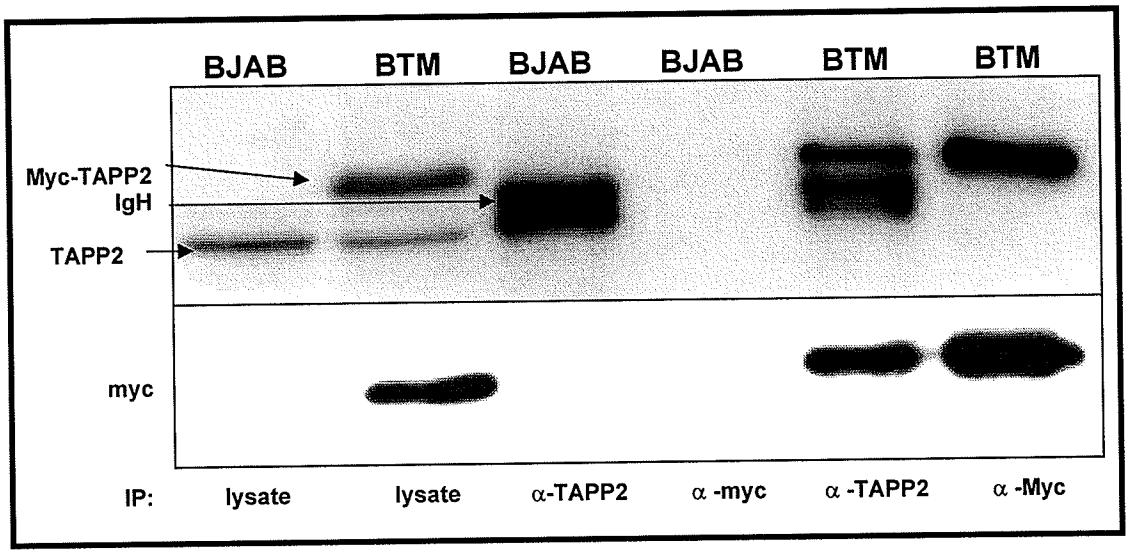

Figure 18. Immunoprecipitate endogenous TAPP2 by anti-TAPP2 Ab. Western blots showing immunoprecipitated TAPP2 by either α-TAPP2 Ab or α-myc antibody. BTM = BJAB expressing myc-TAPP2. Each sample is blotted against either TAPP2 (top) or myc-epitope (bottom). First two lanes are whole cell lysates from the indicated cell line without addition of antibody. Lane 3 to 6; 15 million cells were subjected to immunoprecipitation with 2 ug of indicated antibody.

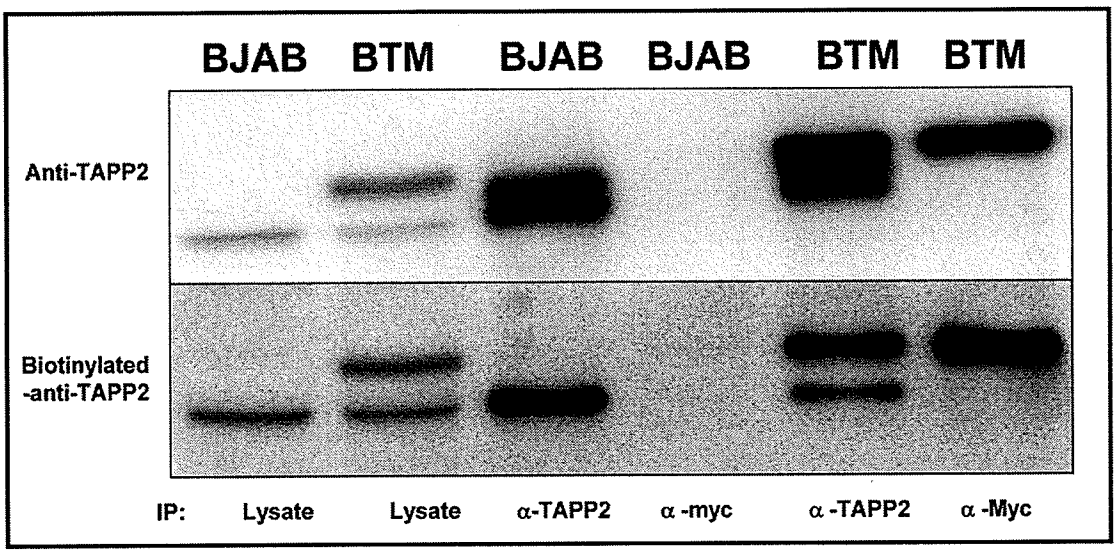

Figure 19. Detection of TAPP2 with biotinylated Ab. The same sample from Figure 18 was blotted against TAPP2 using anti-TAPP2 antibody (top) or biotinylated-anti-TAPP2 Ab (bottom) for comparison.

c) **Elution of TAPP2 associated proteins by epitope competition.** Because non-specifically precipitated contaminant proteins are a major concern and common feature of immunoprecipitation, I wanted to test whether I could specifically elute TAPP2 from the anti-TAPP2 Ab using the epitope peptide for competitive binding. Once this assay was established, we hoped to leave behind non-specific proteins bound to protein G beads or the anti-TAPP2 Ab. As seen in Figure 20, incubation with TAPP2 epitope peptide in PBS for 1 hour at the indicated concentration can release endogenous TAPP2 from the anti-TAPP2 Ab in a dose-dependent manner (left). Similar results were observed when using c-myc peptide to compete with myc-TAPP2 binding to anti-myc Ab (right). The same amount of whole cell lysate were loaded into all the control lanes. Under my assay condition, 10 μg of TAPP2 synthetic peptide gives optimal TAPP2 elution whereas 1 ug myc-peptide gives optimal myc-TAPP2 elution.

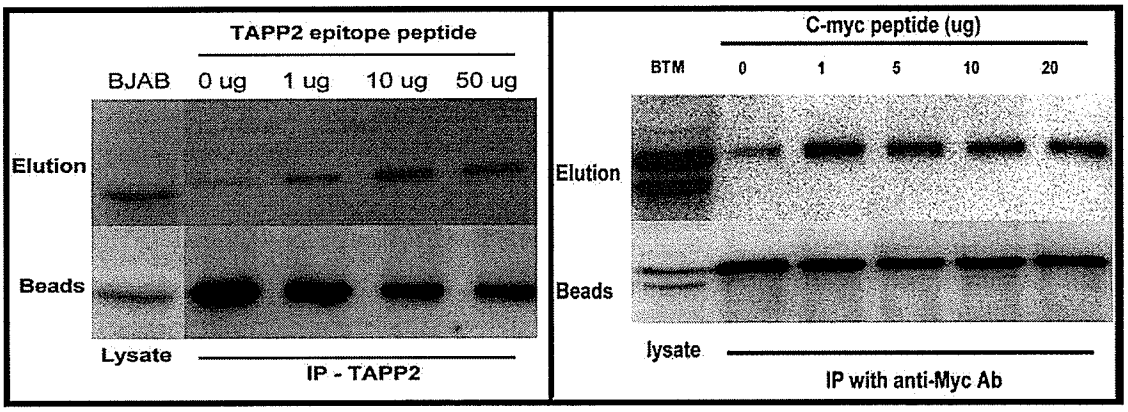

Figure 20. Elution of TAPP2 using epitope peptide competition. (Left) BJAB were subjected to immunoprecipitation with anti-TAPP2 Ab followed by incubation with various concentration of TAPP2 epitope peptide to elute endogenous TAPP2 from the Ab. (Right) BTM cells were subjected to immunoprecipitation with anti-myc Ab followed by incubation with various concentration of c-myc peptide to elute myc-TAPP2 from the anti-myc Ab. All western blots were blotted against TAPP2 and the relative amount can be estimate when compared to the control whole cell lysate.

d) **TAPP2 elution is pH dependent.** As seen in Figure 20, the amount of TAPP2 eluted from the anti-TAPP2 antibody is relatively small and majority of TAPP2 is still bound to the Ab associated with the protein G beads. Since the peptide competition binding assay was done at pH 7.0, I wanted to find a pH condition which provides maximum elution of TAPP2 from the anti-TAPP2 Ab. In the mean time I will monitor the release of anti-TAPP2 Ab from the protein G beads. I performed the same competitive binding assay at pH range from 7 to 3 and I blotted the eluted fraction against TAPP2 and against the rabbit polyclonal antibody. As seen in Figure 21, the quantity of detectable TAPP2 released is reduced as the pH decreased whereas the quantity of anti-TAPP2 Ab fluctuate slightly until the pH reaches around 3.5 and below. While there is large quantity of anti-TAPP2 Ab eluted at low pH, it did not correlate to TAPP2 protein quantitatively. This suggested that TAPP2 protein maybe subjected to degradation at low pH. My results here suggested that maximal TAPP2 elution is at a pH range from 5 to 7.

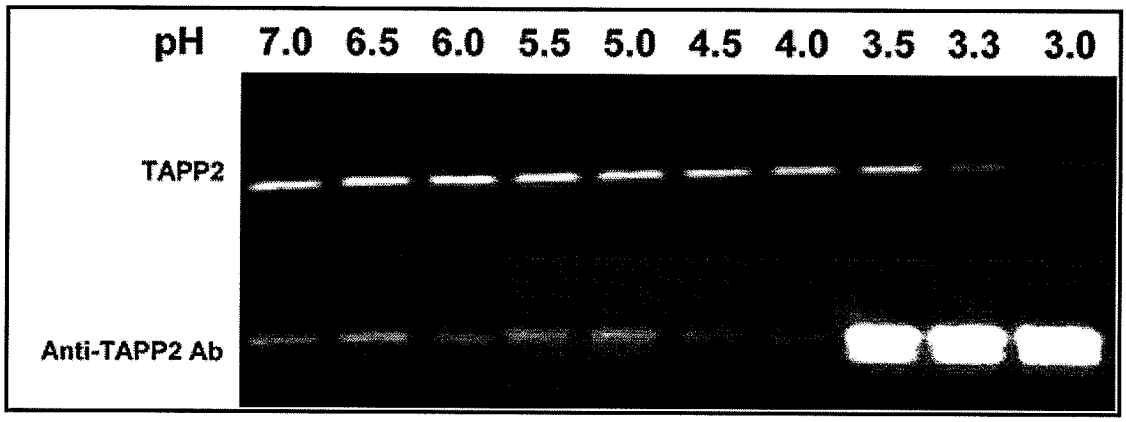

Figure 21. Optimal TAPP2 elution at pH 7.0. Western blot showing the total amount of TAPP2 (top) and the total amount of anti-TAPP2 Ab released (bottom) at indicated pH. Increasing amount of HCl was added to each sample to yield the approximate pH value. 20 μg of peptide was added to PBS with HCl at a final volume of 200μl for individual elution.

e) **Immunoprecipitation of TAPP2 associated proteins in B cells.** In order to identify potential TAPP2 associated proteins in B cells, I performed scale up immunoprecipitation using anti-TAPP2 Ab in TAPP2 over-expressing BJAB cells (Figure 22 clone 4) along with anti-myc Ab to immunoprecipitate myc-tagged TAPP2 expressing BJAB cells (Figure 23 clone 3). By comparing the immunoprecipitates between BTF clone and BTFM clone, we might be able to identify the molecule(s) associated with TAPP2 at the PDZ-B motif. To ensure the clones are minimally altered during transfection and selection, we checked their BCR expression and chose the clones with similar expression as parental BJAB cells. (Figure 24) This is particularly important as I wanted to identify the protein associating with TAPP2 after BCR activation. Based on my previous analysis, TAPP2 membrane recruitment reaches a plateau in about 10 minutes after BCR cross-linking. Therefore, I stimulated at least 80 X 10^6 cells with 10 μg/mL anti-IgM for 10 minutes, followed by immunoprecipitation with anti-TAPP2 Ab or anti-myc Ab along with the control Ab.

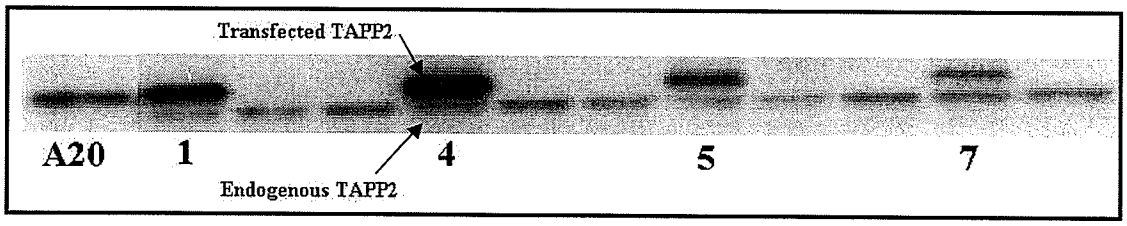

Figure 22. Quantitative expression of TAPP2 pcDNA3.0 in BJAB cells. Western blot showing BJAB cells transfected with TAPP2 pcDNA3.0 (named BTF clones). The upper band represents mouse TAPP2 expressed on human BJAB cells. The lower band represents endogenous TAPP2 in BJAB cells. Although the sequence of TAPP2 is derived from mouse tissue, all the functional domains are conserved between human and mouse. Figure shows that there are 4 positive clones out of 11 selected populations. A20 whole cell lysate were used as control to indicate the position of mouse TAPP2 band. The numbers were used to discriminate among the positive populations only. Note that clone 4 has the highest expression while clone 7 has the lowest. In this study, clone 4 will be used to immunoprecipitate TAPP2 associated protein.

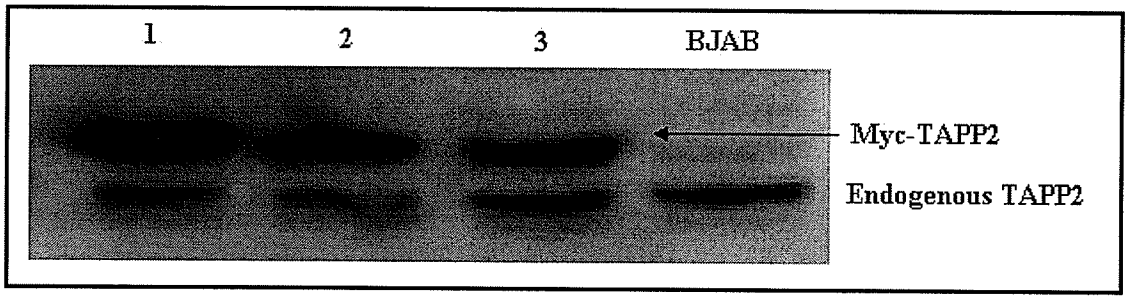

Figure 23. Quantitative expression of TAPP2 pcDNA3.1 in BJAB cells. Western blot showing BJAB cells transfected with myc-epitope tagged TAPP2 (BTFM clones). Figure shows three positive clones with BJAB whole cell lysate as control. Note that clone 1 has the highest expression of myc-TAPP2 while clone 2 and 3 are similar to each other.

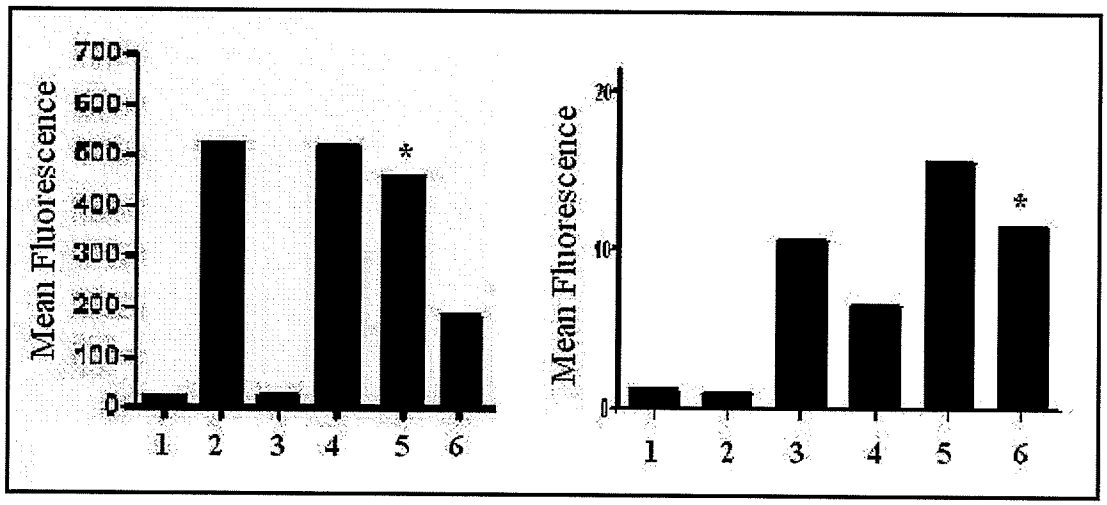

TAPP2 expressing clones (BTF)		Myc-tagged TAPP2 expressing clones (BTFM)	
1	Unstain parental BJAB cells	1	Unstain parental BJAB cells
2	Stained BJAB	2	Isotype Ab stained BJAB
3	Isotype Ab stained BJAB	3	Stained BJAB
4	Empty pcDNA3.0 vector transfected BJAB	4	BTFM clone 1 (correspond to Figure 22)
5	BTF clone 4 (correspond to Figure 21)	5	BTFM clone 2 (correspond to Figure 22)
6	BTF clone 7 (correspond to Figure 21)	6	BTFM clone 3 (correspond to Figure 22)

Figure 24. Surface BCR (IgM) expression on various TAPP2 transfected clones. All cells were stained with FITC-conjugated anti-human IgM except for unstained control and control isotype antibody stain (FITC-conjugated anti-human IgG). Stained cells were all subject to FACS analysis and the value of mean fluorescent is showed. * indicated the clone used for immunoprecipitation. Table on bottom indicates what each column is representing in figure.

As shown in Figure 25, my initial result using 10% pre-cast gel purchased from Bio-Rad showed reasonable protein separation but the bands above 170 kDa and below 40 kDa were not very distinctive. However, the result of this experiment suggested that conventional Coomassie Blue can provide reasonable staining quality for the quantity of immunoprecipitates. Close examination on the gel reveal no visually distinctive bands in the activated immunoprecipitates comparing to the non-activated fraction (compare lane 5 to 6 or lane 8 to 9). Also I did not detect any protein bands which might be specific for TAPP2 PDZ-B motif by comparing immunoprecipitates of BTF and BTFM clones (compare lanes 5 and 6 to lanes 8 and 9). Furthermore, the protein bands above 170 kDa become more faint and less distinguishable from the background.

In order to obtain better resolved bands in the high molecular weight regions, I repeated similar experiment using double the amount of cells (160 millions) and with longer electrophoresis time in hope to resolve higher molecular weight proteins. As seen in Figure 25, running the gel longer unexpectedly caused the proteins to migrate unevenly in the pre-cast gel. Despite the undesirable smearing and spreading of the protein bands below 55 kDa, this result suggested that it is possible to resolve protein bands above 170 kDa with more cells and longer electrophoresis time.

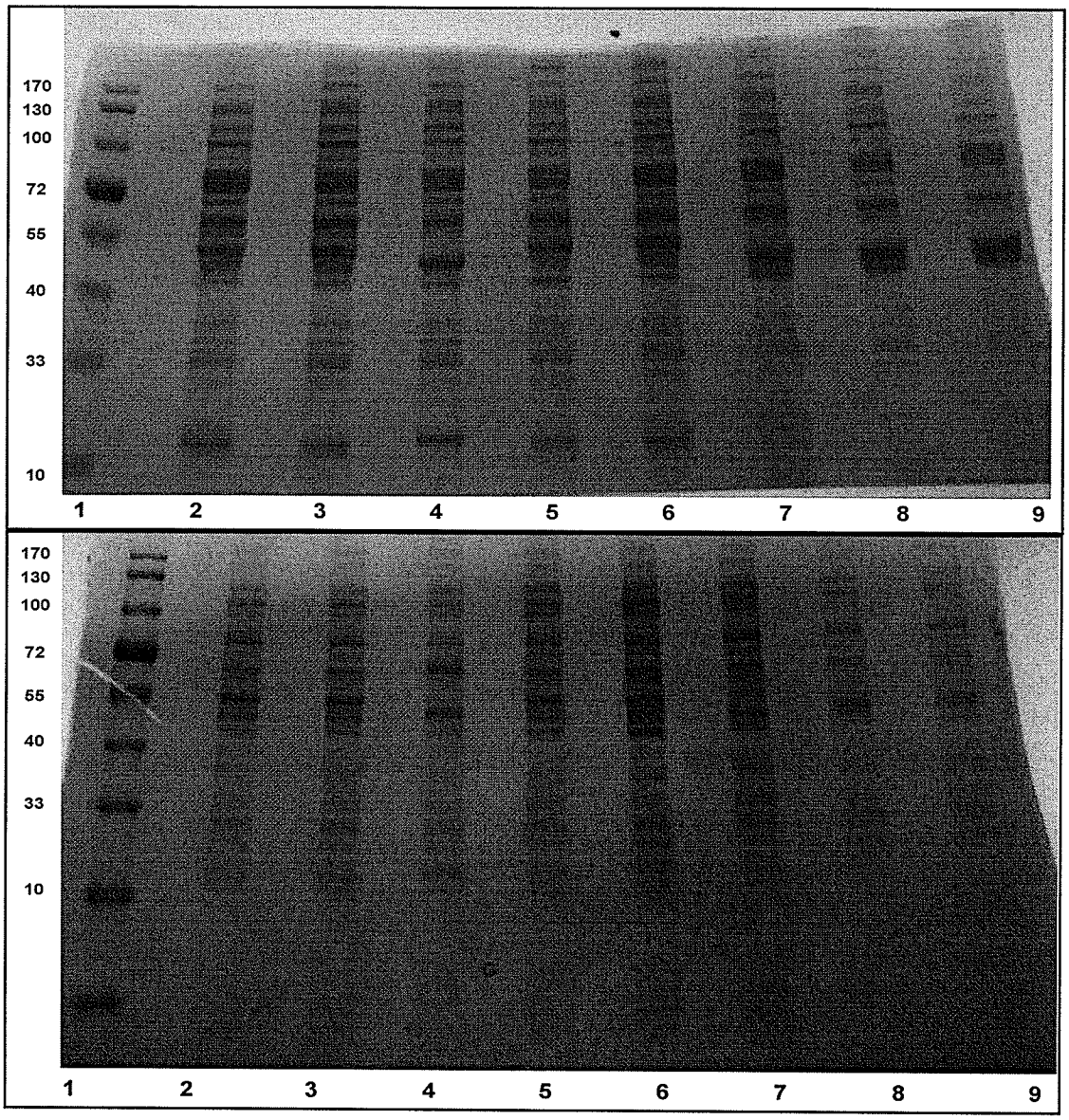

Lane	1	2	3	4	5	6	7	8	9
Cell lines	Marker	BJAB		BTFM			BTF		
Activation	N/A	Yes	No	Yes	No	Yes	Yes	No	Yes
IP Ab (10 ug)	N/A	α-myc		Isotype Ab	α-myc		Isotype Ab	α-TAPP2	

Figure 25. Electrophoresis of anti-TAPP2 and anti-myc immunoprecipitation. (Top) bead-bound fraction and (bottom) the eluted fractions of various immunoprecipitates. Proteins were visualized by Commassie Blue and table on bottom indicates IP conditions. At least 80 million cells were used in each condition.

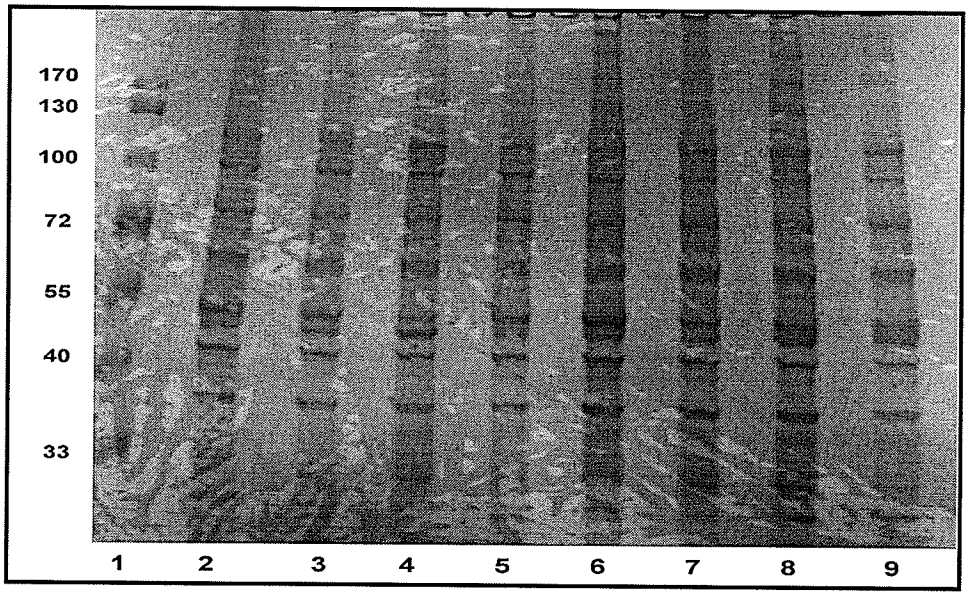

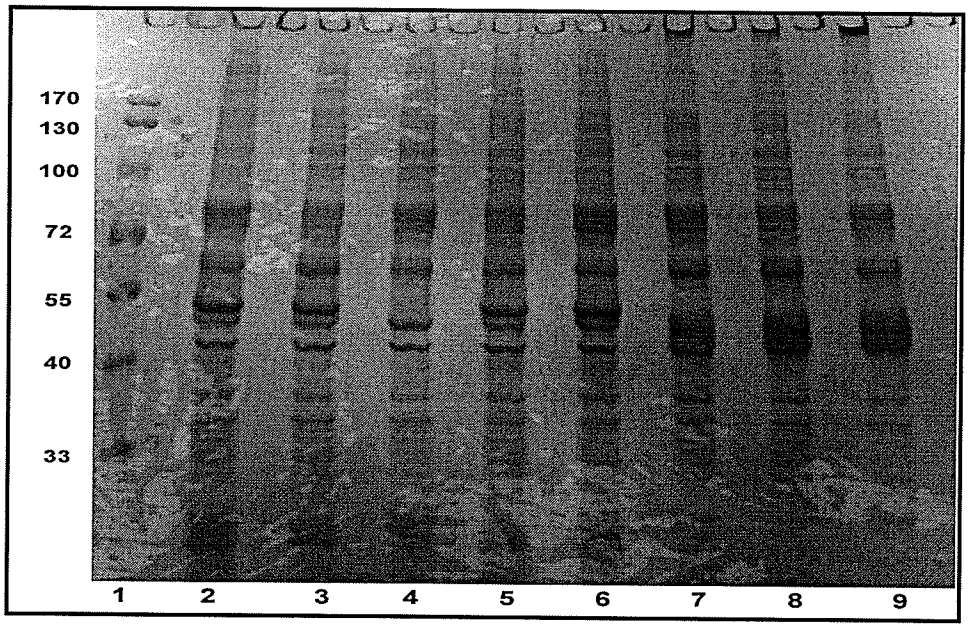

Lane	1	2	3	4	5	6	7	8	9
Cell lines	Marker	BJAB		BTFM			BTF		
Activation	N/A	Yes	No	Yes	No	Yes	Yes	No	Yes
IP Ab (20 ug)	N/A	α-myc		Isotype Ab	α-myc		Isotype Ab	α-TAPP2	

Figure 26. Electrophoresis of anti-TAPP2 and anti-myc immunoprecipitation. (Top) bead-bound and (bottom) eluted fractions of various immunoprecipitates. Proteins were visualized by Commassie Blue and the table on bottom indicates each IP conditions. At least 160 million cells were used in each condition.

To improve protein band resolution and reduce background staining, I utilized 7% acrylamide gel and use GelCode Blue stain for the next experiment. Here I will first focused on immunoprecipitating BTF cells only and the result is shown in Figure 27. In this experiment, GelCode Blue seemed to provide better staining quality and less background. Although it is not as apparent in the figure, close visual examination on the gel revealed a protein band above 170 kDa which was found on TAPP2 immunoprecipitates but not on the control lane (Figure 27). This band was never apparent in Coomassie blue stained gel either due to low staining intensity or poor resolution. Furthermore, the intensity of the band appears stronger in activated cells compared to the non-activated cells in this particular experiment. This is the first time I have visually detected a distinct band found among anti-TAPP2 immunoprecipitates but not on the control antibody immunoprecipitate.

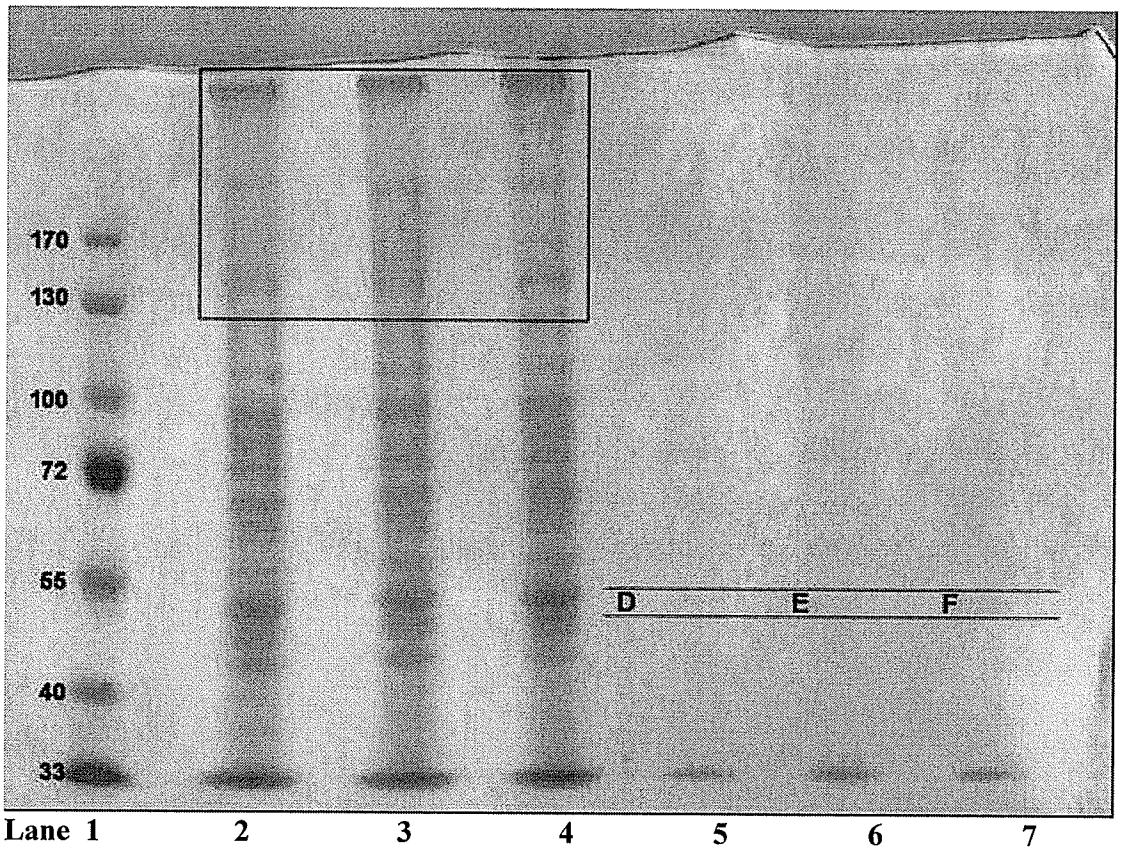

Figure 27. GelCode Blue staining revealed TAPP2 specific associated protein. (Top) Immunoprecipitation of BTF clone using anti-TAPP2 antibody. Immunoprecipitates were separated in 7% polyacrylamide gel stained with GelCode Blue. (From left to right) Lane 1 – protein marker. Lane 2 – control polyclonal rabbit antibody immunoprecipitation on BCR-activated cells. Lane 3 – TAPP2 immunoprecipitation of non-activated cells. Lane 4 – TAPP2 immunoprecipitation on BCR-activated cells. Lanes 2 to 4 were bead-bound fraction whereas lanes 5 to 7 were the corresponding eluted fractions. (Right) The region on bead bound fraction was enlarged at the right to show the distinctive bands. The same band was not visible on control Ab immunoprecipitation. The letter correspond to the gel fragment excised for MS analysis.

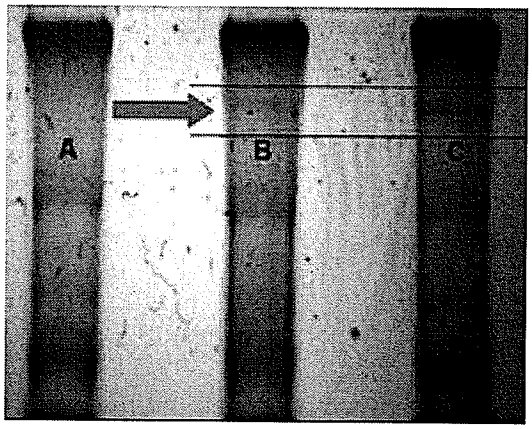

f) **TAPP2 is associated with utrophin in B cells.** After visually identifying a distinct protein band found in TAPP2 immunoprecipitates, I excised the bands along with the corresponding control fragment for in-gel protein digestion as described in method section. The trypsin digested samples were analyzed on HPLC-MS/MS in collaboration with Manitoba Centre for Proteomics. The acquired data were then subjected to global proteomic database search and the candidate proteins identified are selectively listed in Table 2 with confidence threshold for acceptance set at an expectation value of -10 (see complete list in Appendix II). This cutoff value ensures that the identification came from at least two high confidence peptides of the same protein. Among the identified candidates, utrophin scored the highest according to the result from the database search. This suggests that utrophin is readily identified in the gel bands excised from anti-TAPP2 immunoprecipitates. In contrast, utrophin was not found in control band. Close examination of the basis for identification revealed the samples analyzed contain at least 27 peptide fragments corresponding to utrophin (Figure 28). My results suggested that TAPP2 is constitutively associated with utrophin in B cells *in vivo*.

Up to this point, although the eluted fractions (Figure 25 and 26 bottom) showed reasonable band intensity under Coomassie Blue staining, there is no apparent difference between the control and the anti-TAPP2 immunoprecipitates. But in this particular gel stained with GelCode Blue, the eluted fractions become more distinguishable between the control and the anti-TAPP2 immunoprecipitates. Close visual examination of the gel revealed there are two bands on both anti-TAPP2 immunoprecipitates but not on the control lane at the region where TAPP2 is

approximately located (Figure 27 labeled D, E and F). To determine if these bands are indeed TAPP2, I excised these bands and subjected them to the same identification procedure. As showed in table 3, although the control sample (sample D) appeared to have cross contamination (most likely from sample B or C), my results showed that TAPP2 is presence in both eluted-fractions of TAPP2 immunoprecipitates but it is not found in the corresponding control. (see Appendix II for complete list) This is further confirmed by western blot showing the control Ab did not immunoprecipitate TAPP2 non-specifically (Figure 29). The reason for the observed low confidence of identification value for TAPP2 is most likely due to the limited quantity of TAPP2 peptides available in the eluted fraction. In this experiment, I did not see other distinguishable protein bands on the same gel which might be specific for TAPP2. I also did not observe any bands in the eluted fraction which might corresponds to utrophin. Further scale-up for elution might enable one to see utrophin band on the gel. My results here showed that utrophin is specifically immunoprecipitated with TAPP2 and our elution method has the potential to reduce non-specific associated proteins under our assay condition.

Table 2. Selected candidate proteins identified from the gel fragments excised from the bead-bounded fraction indicated in Figure 26.

Log(e)$^+$	MW	Accession	Description
Sample A *– Control Ab immunoprecipitation (BCR-activated)*			
-104.7	468.7	ENSP00000313420	DNS-dependent protein kinase catalytic subunit
-31.1	66.0	ENSP00000252244	Keratin, type II cytoskeletal 1
-28.0	8.8	gi|999627|	Porcine E-Trypsin
-22.7	228.3	ENSP00000327077	Pericentriolar material 1
-18.6	277.0	ENSP00000297183	Eukaryotic translation initiation factor 4E binding protein 3
-10.8	62.0	ENSP00000246662	Keratin, type I cytoskeletal 9
Sample B *– TAPP2 immunoprecipitation (non-activated)*			
-356.3	394.2	ENSP00000356515	Utrophin
-78.4	468.7	ENSP00000313420	DNA-dependent protein kinase catalytic subunit
-38.1	66.0	ENSP00000252244	Keratin, type II cytoskeletal 1
-35.2	62.0	ENSP00000246662	Keratin, type I cytoskeletal 9
-28.5	8.8	gi|999627|	Porcine E-Trypsin
Sample C *– TAPP2 immunoprecipitation (BCR-activated)*			
-457.6	394.2	ENSP00000356515	Utrophin
-79.2	468.7	ENSP00000313420	DNA-dependent protein kinase catalytic subunit
-29.1	277.0	ENSP00000297183	Eukaryotic translation initiation factor 4E binding protein 3
-27.5	66.0	ENSP00000252244	Keratin, type II cytoskeletal 1
-21.1	8.8	gi|999627|	Porcine E-Trypsin

Table 3. Selected candidate proteins identified from the gel fragments excised from the eluted fraction indicated in Figure 26.

Log(e)$^+$	MW	Accession	Description
Sample D *– Control Ab immunoprecipitation (BCR-activated)*			
-59.7	394.2	ENSP00000356515	Utrophin
Sample E *– TAPP2 immunoprecipitation (non-activated)*			
-11.6	34.1	ENSP0000306771	Tandem PH domain containing protein-2 (TAPP2)
-11.5	47.1	ENSP0000234590	Alpha Enolase
-10.1	38.4	ENSP0000313199	Heterogeneous nuclear ribonucleoprotein D0
-9.0	51.2	ENSP0000327539	Heterogeneous nuclear ribonucleoprotein H
-8.0	46.4	ENSP0000326381	Eukaryotic initiation factor 4A-II
-7.7	43.8	ENSP0000302886	Proliferation-associated protein 2G4
-2.1	59.5	ENSP0000252245	Cytokeratin type II
-1.4	551.5	ENSP0000354852	Ryanodine receptor 3
Sample F *– TAPP2 immunoprecipitation (BCR-activated)*			
-3.4	34.1	ENSP0000306771	Tandem PH domain containing protein-2 (TAPP2)
-3.3	47.1	ENSP0000234590	Alpha Enolase
-2.0	110.2	ENSP0000349595	Sarcoplasmic/endoplasmic reticulum calcium ATPase

MAKYGEHEASPDNGQNEFSDIIKSRSDEHNDVQKKTFTKWINARFSKSGKPPINDMFTDLKDGRKLLDLLEGLTGTSLPKERGSTRVHA
LNNVNRVLQVLHQNNVELVNIGGTDIVDGNHKLTLGLLWSIILHWQVKDVMKDVMSDLQQTNSEKILLSWVRQTTRPYSQVNVLNFTTS
WTDGLAFNAVLHRHKPDLFSWDKVVKMSPIERLEHAFSKAQTYLGIEKLLDPEDVAVQLPDKKSIIMYLTSLFEVLPQQVTIDAIREVE
TLPRKYKKECEEEAINIQSTAPEEEHESPRAETPSTVTEVDMDLDSYQIALEEVLTWLLSAEDTFQEQDDISDDVEEVKDQFATHEAFM
MELTAHQSSVGSVLQAGNQLITQGTLSDEEEFEIQEQMTLLNARWEALRVESMDRQSRLHDVLMELQKKQLQQLSAWLTLTEERIQKME
TCPLDDDVKSLQKLLEEHKSLQSDLEAEQVKVNSLTHMVVIVDENSGESATAILEDQLQKLGERWTAVCRWTEERWNRLQEINILWQEL
LEEQCLLKAWLTEKEEALNKVQTSNFKDQKELSVSVRRLAILKEDMEMKRQTLDQLSEIGQDVGQLLDNSKASKKINSDSEELTQRWDS
LVQRLEDSSNQVTQAVAKLGMSQIPQKDLLETVRVREQAITKKSKQELPPPPPPKKRQIHVDIEAKKKFDAISAELLNWILKWKTAIQT
TEIKEYMKMQDTSEMKKKLKALEKEQRERIPRADELNQTGQILVEQMGKEGLPTEEIKNVLEKVSSEWKNVSQHLEDLERKIQLQEDIN
AYFKQLDELEKVIKTKEEWVKHTSISESSRQSLPSLKDSCQRELTNLLGLHPKIEMARASCSALMSQPSAPDFVQRGFDSFLGRYQAVQ
EAVEDRQQHLENELKGQPGHAYLETLKTLKDVLNDSENKAQVSLNVLNDLAKVEKALQEKKTLDEILENQKPALHKLAEETKALEKNVH
PDVEKLYKQEFDDVQGKWNKLKVLVSKDLHLLEEIALTLRAFEADSTVIEKWMDGVKDFLMKQQAAQGDDAGLQRQLDQCSAFVNEIET
IESSLKNMKEIETNLRSGPVAGIKTWVQTRLGDYQTQLEKLSKEIATQKSRLSESQEKAANLKKDLAEMQEWMTQAEEEYLERDFEYKS
PEELESAVEEMKRAKEDVLQKEVRVKILKDNIKLLAAKVPSGGQELTSELNVVLENYQLLCNRIRGKCHTLEEVWSCWIELLHYLDLET
TWLNTLEERMKSTEVLPEKTDAVNEALESLESVLRHPADNRTQIRELGQTLIDGGILDDIISEKLEAFNSRYEDLSHLAESKQISLEKQ
LQVLRETDQMLQVLQESLGELDKQLTTYLTDRIDAFQVPQEAQKIQAEISAHELTLEELRRNMRSQPLTSPESRTARGGSQMDVLQRKL
REVSTKFQLFQKPANFEQRMLDCKRVLDGVKAELHVLDVKDVDPDVIQTHLDKCMKLYKTLSEVKLEVETVIKTGRHIVQKQQTDNPKG
MDEQLTSLKVLYNDLGAQVTEGKQDLERASQLARKMKKEAASLSEWLSATETELVQKSTSEGLLGDLDTEISWAKNVLKDLEKRKADLN
TITESSAALQNLIEGSEPILEERLCVLNAGWSRVRTWTEDWCNTLMNHQNQLEIFDGNVAHISTWLYQAEALLDEIEKKPTSKQEEIVK
RLVSELDDANLQVENVRDQALILMNARGSSSRELVEPKLAELNRNFEKVSQHIKSAKLLIAQEPLYQCLVTTETFETGVPFSDLEKLEN
DIENMLKFVEKHLESSDEDEKMDEESAQIEEVLQRGEEMLHQPMEDNKKEKIRLQLLLLHTRYNKIKAIPIQQRKMGQLASGIRSSLLP
TDYLVEINKILLCMDDVELSLNVPELNTAIYEDFSFQEDSLKNIKDQLDKLGEQIAVIHEKQPDVILEASGPEAIQIRDTLTQLNAKWD
RINRMYSDRKGCFDRAMEEWRQFHCDLNDLTQWITEAEELLVDTCAPGGSLDLEKARIHQQELEVGISSHQPSFAALNRTGDGIVQKLS
QADGSFLKEKLAGLNQRWDAIVAEVKDRQPRLKGESKQVMKYRHQLDEIICWLTKAEHAMQKRSTTELGENLQELRDLTQEMEVHAEKL
KWLNRTELEMLSDKSLSLPERDKISESLRTVNMTWNKICREVPTTLKECIQEPSSVSQTRIAAHPNVQKVVLVSSASDIPVQSHRTSEI
SIPADLDKTITELADWLVLIDQMLKSNIVTVGDVEEINKTVSRMKITKADLEQRHPQLDYVFTLAQNLKNKASSSDMRTAITEKLERVK
NQWDGTQHGVELRQQQLEDMIIDSLQLLEEYGSDDTRNVKETTEYLKTSWINLKQSIADRQNALEAEWRTVQASRRDLENFLKWIQEAE
TTVNVLVDASHRENALQDSILARELKQQMQDIQAEIDAHNDIFKSIDGNRQKMVKALGNSEEATMLQHRLDDMNQRWNDLKAKSASIRA
HLEASAEKWNRLLMSLEELIKWLNMKDEELKKQMPIGGDVPALQLQYDHCKALRRELKEKEYSVLNAVDQARVFLADQPIEAPEEPRRN
LQSKTELTPEERAQKIAKAMRKQSSEVKEKWESLNAVTSNWQKQVDKALEKLRDLQGAMDDLDADMKEAESVRNGWKPVGDLLIDSLQD
HIEKIMAFREEIAPINFKVKTVNDLSSQLSPLDLHPSLKMSRQLDDLNMRWKLLQVSVDDRLKQLQEAHRDFGPSSQHFLSTSVQLPWQ
RSISHNKVPYYINHQTQTTCWDHPKMTELFQSLADLNNVRFSAYRTAIKIRRLQKALCLDLLELSTTNEIFKQHKLNQNDQLLSVPDVI
NCLTTTYDGLEQMHKDLVNVPLCVDMCLNWLLNVYDTGRTGKIRVQSLKIGLMSLSKGLLEEKYRYLFKEVAGPTEMCDQRQLGLLLHD
AIQIPRQLGEVAAFGGSNIEPSVRSCFQQNNNKPEISVKEFIDWMHLEPQSMVWLPVLHRVAAAETAKHQAKCNICKECPIVGFRYRSL
KHFNYDVCQSCFFSGRTAKGHKLHYPMVEYCIPTTSGEDVRDFTKVLKNKFRSKKYFAKHPRLGYLPVQTVLEGDNLETPITLISMWPE
HYDPSQSPQLFHDDTHSRIEQYATRLAQMERTNGSFLTDSSSTTGSVEDEHALIQQYCQTLGGESPVSQPQSPAQILKSVEREERGELE
RIIADLEEEQRNLQVEYEQLKDQHLRRGLPVGSPPESIISPHHTSEDSELIAEAKLLRQHKGRLEARMQILEDHNKQLESQLHRLRQLL
EQPESDSRINGVSPWASPQHSALSYSLDPDASGPQFHQAAGEDLLAPPHDTSTDLTEVMEQIHSTFPSCCPNVPSRPQAM

Figure 28. Identified peptides correspond to utrophin. Amino acid sequence of utrophin showing the fragments (underlined) which identified via peptide fingerprinting by mass spectrometry.

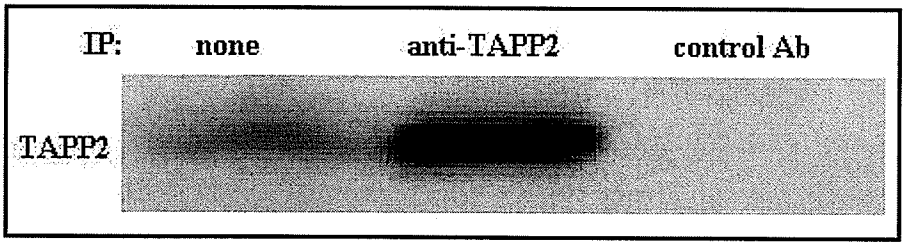

Figure 29. Specificity of anti-TAPP2 antibody in immunoprecipitating TAPP2. Western blot showing TAPP2 is specifically immunoprecipitated by anti-TAPP2 antibody but not the control Ab (polyclonal rabbit IgG). Left lane shows BJAB whole cell lysate as positive control.

g) **Other potential associated proteins of TAPP2.** To determine if utrophin might associate with TAPP2 in another B cell model, I immunoprecipitated TAPP2 from the human B cell line Ramos. I employed silver stain in this experiment due to the low levels of protein in the eluted fractions. Conventional silver stain is the most sensitive method for protein staining but it is usually not recommended for mass spectrometer because the staining procedure can result in formation of covalent bond between peptides thereby generating false mass signal during analysis. Also it has poor proportionality of staining intensity and does not correlate to the actual amount of proteins. This might be overcome by the currently available mass spectrometry compatible silver stain which is suggested to minimized covalent bond formation.

I immunoprecipitated TAPP2 from Ramos B cells in addition to BTF cells. As seen in Figure 30, TAPP2 immunoprecipitation on BTF cells yielded reproducible bands where utrophin was identified previously (as indicated by an arrow) and similar bands were observed on Ramos immunoprecipitates. Although the protein bands on Ramos were less intense due to difference in cell size and quantity of cell used, there are two separate regions that seemed to have specific TAPP2 immunoprecipitated proteins but not on the control immunoprecipitation. Close examination of the gel revealed numerous bands of high molecular weight on Ramos cells which seem to be specific for TAPP2 in addition to a band near 100 kDa. These bands were excised (labeled as B01 to B06 in Figure 30) and subject to the same identification protocol as described previously. The complete result is listed in Appendix III. Unfortunately, sample B01, B02 and B03 did not yield any specific identification other than the common contaminant proteins. This can be due to various reasons. Although proteins

bands are clearly visible, the concentration might not be high enough for mass spectrometer detection since silver stain can detect less than one nano gram of protein. More importantly, the procedure for gel processing is subject to sample loss. Furthermore, the intensity of the band does not correlated to the actual protein concentration because the silver stain signal will continue to develop until it is stopped by applying acetic acid solution. The effect of over-developed signal is apparent in region between 40 to 55 kDa. Regardless, the protein bands labeled B04, B05 and B06 have been identified with a list of potential candidates (Appendix III). Among these candidates, γ-tubulin complex component 2 (GCP-2) and polypyrimidine tract-binding (PTB) protein-associated splicing factor (PSF) appeared to be potential TAPP2 associated protein in Ramos cells.

The sensitivity of silver stain enables us to visualize the effectiveness of our elution method. As seen in Figure 31, the non-specifically immunoprecipitated proteins showed in the bead-bound fractions of the control Ab lane (Figure 30) are absent on the eluted-fraction. On the other hand, the eluted protein bands on Ramos cells are too weak for comparison. To confirm the presence of TAPP2, I cut the bands at the region labeled E1 to E6 for mass spectrometer analysis and identification. These regions are most likely where TAPP2 is located. The result is shown in Appendix IV. The mass spectrometer analysis and database search identified TAPP2 in sample E3 but not E2, whereas actin is found on both samples E5 and E6. This suggested that TAPP2 might also be associated with the cytoskeleton and play a role in actin remodeling.

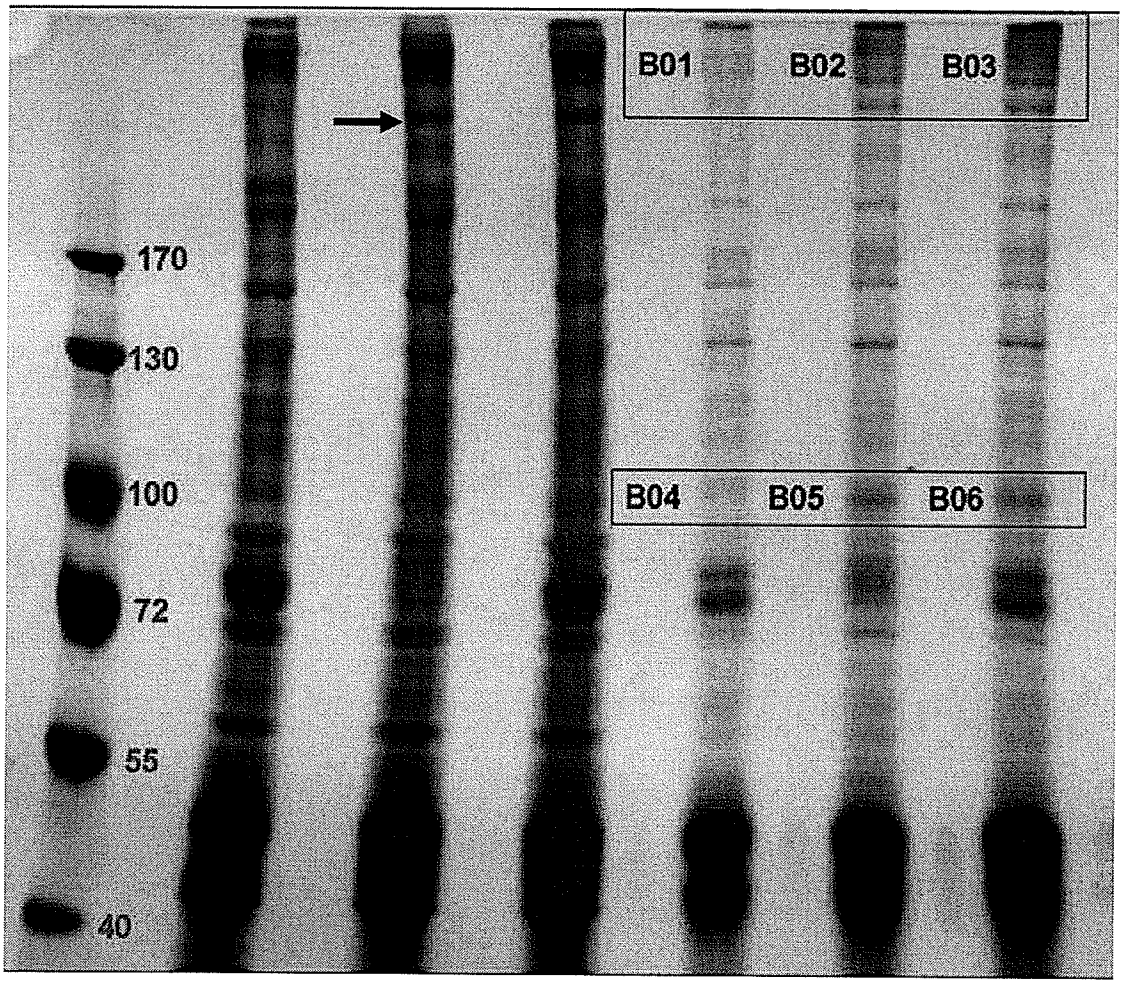

Cells	BTF	BTF	BTF	Ramos	Ramos	Ramos
IP Ab	Control	α-TAPP2	α-TAPP2	Control	α-TAPP2	α-TAPP2
Stimulation	α-IgM	none	α-IgM	α-IgM	none	α-IgM

Figure 30. TAPP2 immunoprecipitation on BTF and Ramos cells. The figure shows the bead-bound fractions of the immunoprecipitates and the labeled regions indicate where the bands were excised for identification. 160 and 180 million BTF and Ramos cells were used respectively for each individual condition. Bottom table shows the description of each lane. Protein bands were visualized with SilverSNAP® stain. Black arrow indicates similar bands were observed as in Figure 19 right panel where utrophin was identified.

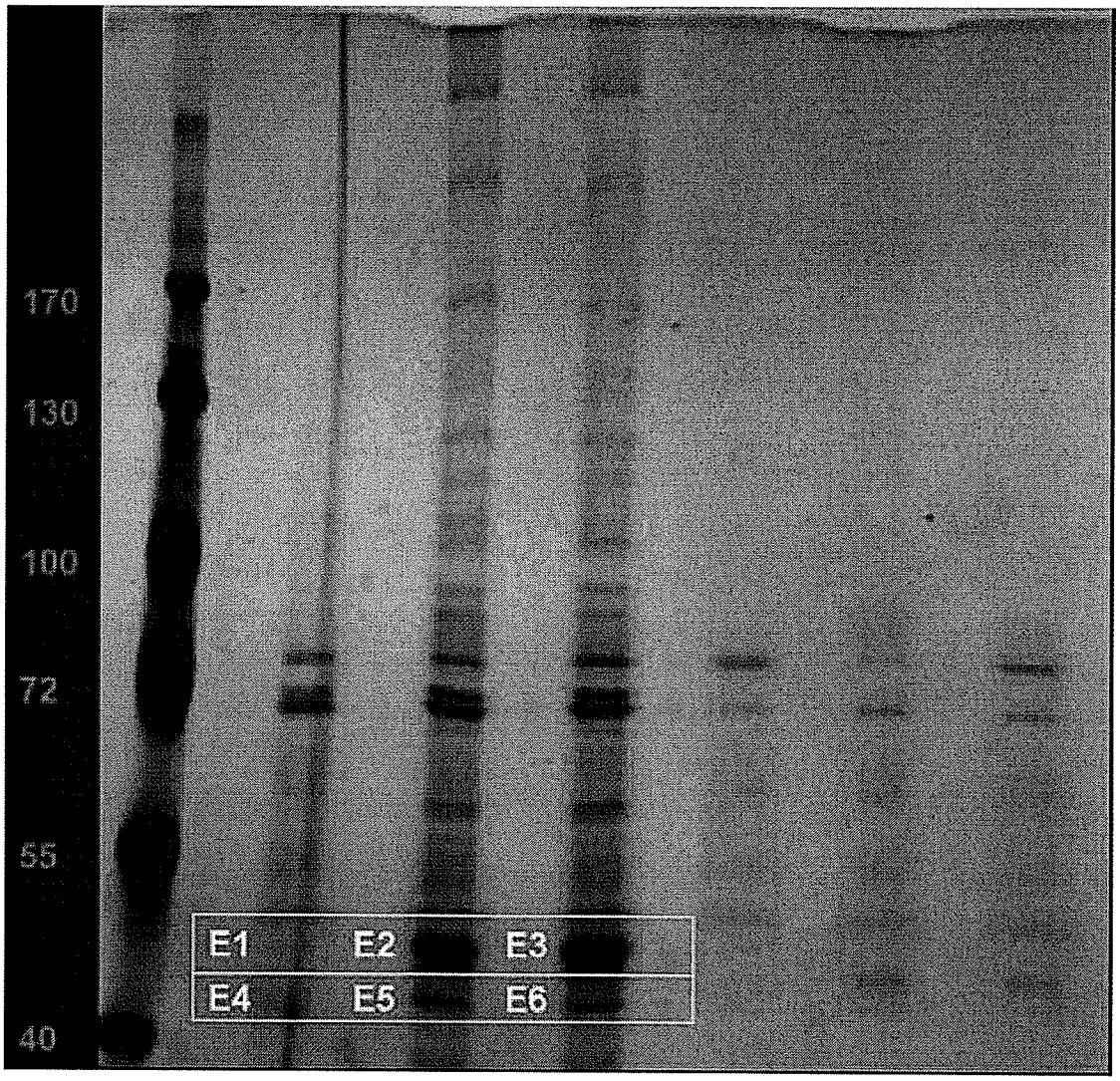

Cells	BTF	BTF	BTF	Ramos	Ramos	Ramos
IP Ab	Control	α-TAPP2	α-TAPP2	Control	α-TAPP2	α-TAPP2
Stimulation	α-IgM	none	α-IgM	α-IgM	none	α-IgM

Figure 31. The corresponding eluted fractions from TAPP2 immunoprecipitation on BTF and Ramos cells. In this SilverSNAP® stained gel, two regions were excised for mass spectrometer identification. The complete list of identification are presented in Appendix IV.

Chapter Discussion

In this section I showed utrophin as a TAPP2 associated protein in human B cells with the highest confidence of identification. This is the very first immunoprecipitation of endogenous TAPP2 associating partner without the use of ectopic expression. Utrophin is a homologue of dystrophin which links the actin cytoskeleton to the β-dystroglycan complex in the plasma membrane. It is ubiquitously expressed and currently very little is known in regarding to its role in lymphocyte activation. [156]

The identification of utrophin was derived from the bead-bound fractions of BTF cells. Although we failed to identify utrophin in Ramos cell due to low protein concentration, further scale up is necessary to overcome such problem. In the course of optimizing the condition for TAPP2 elution, I determined that optimal elution is near neutral pH. Although I can incubate the immunoprecipitates for longer times in the hope of releasing more TAPP2 complexes from the antibody, it is not practical as we do not know the dissociation kinetics of other non-specifically bounded proteins. The ideal condition is to elute maximal amount of TAPP2 while reducing the non-specific protein release from beads. As seen in most cases, reducing non-specific protein precipitation is a common challenge for immunoprecipitation. However, the efficiency of my elution method in reducing non-specific background bands became apparent when using silver stain as seen in Figure 31. In this gel, there are many protein bands which seemed to be TAPP2 specific, but we know that the silver stain procedure can bias the actual quantity of the protein, which may reach below the general detection limit of the mass spectrometer as seen in sample B01 to B03. Therefore, the likelihood of detecting proteins in these bands with high confident is small. Silver stain will not give consistent

result unless a known amount of proteins are used as the control for comparison. On the other hand, although the GelCode blue stained gel did not yield high resolved bands as silver stain on the eluted fractions; a faint band was visible and identified to contain TAPP2. Therefore, among the three different staining methods, GelCode Blue stain provides good sensitivity and seem to set the lower limit for MS detection for my application.

Although my results showed that utrophin immunoprecipitated with TAPP2, the nature of association is currently unknown. Utrophin is a homologue of dystrophin and they both known to bind syntrophins through their syntrophin binding sequence. [156] Since syntrophins contain PDZ domains, I speculate TAPP2 might interact with syntrophins via its PDZ-B domain, similar to TAPP1, and this association can link TAPP2 indirectly to utrophin in B cells. Such speculation can be easily tested by immunoprecipitation using BTM cells or BJAB expressing TAPP2-mPDZ. But currently there is no data showing which syntrophin isoforms are expressed in B cells. I do not exclude the possibility that TAPP2 can associate with utrophin via other forms of interactions, either directly or indirectly. As seen in Figure 31, there are many more candidate proteins visible in the TAPP2 immunoprecipitates than in the control. In addition, so far there is no apparent difference between activated and non-activated TAPP2 immunoprecipitates. But I do not exclude the possibility that there is small quantitatively difference between activated and non-activated cells beyond my detection limit. Regardless, further scale-up immunoprecipitation is necessary in identifying more candidates to elucidate TAPP2 signaling complex. Any additional identified proteins can be validated by reverse immunoprecipitation to detect the presence of TAPP2.

Chapter Summary

In this section, I have generated BJAB clones expressing various forms of TAPP2 and characterized their surface IgM expression. I have tested and confirmed the ability of anti-TAPP2 antibody in immunoprecipitating endogenous TAPP2. I have also established the condition to elute TAPP2 from anti-TAPP2 antibody by epitope peptide competitive binding assay and my result showed optimal release is near neutral pH. I have identified utrophin as one of the TAPP2 associated protein with highest confident of identification. Although the nature of the association is unknown, this opens up a new area of research as very little is known about the function of utrophin in lymphocyte activation and immune regulation.

THESIS DISCUSSION AND IMPLICATION

My methodology simulates the effect of exogenous superoxide in B cells at the site of infection, where BCR are being cross-linked by antigen and superoxide are being produced by inflammatory cells. Here I showed hydrogen peroxide triggers recruitment of PI(3,4)P2-binding protein but not PI(3,4,5)P3-binding protein. I also showed that hydrogen peroxide synergizes with BCR signaling in PI3K-dependent recruitment of PH-domain adaptor proteins. In addition, I showed that utrophin is associated with TAPP2 *in vivo* immunoprecipitation. Our results shed light on the biological function of TAPP2 in B cell activation and I will discuss the possible role of TAPP2 in the context of immune cell function.

PI(3,4)P2 can be generated by phosphorylation of PI(3)P by PI4K, phosphorylation of PI(4)P by PI3K, or dephosphorylation of PI(3,4,5)P3 by SHIP. [124, 157] Under negative regulation, PI(3,4)P2 is dephosphorylated by PTEN or type 1α inositol polyphosphate 4-phosphatase back to PI(4)P or PI(3)P respectively (Figure 32). [123, 158] Whereas PTEN knockout mice are embryonic lethal and show high incident of tumor, SHIP knockouts are viable with no obvious increase on rates of cancer development. [127] This suggested that PI(3,4,5)P3 alone cannot account for the malignant transformation in these mice and implicated that PI(3,4)P2 also play a role. This is demonstrated in studies on Akt, a well recognized survival element in PI3K signaling. Akt has a PH domain which binds to both PI(3,4,5)P3 and PI(3,4)P2 and it has been shown that PI(3,4)P2 is necessary to regulate Akt activity. [107, 118] Furthermore, phosphatidylinositol 4-phosphatase has recently been described as tumor suppressor in malignant cells. [159] These results collectively suggest that the PI(3,4)P2 pathway is

also significant in cell survival and transformation. My results showed low level of H_2O_2 can selectively recruit PI(3,4)P2 binding proteins but not PIP3 binding proteins. This suggested that a connection may exist between low level of oxidant and activation of cell survival pathway, which is likely to involve PI(3,4)P2. Although an association between oxidant and cancer is abundantly described in the literature, the underlying mechanism is largely unknown. Such a connection is implicated by studies involving $gp91^{phox}$ transgenic and Prx II knockout mice. [56, 57, 82]

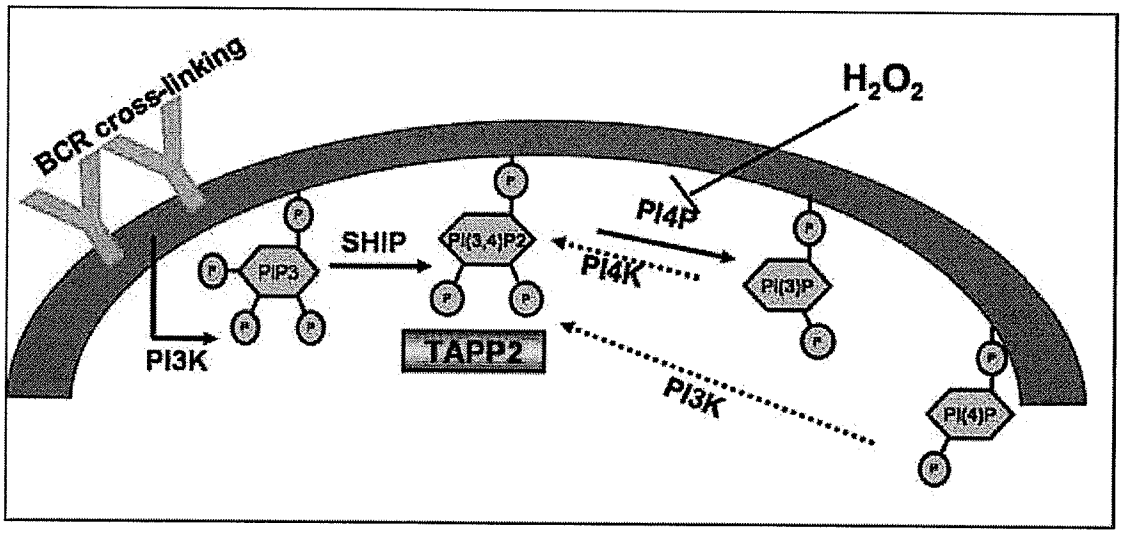

Figure 32. Model of TAPP2 recruitment in BJAB cell upon peroxide stimulation. Unlike PI(4,5)P2, PI(3)P and PI(4)P are present at low level in quiescent cells. Therefore, PI(3)P and PI(4)P are unlikely to contribute the rapid increase of PI(3,4)P2 upon BCR activation. On the other hand, it has been showed that PI4P can breakdown PI(3,4)P2 to generate and contribute PI(3)P pool. Although it has not been directly demonstrated, oxidative inhibition of PI4P might leads to increase of PI(3,4)P2 through SHIP.

Utrophin is a component of the dystrophin glycoprotein complex (DGC) which is involved in brain development, synapse formation and plasticity, as well as water and ion homeostasis. [160] Although it is ubiquitously expressed, its function in B lymphocytes remains unexplored. Dystrophin, a close homologue of utrophin, was identified as the gene commonly mutated in Ducheene muscular dystrophy (DMD). Dystrophin plays a major role in postsynaptic membrane differentiation at the neuromuscular junction. In this regard, Utrophin has been viewed as an excellent candidate to replace dystrophin and to treat DMD. [161] Due to the major function of utrophin in neuromuscular junction, it is tempting to speculate a possible involvement of utrophin in immune synapse formation or development. While a direct connection between utrophin and immune synapse has not been demonstrated, there is strong evidence for utrophin in mediating cell-to-cell contact. [162, 163] Utrophin expression can be up-regulated by calcineurin, heregulin, nitric oxide, IL-6 and the GTPase RhoA. [164-168] It has been shown that upregulation by RhoA is correlated with enhanced utrophin membrane association. [169]

TAPP1 and TAPP2 are the only known proteins which specifically bind to PI(3,4)P2 with high affinity. [98] The PI(3,4)P2 effector signaling pathway in B cells upon PI3K activation remains undefined. Furthermore, the role of utrophin in lymphocyte function is currently unknown. Here I show the very first evidence that utrophin plays a role in PI3K pathway in B cell. My data shows that TAPP2 is constitutively associated with utrophin. (Figure 19) Whether the association is up- or down-regulated at the membrane after BCR cross-linking remains unknown. As mentioned above, TAPP1 has been shown associated with syntrophin. Therefore it is very likely for TAPP2 to associate with utrophin through interaction with syntrophin via its PDZ domain. While we can

provide a reasonable link between TAPP2 PDZ-B domain and utrophin, the function of TAPP2 at the N-terminal is entirely unknown. Interestingly, although the N-terminal PH domain does not bind to any lipid tested, other PH domains have been shown to regulate GTPase. [99] Thus one possibility is that TAPP2 can regulate GTPase through its N-terminal PH domain at the plasma membrane (Figure 33).

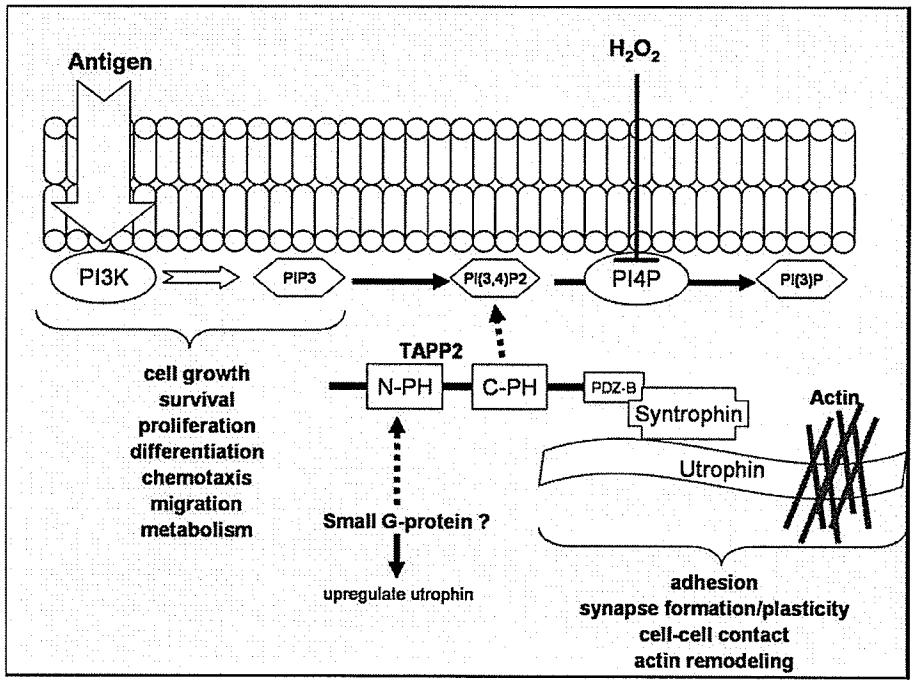

Figure 33. The role of TAPP2 in PI3K signaling. Diagram depicts the potential links between TAPP2 and its downstream signaling targets. Although PIP3 is the most studied regarding to PI3K signaling, PI(3,4)P2 might share a role in some of the signaling outcomes described above. Interaction between utrophin and actin implicates a role of TAPP2 in cytoskeleton remodeling processes such as adhesion and lymphocyte homing. Although it has not been tested, the N-PH domain of TAPP2 might associate with small G-protein which has been showed to upregulate utrophin.

TAPP2 is likely to function as an adaptor molecule which links BCR signaling to cytoskeleton remodeling. In terms of biological function, TAPP2 likely regulates B lymphocyte migration to the site of inflammation. It has been show that integrin signaling can mediate PI(3,4)P2 synthesis in other systems. [170] In addition, ROS has been shown to be required for lymphocyte trans-endothelial migration. [171] I have showed that TAPP2 responds to ROS and binds to PI(3,4)P2 produced on the membrane and utrophin is constitutively associate with TAPP2. To fit my data into the current model of immune response, I speculate that further generation of PI(3,4)P2 in inflammatory sites will allow TAPP2 to accumulate at the junction between B cell and endothelial cell where lymphocyte trans-endothelial migration occur. In the mean time, the cytoskeleton remodeling occurs and utrophin will play a role in synapse formation and/or stabilization. This form of cell contact is distinct from immune synapse formation, since various studies have suggested that the composition and property of cell junction is very diverse. [172] In addition, TAPP2 might not likely to play a role in immune synapse formation since it has been showed that PI(3,4)P2 is not found in immune synapse on T cell side. [173] This does not exclude the possibility that TAPP2 might recruited to the plasma membrane via other forms of protein interaction. Although it has not been directly demonstrate.

While this thesis was being written, our laboratory has generated preliminary data from various TAPP2 expressing mutants which I made during the years of my study. Briefly, BJAB cells over-expressing full length wild-type TAPP2 show enhance adhesion phenotype, while the mutant TAPP2 shows reduced adhesion compared to the wild-type BJAB cells. My data can could be a potential link between PI(3,4)P2, 5-phosphatase,

integrin, ROS, and utrophin in an uncharacterized pathway which plays a role in cell-to-cell and/or cell-matrix contact. TAPP2 may be an important link between the extracellular signals to the downstream effectors of cell adhesion. Elucidating the function of TAPP2 is biologically important since our understanding of PI3K signaling in PI(3,4)P2 pathway is still at infancy.

Future Direction

TAPP2 associating proteins - It would be important to further confirm the association between utrophin and TAPP2 through complementary immunoprecipitation. Also, although it has not been identified with great confidence, it is likely that TAPP2 can associate with other candidate proteins (Figure 31). Further scale up immunoprecipitation in various B cell lines would be a logical approach. Any identified TAPP2-specific associated proteins would be confirmed by western blotting through complementary immunoprecipitation.

Nature of molecular association – Whether the PDZ-B region of TAPP2 is involved in utrophin association can be tested by using myc-TAPP2 expressing cells (Figure 23). As this region is blocked by myc-epitope, it can be immunoprecipitated by anti-myc antibody without immunoprecipitating endogenous TAPP2 (Figure 18). Ideally, BJAB cells expressing a vector encoding myc-epitope at the N-terminal end of TAPP2-mPDZ should be use for this purpose. Also, whether the association is quantitatively dependent on the nature of stimuli would be important to test. Since I have shown that superoxide can synergize TAPP2 membrane recruitment, it would be interesting to see if this correlates with the quantity of utrophin association or if the association is being distinctively regulated due to the nature of stimuli.

Co-localization experiment - Regarding the cellular distribution of TAPP2 with respect to utrophin, it would be interesting to see if TAPP2 co-localize with utrophin before and after BCR and/or H_2O_2 stimulation. This can be done by intracellular staining with our anti-TAPP2 antibody and the commercially available anti-utrophin antibody. Other

potential candidate proteins can be tested in similar way as long as the antibody is available.

Functional analyses – This can be done by various stable transfectants which I have generated on both BJAB and A20 cells (Appendix I, V-VIII and Figure 22). With the gain-of-function (on BJAB) and lost-of-function mutants (both A20 and BJAB), we can test cell survival in response to H_2O_2, chemotaxis, adhesion, NFkB activation, and downstream signaling of PI3K such as Akt and MAPK phosphorylation. These results will give us valuable insight on the biological functions of TAPP2 as effector of PI(3,4)P2 in overall PI3K signaling.

APPENDIXIES

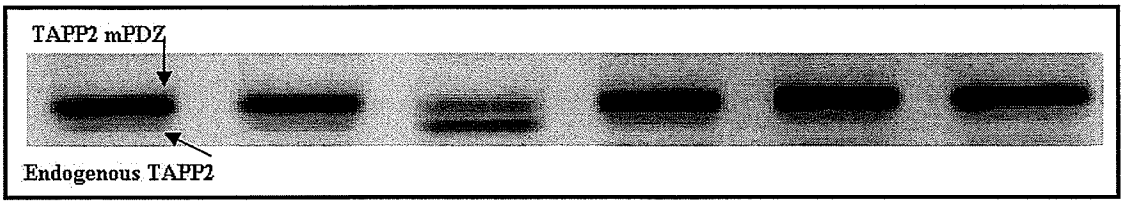

I. Quantitative expression of TAPP2-mPDZ pcDNA3.0 in BJAB cells. Western blot showing BJAB cells transfected with TAPP2-mPDZ pcDNA3.0. Note that all clones are positive in expressing TAPP2-mPDZ. The clones in lane 3 express the least amount of TAPP2-mPDZ while the expression level of the remaining clones is similar.

II. Identified candidate proteins in selected protein bands from TAPP2 immunoprecipitation on BTF cells. The following list labeled A to D represents the bands cut from various region of the gel showed in Figure 27.

Sample A			
Log(e)$^+$	**MW**	**Accession**	**Description**
-104.7	468.7	ENSP00000313420	DNS-dependent protein kinase catalytic subunit
-31.1	66.0	ENSP00000252244	Keratin, type II cytoskeletal 1
-28.0	8.8	gi|999627|	Porcine E-Trypsin
-22.7	228.3	ENSP00000327077	Pericentriolar material 1
-18.6	277.0	ENSP00000297183	Eukaryotic translation initiation factor 4E binding protein 3
-10.8	62.0	ENSP00000246662	Keratin, type I cytoskeletal 9
-9.8	219.8	ENSP00000324463	Nuclear protein ZAP3
-9.2	242.8	ENSP00000369435	Predicted: member of CAD enzyme
-7.3	191.5	ENSP00000269122	Clathrin heavy chain 1
-3.8	42.0	ENSP00000306469	Predicted: actin-like protein
-3.7	18.0	ENSP00000272317	40S ribosomal protein S27a
-3.7	45.9	ENSP00000349435	60S ribosomal protein L3
-3.2	135.5	ENSP00000305790	Splicing factor 3B subunit 3
-2.2	50.4	ENSP00000217182	Elongation factor 1-alpha 2
-2.0	36.0	ENSP00000369245	Immunoglobulin gamma-4 chain constant region
-1.9	228.7	ENSP00000277536	No description
-1.4	532.0	ENSP00000351750	Dynein heavy chain, cytosolic
-1.2	39.9	ENSP00000188376	Phosphate carrier protein, mitochondrial precursor
-1.2	36.3	ENSP00000244295	No description
Sample B			
Log(e)$^+$	**MW**	**Accession**	**Description**
-356.3	394.2	ENSP00000356515	Utrophin
-78.4	468.7	ENSP00000313420	DNA-dependent protein kinase catalytic subunit
-38.1	66.0	ENSP00000252244	Keratin, type II cytoskeletal 1
-35.2	62.0	ENSP00000246662	Keratin, type I cytoskeletal 9
-28.5	8.8	gi|999627|	Porcine E-Trypsin
-12.4	60.0	ENSP0000369317	No description
-11.2	242.8	ENSP0000369435	No description
-6.0	35.9	ENSP0000369242	No description
-5.0	58.8	ENSP0000269576	Keratin, type 1 cytoskeletal 10
-4.4	228.3	ENSP00000327077	Pericentriolar material 1
-3.6	532.0	ENSP00000351750	Dynein heavy chain, cytosolic
-3.2	18.0	ENSP00000272317	40S ribosomal protein S27a
-2.7	50.4	ENSP00000217182	Elongation factor 1-alpha 2
-2.2	135.5	ENSP00000305790	Splicing factor 3B subunit 3
-2.2	346.7	ENSP00000339299	Triple functional domain protein
-2.1	191.5	ENSP00000269122	Clathrin heavy chain 1
-1.8	100.8	ENSP00000357031	No description
-1.6	277.0	ENSP00000297183	Eukaryotic translation initiation factor 4E binding protein 3
-1.4	55.1	ENSP00000322453	Predicted: similar to ring finger protein 129
-1.2	228.7	ENSP00000277536	No description
-1.1	856.8	ENSP00000354508	Bullous pemphigoid antigen 1 isoforms 1/2/3/4/5/8

Sample C			
Log(e)$^+$	**MW**	**Accession**	**Description**
-457.6	394.2	ENSP00000356515	Utrophin
-79.2	468.7	ENSP00000313420	DNA-dependent protein kinase catalytic subunit
-29.1	277.0	ENSP00000297183	Eukaryotic translation initiation factor 4E binding protein 3
-27.5	66.0	ENSP00000252244	Keratin, type II cytoskeletal 1
-21.1	8.8	gi|999627|	Porcine E-Trypsin
-11.4	242.8	ENSP00000369435	No description
-5.6	62.0	ENSP00000246662	Keratin, type I cytoskeletal 9
-5.3	228.3	ENSP00000327077	Pericentriolar material 1
-3.3	135.5	ENSP00000305790	Splicing factor 3B subunit 3
-3.3	426.5	ENSP00000354923	Dystrophin
-2.3	228.7	ENSP00000277536	No description
-1.6	18.5	ENSP00000287144	Predicted: similar to 60S ribosomal protein L29
-1.5	59.5	ENSP00000252245	Cytokeratin type II
-1.2	532.0	ENSP00000351750	Dynein heavy chain, cytosolic
-1.2	44.7	ENSP00000315137	Sphingosine-1-phosphate phosphatase 2
Sample D			
Log(e)$^+$	**MW**	**Accession**	**Description**
-59.7	394.2	ENSP00000356515	Utrophin
-13.9	66.0	ENSP00000252244	Keratin, type II cytoskeletal 1
-3.4	73.5	ENSP00000308972	No description
-1.8	8.8	gi|999627|	Porcine E-Trypsin
-1.1	628.7	ENSP00000367263	No description
Sample E			
Log(e)$^+$	**MW**	**Accession**	**Description**
-26.5	66.0	ENSP00000252244	Keratin, type II cytoskeletal 1
-24.7	38.6	ENSP00000350456	No description
-18.5	35.9	ENSP00000361626	No description
-17.0	62.0	ENSP00000246662	Keratin, type I cytoskeletal 9
-14.8	50.1	ENSP0000339063	No description
-12.7	8.8	gi|999627|	Porcine E-Trypsin
-11.6	34.1	ENSP0000306771	Tandem PH domain containing protein-2
-11.5	47.1	ENSP0000234590	Alpha Enolase
-10.1	38.4	ENSP0000313199	Heterogeneous nuclear ribonucleoprotein D0
-9.0	51.2	ENSP0000327539	Heterogeneous nuclear ribonucleoprotein H
-8.0	46.4	ENSP0000326381	Eukaryotic initiation factor 4A-II
-7.7	43.8	ENSP0000302886	Proliferation-associated protein 2G4
-2.1	59.5	ENSP0000252245	Cytokeratin type II
-1.8	143.0	ENSP0000369302	No description
-1.4	551.5	ENSP0000354852	Ryanodine receptor 3
Sample F			
Log(e)$^+$	**MW**	**Accession**	**Description**
-21.1	38.6	ENSP0000350456	No description
-3.4	34.1	ENSP0000306771	Tandem PH domain containing protein-2
-3.3	47.1	ENSP0000234590	Alpha Enolase
-2.0	110.2	ENSP0000349595	Sarcoplasmic/endoplasmic reticulum calcium ATPase
-1.5	53.2	ENSP0000360327	No description
-1.3	82.3	ENSP0000316983	No description
-1.2	19.5	ENSP0000366414	No description
-1.1	49.9	ENSP0000369784	No description

III. Identified candidate proteins in selected protein bands (bead-bound) from TAPP2 immunoprecipitation on Ramos cells.

Sample B01			
Log(e)$^+$	**MW**	**Accession**	**Description**
-18.0	66.0	ENSP00000252244	Keratin, type II cytoskeletal 1
-7.9	8.8	gi|999627|	Porcine E-Trypsin
-1.4	531.8	ENSP00000261887	Guanine nucleotide exchange factor p532
Sample B02			
-24.0	66.0	ENSP00000252244	Keratin, type II cytoskeletal 1
-18.7	8.8	gi|999627|	Porcine E-Trypsin
-1.8	160.7	ENSP00000344446	No description
Sample B03			
-11.9	66.0	ENSP00000252244	Keratin, type II cytoskeletal 1
-11.7	8.8	gi|999627|	Porcine E-Trypsin
-8..8	62.0	ENSP00000246662	Keratin, type 1 cytoskeletal 9
-1.3	152.9	ENSP00000371308	No description
Sample B04			
-8.0	8.8	gi|999627|	Porcine E-Trypsin
-5.6	66.0	ENSP00000252244	Keratin, type II cytoskeletal 1
-1.2	96.8	ENSP00000263798	Tyrosine-protein kinase receptor TYRO3 precursor
-1.1	127.0	ENSP00000288235	Myosin Ie
Sample B05			
-10.6	76.1	ENSP00000349748	PTB-associated splicing factor (PSF)
-8.3	8.8	gi|999627|	Porcine E-Trypsin
-3.4	102.5	ENSP00000252936	Gamma-tubulin complex component 2
-1.3	242.8	ENSP00000369435	No description
-1.1	22.8	ENSP00000357564	No description
Sample B06			
-16.1	66.0	ENSP00000252244	Keratin, type II cytoskeletal 1
-11.1	76.1	ENSP00000349748	PTB-associated splicing factor (PSF)
-10.4	62.0	ENSP00000246662	Keratin, type 1 cytoskeletal 9
-9.1	103.5	ENSP00000364832	No description
-8.6	102.5	ENSP00000252936	Gamma-tubulin complex component 2
-7.2	8.8	gi|999627|	Porcine E-Trypsin
-3.5	60.0	ENSP00000252252	Keratin, type II cytoskeletal 6F
-1.5	37.6	ENSP00000342749	Mesoderm specific transcript isoform a
-1.4	60.1	ENSP00000266534	No description

IV. Identified candidate proteins in selected protein bands (eluted fractions) from TAPP2 immunoprecipitation on BTF cells.

Sample E1			
Log(e)$^+$	**MW**	**Accession**	**Description**
-44.3	62.0	ENSP00000246662	Keratin, type 1 cytoskeletal 9
-14.2	8.8	gi|999627|	Porcine E-Trypsin
-8.8	66.0	ENSP00000252244	Keratin, type II cytoskeletal 1
-2.6	156.3	ENSP00000339381	Regulator of G-protein signaling 12
-1.5	120.2	ENSP00000351113	No description
Sample E2			
-12.2	8.8	gi|999627|	Porcine E-Trypsin
-11.1	66.0	ENSP00000252244	Keratin, type II cytoskeletal 1
-4.3	35.9	ENSP00000361626	No description
-3.4	62.0	ENSP00000246662	Keratin, type 1 cytoskeletal 9
-1.6	60.5	ENSP00000243639	No description
Sample E3			
-39.8	62.0	ENSP00000246662	Keratin, type 1 cytoskeletal 9
-21.5	8.8	gi|999627|	Porcine E-Trypsin
-13.0	66.0	ENSP00000252244	Keratin, type II cytoskeletal 1
-7.3	34.1	ENSP00000306771	Tandem PH domain-containing protein-2
-3.6	35.9	ENSP00000361626	No description
-3.0	50.4	ENSP00000217182	Elongation factor 1-alpha 2
-1.1	48.8	ENSP00000345649	No description
Sample E4			
-10.1	62.0	ENSP00000246662	Keratin, type 1 cytoskeletal 9
-7.4	66.0	ENSP00000252244	Keratin, type II cytoskeletal 1
-3.4	8.8	gi|999627|	Porcine E-Trypsin
-1.7	160.2	ENSP00000312671	No description
Sample E5			
-8.9	8.8	gi|999627|	Porcine E-Trypsin
-2.5	42.0	ENSP00000224784	Alpha-actin 2
-1.1	44.6	ENSP00000289350	No description
Sample E6			
-8.8	41.7	ENSP00000349960	Beta-actin
-7.0	8.8	gi|999627|	Porcine E-Trypsin
-2.0	101.1	ENSP00000372443	No description
-1.1	38.4	ENSP00000332504	C-C chemokine receptor type 10

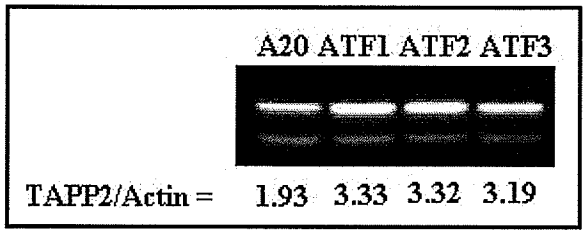

V. A20 cells expressing TAPP2 full length pcDNA3.0 (ATF). Western blot showing A20 cells stably transfected with TAPP2 full length pcDNA3.0. A20 whole cell lysate is shown on the left as control. Top bands are TAPP2 whereas bottom bands are actin. The ratio of TAPP2 over actin is shown. ATF1 and ATF2 have similar expression whereas ATF3 has the lowest among the positive clones.

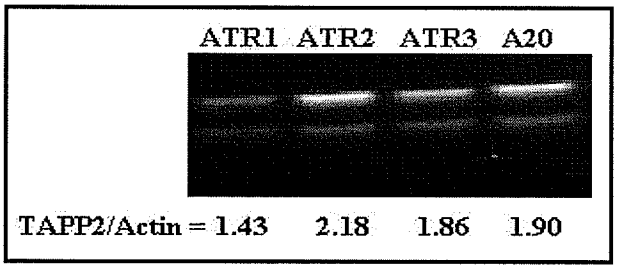

VI. A20 cells expressing TAPP2 full length R218L pcDNA3.0 (ATR). Western blot showing A20 cells stably transfected with TAPP2 PH mutant on pcDNA3.0 vector. This mutant cannot target TAPP2 to the membrane due to mutation in PH domain. A20 whole cell lysate is shown on the right as control. ATR2 has highest expression followed by ATR3 and ATR1.

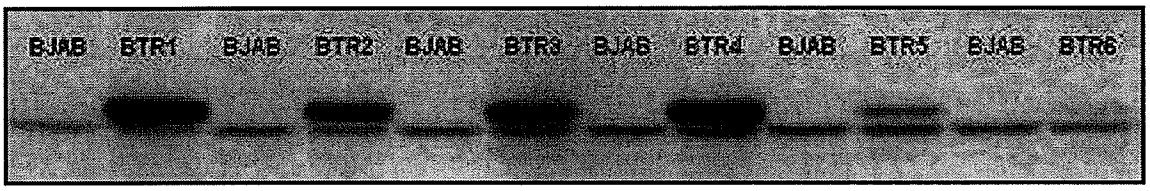

VII. BJAB cells expressing TAPP2 full length R218L pcDNA3.0 (BTR). Western blot showing BJAB cells stably transfected with TAPP2 PH mutant on pcDNA3.0 vector. Clone BTR1 and BTR4 has similar expression followed by BTR3, BTR2 then BTR5. BTR6 clone being the least over-expressed.

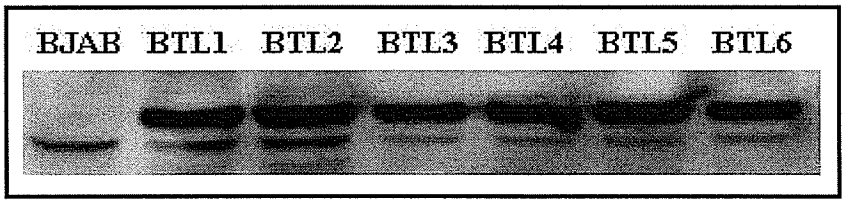

VIII. BJAB cell expressing membrane targeting TAPP2 on pcDNA3.1 (BTL). Western blot showing BJAB clones stably transfected with TAPP2 with human lyn inserted at the N-terminal. This vector will not express myc-epitope since the stop codon is present before myc translation. This form of TAPP2 is constitutively targeted on the plasma membrane. According to signal counting and repeated blots, the order of expression is as follows: BTL1>BTL3>BTL4>BTL6>BTL5.

REFERENCES

1. Bokoch, G.M. and U.G. Knaus, *NADPH oxidases: not just for leukocytes anymore!* Trends Biochem Sci, 2003. **28**(9): p. 502-8.
2. Szanto, I., et al., *Expression of NOX1, a superoxide-generating NADPH oxidase, in colon cancer and inflammatory bowel disease.* J Pathol, 2005. **207**(2): p. 164-76.
3. Banfi, B., et al., *A Ca(2+)-activated NADPH oxidase in testis, spleen, and lymph nodes.* J Biol Chem, 2001. **276**(40): p. 37594-601.
4. Heidari, Y., A.M. Shah, and C. Gove, *NOX-2S is a new member of the NOX family of NADPH oxidases.* Gene, 2004. **335**: p. 133-40.
5. Woo, C.H., et al., *Involvement of cytosolic phospholipase A2, and the subsequent release of arachidonic acid, in signalling by rac for the generation of intracellular reactive oxygen species in rat-2 fibroblasts.* Biochem J, 2000. **348 Pt 3**: p. 525-30.
6. Woo, C.H., et al., *Leukotriene B(4) stimulates Rac-ERK cascade to generate reactive oxygen species that mediates chemotaxis.* J Biol Chem, 2002. **277**(10): p. 8572-8.
7. Ha, Y.J. and J.R. Lee, *Role of TNF receptor-associated factor 3 in the CD40 signaling by production of reactive oxygen species through association with p40phox, a cytosolic subunit of nicotinamide adenine dinucleotide phosphate oxidase.* J Immunol, 2004. **172**(1): p. 231-9.
8. Boveris, A. and B. Chance, *The mitochondrial generation of hydrogen peroxide. General properties and effect of hyperbaric oxygen.* Biochem J, 1973. **134**(3): p. 707-16.
9. Chance, B., H. Sies, and A. Boveris, *Hydroperoxide metabolism in mammalian organs.* Physiol Rev, 1979. **59**(3): p. 527-605.
10. Szeto, H.H., *Mitochondria-targeted peptide antioxidants: novel neuroprotective agents.* Aaps J, 2006. **8**(3): p. E521-31.
11. Reth, M., *Hydrogen peroxide as second messenger in lymphocyte activation.* Nat Immunol, 2002. **3**(12): p. 1129-34.
12. Genova, M.L., et al., *Mitochondrial production of oxygen radical species and the role of Coenzyme Q as an antioxidant.* Exp Biol Med (Maywood), 2003. **228**(5): p. 506-13.
13. Kamiguti, A.S., et al., *Expression and activity of NOX5 in the circulating malignant B cells of hairy cell leukemia.* J Immunol, 2005. **175**(12): p. 8424-30.
14. Dusi, S., et al., *Nicotinamide-adenine dinucleotide phosphate oxidase assembly and activation in EBV-transformed B lymphoblastoid cell lines of normal and chronic granulomatous disease patients.* J Immunol, 1998. **161**(9): p. 4968-74.
15. Jones, O.T.G. and J.D. Wood, *Oxidant Production by Human B Lymphocytes: Detection of Activity and Identification of Components Involved.* Methods, 1996. **9**(3): p. 619-27.
16. Vignais, P.V., *The superoxide-generating NADPH oxidase: structural aspects and activation mechanism.* Cell Mol Life Sci, 2002. **59**(9): p. 1428-59.
17. Babior, B.M., *NADPH oxidase.* Curr Opin Immunol, 2004. **16**(1): p. 42-7.

18. Moncada, S., R.M. Palmer, and E.A. Higgs, *Nitric oxide: physiology, pathophysiology, and pharmacology.* Pharmacol Rev, 1991. **43**(2): p. 109-42.
19. Fukumura, D., S. Kashiwagi, and R.K. Jain, *The role of nitric oxide in tumour progression.* Nat Rev Cancer, 2006. **6**(7): p. 521-34.
20. Beckman, J.S., et al., *Apparent hydroxyl radical production by peroxynitrite: implications for endothelial injury from nitric oxide and superoxide.* Proc Natl Acad Sci U S A, 1990. **87**(4): p. 1620-4.
21. Hancock, J.T., L.M. Henderson, and O.T. Jones, *Superoxide generation by EBV-transformed B lymphocytes. Activation by IL-1 beta, TNF-alpha and receptor independent stimuli.* Immunology, 1990. **71**(2): p. 213-7.
22. Suzuki, Y. and Y. Ono, *Involvement of reactive oxygen species produced via NADPH oxidase in tyrosine phosphorylation in human B- and T-lineage lymphoid cells.* Biochem Biophys Res Commun, 1999. **255**(2): p. 262-7.
23. Lee, J.R. and G.A. Koretzky, *Production of reactive oxygen intermediates following CD40 ligation correlates with c-Jun N-terminal kinase activation and IL-6 secretion in murine B lymphocytes.* Eur J Immunol, 1998. **28**(12): p. 4188-97.
24. Singh, D.K., et al., *The strength of receptor signaling is centrally controlled through a cooperative loop between Ca2+ and an oxidant signal.* Cell, 2005. **121**(2): p. 281-93.
25. Orie, N.N., W. Zidek, and M. Tepel, *Tyrosine and calcium/calmodulin kinases are common signaling components in the generation of reactive oxygen species in human lymphocytes.* Life Sci, 1999. **65**(20): p. 2135-42.
26. Mizuki, K., et al., *Functional modules and expression of mouse p40(phox) and p67(phox), SH3-domain-containing proteins involved in the phagocyte NADPH oxidase complex.* Eur J Biochem, 1998. **251**(3): p. 573-82.
27. Porter, C.D., et al., *p22-phox-deficient chronic granulomatous disease: reconstitution by retrovirus-mediated expression and identification of a biosynthetic intermediate of gp91-phox.* Blood, 1994. **84**(8): p. 2767-75.
28. Dorseuil, O., et al., *Inhibition of superoxide production in B lymphocytes by rac antisense oligonucleotides.* J Biol Chem, 1992. **267**(29): p. 20540-2.
29. Lopes, L.R., et al., *Phosphorylated p40PHOX as a negative regulator of NADPH oxidase.* Biochemistry, 2004. **43**(12): p. 3723-30.
30. Benna, J.E., et al., *Phosphorylation of the respiratory burst oxidase subunit p67(phox) during human neutrophil activation. Regulation by protein kinase C-dependent and independent pathways.* J Biol Chem, 1997. **272**(27): p. 17204-8.
31. Dang, P.M., et al., *Phosphorylation of the NADPH oxidase component p67(PHOX) by ERK2 and P38MAPK: selectivity of phosphorylated sites and existence of an intramolecular regulatory domain in the tetratricopeptide-rich region.* Biochemistry, 2003. **42**(15): p. 4520-6.
32. Park, H.S., et al., *Phosphorylation of the leucocyte NADPH oxidase subunit p47(phox) by casein kinase 2: conformation-dependent phosphorylation and modulation of oxidase activity.* Biochem J, 2001. **358**(Pt 3): p. 783-90.
33. Decoursey, T.E. and E. Ligeti, *Regulation and termination of NADPH oxidase activity.* Cell Mol Life Sci, 2005. **62**(19-20): p. 2173-93.

34. van Reyk, D.M., et al., *The intracellular oxidation of 2',7'-dichlorofluorescin in murine T lymphocytes.* Free Radic Biol Med, 2001. **30**(1): p. 82-8.
35. Rhee, S.G., *Redox signaling: hydrogen peroxide as intracellular messenger.* Exp Mol Med, 1999. **31**(2): p. 53-9.
36. Rhee, S.G., H.Z. Chae, and K. Kim, *Peroxiredoxins: a historical overview and speculative preview of novel mechanisms and emerging concepts in cell signaling.* Free Radic Biol Med, 2005. **38**(12): p. 1543-52.
37. Demple, B. and L. Harrison, *Repair of oxidative damage to DNA: enzymology and biology.* Annu Rev Biochem, 1994. **63**: p. 915-48.
38. Imlay, J.A., S.M. Chin, and S. Linn, *Toxic DNA damage by hydrogen peroxide through the Fenton reaction in vivo and in vitro.* Science, 1988. **240**(4852): p. 640-2.
39. Chiaramonte, R., et al., *Oxidative stress signalling in the apoptosis of Jurkat T-lymphocytes.* J Cell Biochem, 2001. **82**(3): p. 437-44.
40. Barbouti, A., et al., *DNA damage and apoptosis in hydrogen peroxide-exposed Jurkat cells: bolus addition versus continuous generation of H(2)O(2).* Free Radic Biol Med, 2002. **33**(5): p. 691-702.
41. Frossi, B., et al., *H(2)O(2) induces translocation of APE/Ref-1 to mitochondria in the Raji B-cell line.* J Cell Physiol, 2002. **193**(2): p. 180-6.
42. Devadas, S., et al., *Discrete generation of superoxide and hydrogen peroxide by T cell receptor stimulation: selective regulation of mitogen-activated protein kinase activation and fas ligand expression.* J Exp Med, 2002. **195**(1): p. 59-70.
43. Green, D.R., *Overview: apoptotic signaling pathways in the immune system.* Immunol Rev, 2003. **193**: p. 5-9.
44. Zimmermann, K.C., C. Bonzon, and D.R. Green, *The machinery of programmed cell death.* Pharmacol Ther, 2001. **92**(1): p. 57-70.
45. Um, H.D., J.M. Orenstein, and S.M. Wahl, *Fas mediates apoptosis in human monocytes by a reactive oxygen intermediate dependent pathway.* J Immunol, 1996. **156**(9): p. 3469-77.
46. Williams, M.S. and P.A. Henkart, *Role of reactive oxygen intermediates in TCR-induced death of T cell blasts and hybridomas.* J Immunol, 1996. **157**(6): p. 2395-402.
47. Kasahara, Y., et al., *Involvement of reactive oxygen intermediates in spontaneous and CD95 (Fas/APO-1)-mediated apoptosis of neutrophils.* Blood, 1997. **89**(5): p. 1748-53.
48. Dumont, A., et al., *Hydrogen peroxide-induced apoptosis is CD95-independent, requires the release of mitochondria-derived reactive oxygen species and the activation of NF-kappaB.* Oncogene, 1999. **18**(3): p. 747-57.
49. Sato, T., et al., *Fas-mediated apoptosome formation is dependent on reactive oxygen species derived from mitochondrial permeability transition in Jurkat cells.* J Immunol, 2004. **173**(1): p. 285-96.
50. Suzuki, Y., Y. Ono, and Y. Hirabayashi, *Rapid and specific reactive oxygen species generation via NADPH oxidase activation during Fas-mediated apoptosis.* FEBS Lett, 1998. **425**(2): p. 209-12.

51. Reinehr, R., et al., *Involvement of NADPH oxidase isoforms and Src family kinases in CD95-dependent hepatocyte apoptosis.* J Biol Chem, 2005. **280**(29): p. 27179-94.
52. Medan, D., et al., *Regulation of Fas (CD95)-induced apoptotic and necrotic cell death by reactive oxygen species in macrophages.* J Cell Physiol, 2005. **203**(1): p. 78-84.
53. Diaz-Llera, S., et al., *Hydrogen peroxide induced mutations at the HPRT locus in primary human T-lymphocytes.* Mutat Res, 2000. **469**(1): p. 51-61.
54. Turner, D.R., et al., *Mitotic recombination is an important mutational event following oxidative damage.* Mutat Res, 2003. **522**(1-2): p. 21-6.
55. Kim, H.W., et al., *Mutagenicity of reactive oxygen and nitrogen species as detected by co-culture of activated inflammatory leukocytes and AS52 cells.* Carcinogenesis, 2003. **24**(2): p. 235-41.
56. Skalnik, D.G., et al., *Targeting of transgene expression to monocyte/macrophages by the gp91-phox promoter and consequent histiocytic malignancies.* Proc Natl Acad Sci U S A, 1991. **88**(19): p. 8505-9.
57. Skalnik, D.G., et al., *Restriction of neuroblastoma to the prostate gland in transgenic mice.* Mol Cell Biol, 1991. **11**(9): p. 4518-27.
58. Szatrowski, T.P. and C.F. Nathan, *Production of large amounts of hydrogen peroxide by human tumor cells.* Cancer Res, 1991. **51**(3): p. 794-8.
59. Olinski, R., P. Jaruga, and T.H. Zastawny, *Oxidative DNA base modifications as factors in carcinogenesis.* Acta Biochim Pol, 1998. **45**(2): p. 561-72.
60. Waris, G. and H. Ahsan, *Reactive oxygen species: role in the development of cancer and various chronic conditions.* J Carcinog, 2006. **5**: p. 14.
61. Engel, R.H. and A.M. Evens, *Oxidative stress and apoptosis: a new treatment paradigm in cancer.* Front Biosci, 2006. **11**: p. 300-12.
62. Lee, S.R., et al., *Reversible inactivation of protein-tyrosine phosphatase 1B in A431 cells stimulated with epidermal growth factor.* J Biol Chem, 1998. **273**(25): p. 15366-72.
63. Leslie, N.R., et al., *Redox regulation of PI 3-kinase signalling via inactivation of PTEN.* Embo J, 2003. **22**(20): p. 5501-10.
64. Meng, T.C., T. Fukada, and N.K. Tonks, *Reversible oxidation and inactivation of protein tyrosine phosphatases in vivo.* Mol Cell, 2002. **9**(2): p. 387-99.
65. Lee, K. and W.J. Esselman, *Inhibition of PTPs by H(2)O(2) regulates the activation of distinct MAPK pathways.* Free Radic Biol Med, 2002. **33**(8): p. 1121-32.
66. Irish, J.M., et al., *Kinetics of B cell receptor signaling in human B cell subsets mapped by phosphospecific flow cytometry.* J Immunol, 2006. **177**(3): p. 1581-9.
67. Schieven, G.L., et al., *p72syk tyrosine kinase is activated by oxidizing conditions that induce lymphocyte tyrosine phosphorylation and Ca2+ signals.* J Biol Chem, 1993. **268**(22): p. 16688-92.
68. Schieven, G.L., et al., *Reactive oxygen intermediates activate NF-kappa B in a tyrosine kinase-dependent mechanism and in combination with vanadate activate the p56lck and p59fyn tyrosine kinases in human lymphocytes.* Blood, 1993. **82**(4): p. 1212-20.

69. Qin, S., et al., *Syk-dependent and -independent signaling cascades in B cells elicited by osmotic and oxidative stress.* J Biol Chem, 1997. **272**(4): p. 2098-103.
70. Qin, S., E.R. Stadtman, and P.B. Chock, *Regulation of oxidative stress-induced calcium release by phosphatidylinositol 3-kinase and Bruton's tyrosine kinase in B cells.* Proc Natl Acad Sci U S A, 2000. **97**(13): p. 7118-23.
71. Qin, S. and P.B. Chock, *Bruton's tyrosine kinase is essential for hydrogen peroxide-induced calcium signaling.* Biochemistry, 2001. **40**(27): p. 8085-91.
72. Qin, S. and P.B. Chock, *Implication of phosphatidylinositol 3-kinase membrane recruitment in hydrogen peroxide-induced activation of PI3K and Akt.* Biochemistry, 2003. **42**(10): p. 2995-3003.
73. He, J., et al., *Syk is required for p38 activation and G2/M arrest in B cells exposed to oxidative stress.* Antioxid Redox Signal, 2002. **4**(3): p. 509-15.
74. Lee, M. and W.S. Koh, *Raf-independent and MEKK1-dependent activation of NF-kappaB by hydrogen peroxide in 70Z/3 pre-B lymphocyte tumor cells.* J Cell Biochem, 2003. **88**(3): p. 545-56.
75. Haddad, J.J., *Antioxidant and prooxidant mechanisms in the regulation of redox(y)-sensitive transcription factors.* Cell Signal, 2002. **14**(11): p. 879-97.
76. Gius, D., et al., *Intracellular oxidation/reduction status in the regulation of transcription factors NF-kappaB and AP-1.* Toxicol Lett, 1999. **106**(2-3): p. 93-106.
77. Reynaert, N.L., et al., *Dynamic redox control of NF-kappaB through glutaredoxin-regulated S-glutathionylation of inhibitory kappaB kinase beta.* Proc Natl Acad Sci U S A, 2006. **103**(35): p. 13086-91.
78. Pineda-Molina, E., et al., *Glutathionylation of the p50 subunit of NF-kappaB: a mechanism for redox-induced inhibition of DNA binding.* Biochemistry, 2001. **40**(47): p. 14134-42.
79. Gilston, V., et al., *Hydrogen peroxide and tumour necrosis factor-alpha induce NF-kappaB-DNA binding in primary human T lymphocytes in addition to T cell lines.* Free Radic Res, 2001. **35**(6): p. 681-91.
80. Moon, E.Y., et al., *Reactive oxygen species augment B-cell-activating factor expression.* Free Radic Biol Med, 2006. **40**(12): p. 2103-11.
81. Mackay, F., et al., *Mice transgenic for BAFF develop lymphocytic disorders along with autoimmune manifestations.* J Exp Med, 1999. **190**(11): p. 1697-710.
82. Moon, E.Y., et al., *Reactive oxygen species induced by the deletion of peroxiredoxin II (PrxII) increases the number of thymocytes resulting in the enlargement of PrxII-null thymus.* Eur J Immunol, 2004. **34**(8): p. 2119-28.
83. Moon, E.Y., et al., *T lymphocytes and dendritic cells are activated by the deletion of peroxiredoxin II (Prx II) gene.* Immunol Lett, 2006. **102**(2): p. 184-90.
84. Bleesing, J.J., et al., *Patients with chronic granulomatous disease have a reduced peripheral blood memory B cell compartment.* J Immunol, 2006. **176**(11): p. 7096-103.
85. Okkenhaug, K. and B. Vanhaesebroeck, *PI3K in lymphocyte development, differentiation and activation.* Nat Rev Immunol, 2003. **3**(4): p. 317-30.
86. Vanhaesebroeck, B., et al., *P110delta, a novel phosphoinositide 3-kinase in leukocytes.* Proc Natl Acad Sci U S A, 1997. **94**(9): p. 4330-5.

87. Chantry, D., et al., *p110delta, a novel phosphatidylinositol 3-kinase catalytic subunit that associates with p85 and is expressed predominantly in leukocytes.* J Biol Chem, 1997. **272**(31): p. 19236-41.
88. Foster, F.M., et al., *The phosphoinositide (PI) 3-kinase family.* J Cell Sci, 2003. **116**(Pt 15): p. 3037-40.
89. Donahue, A.C. and D.A. Fruman, *PI3K signaling controls cell fate at many points in B lymphocyte development and activation.* Semin Cell Dev Biol, 2004. **15**(2): p. 183-97.
90. Arron, J.R., et al., *A positive regulatory role for Cbl family proteins in tumor necrosis factor-related activation-induced cytokine (trance) and CD40L-mediated Akt activation.* J Biol Chem, 2001. **276**(32): p. 30011-7.
91. Panchamoorthy, G., et al., *p120cbl is a major substrate of tyrosine phosphorylation upon B cell antigen receptor stimulation and interacts in vivo with Fyn and Syk tyrosine kinases, Grb2 and Shc adaptors, and the p85 subunit of phosphatidylinositol 3-kinase.* J Biol Chem, 1996. **271**(6): p. 3187-94.
92. Hartley, D., H. Meisner, and S. Corvera, *Specific association of the beta isoform of the p85 subunit of phosphatidylinositol-3 kinase with the proto-oncogene c-cbl.* J Biol Chem, 1995. **270**(31): p. 18260-3.
93. Beckwith, M., G. Jorgensen, and D.L. Longo, *The protein product of the proto-oncogene c-cbl forms a complex with phosphatidylinositol 3-kinase p85 and CD19 in anti-IgM-stimulated human B-lymphoma cells.* Blood, 1996. **88**(9): p. 3502-7.
94. Deane, J.A. and D.A. Fruman, *Phosphoinositide 3-kinase: diverse roles in immune cell activation.* Annu Rev Immunol, 2004. **22**: p. 563-98.
95. Reif, K., et al., *Cutting edge: differential roles for phosphoinositide 3-kinases, p110gamma and p110delta, in lymphocyte chemotaxis and homing.* J Immunol, 2004. **173**(4): p. 2236-40.
96. El Sheikh, S.S., et al., *Topographical expression of class IA and class II phosphoinositide 3-kinase enzymes in normal human tissues is consistent with a role in differentiation.* BMC Clin Pathol, 2003. **3**(1): p. 4.
97. Gold, M.R. and R. Aebersold, *Both phosphatidylinositol 3-kinase and phosphatidylinositol 4-kinase products are increased by antigen receptor signaling in B cells.* J Immunol, 1994. **152**(1): p. 42-50.
98. Lemmon, M.A., *Phosphoinositide recognition domains.* Traffic, 2003. **4**(4): p. 201-13.
99. Lemmon, M.A., *Pleckstrin homology domains: not just for phosphoinositides.* Biochem Soc Trans, 2004. **32**(Pt 5): p. 707-11.
100. Thomas, C.C., et al., *Crystal structure of the phosphatidylinositol 3,4-bisphosphate-binding pleckstrin homology (PH) domain of tandem PH-domain-containing protein 1 (TAPP1): molecular basis of lipid specificity.* Biochem J, 2001. **358**(Pt 2): p. 287-94.
101. Lemmon, M.A. and K.M. Ferguson, *Signal-dependent membrane targeting by pleckstrin homology (PH) domains.* Biochem J, 2000. **350 Pt 1**: p. 1-18.
102. Dowler, S., et al., *Identification of pleckstrin-homology-domain-containing proteins with novel phosphoinositide-binding specificities.* Biochem J, 2000. **351**(Pt 1): p. 19-31.

103. Lodowski, D.T., et al., *Keeping G proteins at bay: a complex between G protein-coupled receptor kinase 2 and Gbetagamma.* Science, 2003. **300**(5623): p. 1256-62.
104. Jaffe, A.B., P. Aspenstrom, and A. Hall, *Human CNK1 acts as a scaffold protein, linking Rho and Ras signal transduction pathways.* Mol Cell Biol, 2004. **24**(4): p. 1736-46.
105. Kim, O., J. Yang, and Y. Qiu, *Selective activation of small GTPase RhoA by tyrosine kinase Etk through its pleckstrin homology domain.* J Biol Chem, 2002. **277**(33): p. 30066-71.
106. Snyder, J.T., et al., *The pleckstrin homology domain of phospholipase C-beta2 as an effector site for Rac.* J Biol Chem, 2003. **278**(23): p. 21099-104.
107. Frech, M., et al., *High affinity binding of inositol phosphates and phosphoinositides to the pleckstrin homology domain of RAC/protein kinase B and their influence on kinase activity.* J Biol Chem, 1997. **272**(13): p. 8474-81.
108. Dowler, S., et al., *DAPP1: a dual adaptor for phosphotyrosine and 3-phosphoinositides.* Biochem J, 1999. **342 (Pt 1)**: p. 7-12.
109. Stephens, L., et al., *Protein kinase B kinases that mediate phosphatidylinositol 3,4,5-trisphosphate-dependent activation of protein kinase B.* Science, 1998. **279**(5351): p. 710-4.
110. Kanai, F., et al., *The PX domains of p47phox and p40phox bind to lipid products of PI(3)K.* Nat Cell Biol, 2001. **3**(7): p. 675-8.
111. Karathanassis, D., et al., *Binding of the PX domain of p47(phox) to phosphatidylinositol 3,4-bisphosphate and phosphatidic acid is masked by an intramolecular interaction.* Embo J, 2002. **21**(19): p. 5057-68.
112. Saito, K., et al., *BTK regulates PtdIns-4,5-P2 synthesis: importance for calcium signaling and PI3K activity.* Immunity, 2003. **19**(5): p. 669-78.
113. Marshall, A.J., et al., *TAPP1 and TAPP2 are targets of phosphatidylinositol 3-kinase signaling in B cells: sustained plasma membrane recruitment triggered by the B-cell antigen receptor.* Mol Cell Biol, 2002. **22**(15): p. 5479-91.
114. Krahn, A.K., et al., *Two distinct waves of membrane-proximal B cell antigen receptor signaling differentially regulated by SRC homology 2-containing inositol polyphosphate 5-phosphatase.* J Immunol, 2004. **172**(1): p. 331-9.
115. Fruman, D.A., *Phosphoinositide 3-kinase and its targets in B-cell and T-cell signaling.* Curr Opin Immunol, 2004. **16**(3): p. 314-20.
116. Astoul, E., S. Watton, and D. Cantrell, *The dynamics of protein kinase B regulation during B cell antigen receptor engagement.* J Cell Biol, 1999. **145**(7): p. 1511-20.
117. Andjelkovic, M., et al., *Role of translocation in the activation and function of protein kinase B.* J Biol Chem, 1997. **272**(50): p. 31515-24.
118. Scheid, M.P., et al., *Phosphatidylinositol (3,4,5)P3 is essential but not sufficient for protein kinase B (PKB) activation; phosphatidylinositol (3,4)P2 is required for PKB phosphorylation at Ser-473: studies using cells from SH2-containing inositol-5-phosphatase knockout mice.* J Biol Chem, 2002. **277**(11): p. 9027-35.
119. Marshall, A.J., et al., *A novel B lymphocyte-associated adaptor protein, Bam32, regulates antigen receptor signaling downstream of phosphatidylinositol 3-kinase.* J Exp Med, 2000. **191**(8): p. 1319-32.

120. Allam, A. and A.J. Marshall, *Role of the adaptor proteins Bam32, TAPP1 and TAPP2 in lymphocyte activation.* Immunol Lett, 2005. **97**(1): p. 7-17.
121. Niiro, H., et al., *The B lymphocyte adaptor molecule of 32 kD (Bam32) regulates B cell antigen receptor signaling and cell survival.* J Exp Med, 2002. **195**(1): p. 143-9.
122. Fournier, E., et al., *The B cell SH2/PH domain-containing adaptor Bam32/DAPP1 is required for T cell-independent II antigen responses.* Curr Biol, 2003. **13**(21): p. 1858-66.
123. Haas-Kogan, D., et al., *Protein kinase B (PKB/Akt) activity is elevated in glioblastoma cells due to mutation of the tumor suppressor PTEN/MMAC.* Curr Biol, 1998. **8**(21): p. 1195-8.
124. Brauweiler, A., et al., *Differential regulation of B cell development, activation, and death by the src homology 2 domain-containing 5' inositol phosphatase (SHIP).* J Exp Med, 2000. **191**(9): p. 1545-54.
125. Wu, Y., et al., *Interaction of the tumor suppressor PTEN/MMAC with a PDZ domain of MAGI3, a novel membrane-associated guanylate kinase.* J Biol Chem, 2000. **275**(28): p. 21477-85.
126. Das, S., J.E. Dixon, and W. Cho, *Membrane-binding and activation mechanism of PTEN.* Proc Natl Acad Sci U S A, 2003. **100**(13): p. 7491-6.
127. Sly, L.M., et al., *SHIP, SHIP2, and PTEN activities are regulated in vivo by modulation of their protein levels: SHIP is up-regulated in macrophages and mast cells by lipopolysaccharide.* Exp Hematol, 2003. **31**(12): p. 1170-81.
128. Liu, Q., et al., *The inositol polyphosphate 5-phosphatase ship is a crucial negative regulator of B cell antigen receptor signaling.* J Exp Med, 1998. **188**(7): p. 1333-42.
129. Isnardi, I., et al., *The SH2 domain-containing inositol 5-phosphatase SHIP1 is recruited to the intracytoplasmic domain of human FcgammaRIIB and is mandatory for negative regulation of B cell activation.* Immunol Lett, 2006. **104**(1-2): p. 156-65.
130. Anzelon, A.N., H. Wu, and R.C. Rickert, *Pten inactivation alters peripheral B lymphocyte fate and reconstitutes CD19 function.* Nat Immunol, 2003. **4**(3): p. 287-94.
131. Suzuki, A., et al., *Critical roles of Pten in B cell homeostasis and immunoglobulin class switch recombination.* J Exp Med, 2003. **197**(5): p. 657-67.
132. Suzuki, A., et al., *Functional analysis of the tumour suppressor gene PTEN in murine B cells and keratinocytes.* Biochem Soc Trans, 2004. **32**(Pt 2): p. 362-5.
133. Helgason, C.D., et al., *A dual role for Src homology 2 domain-containing inositol-5-phosphatase (SHIP) in immunity: aberrant development and enhanced function of b lymphocytes in ship -/- mice.* J Exp Med, 2000. **191**(5): p. 781-94.
134. Okkenhaug, K., et al., *Impaired B and T cell antigen receptor signaling in p110delta PI 3-kinase mutant mice.* Science, 2002. **297**(5583): p. 1031-4.
135. Clayton, E., et al., *A crucial role for the p110delta subunit of phosphatidylinositol 3-kinase in B cell development and activation.* J Exp Med, 2002. **196**(6): p. 753-63.

136. Jou, S.T., et al., *Essential, nonredundant role for the phosphoinositide 3-kinase p110delta in signaling by the B-cell receptor complex.* Mol Cell Biol, 2002. **22**(24): p. 8580-91.
137. Bae, Y.S., et al., *Platelet-derived growth factor-induced H(2)O(2) production requires the activation of phosphatidylinositol 3-kinase.* J Biol Chem, 2000. **275**(14): p. 10527-31.
138. Park, H.S., et al., *Sequential activation of phosphatidylinositol 3-kinase, beta Pix, Rac1, and Nox1 in growth factor-induced production of H2O2.* Mol Cell Biol, 2004. **24**(10): p. 4384-94.
139. Remans, P.H., et al., *Rap1 signaling is required for suppression of Ras-generated reactive oxygen species and protection against oxidative stress in T lymphocytes.* J Immunol, 2004. **173**(2): p. 920-31.
140. Halstead, J.R., et al., *A novel pathway of cellular phosphatidylinositol(3,4,5)-trisphosphate synthesis is regulated by oxidative stress.* Curr Biol, 2001. **11**(6): p. 386-95.
141. Van der Kaay, J., et al., *Distinct phosphatidylinositol 3-kinase lipid products accumulate upon oxidative and osmotic stress and lead to different cellular responses.* J Biol Chem, 1999. **274**(50): p. 35963-8.
142. Yokogawa, T., et al., *Evidence that 3'-phosphorylated polyphosphoinositides are generated at the nuclear surface: use of immunostaining technique with monoclonal antibodies specific for PI 3,4-P(2).* FEBS Lett, 2000. **473**(2): p. 222-6.
143. Salim, K., et al., *Distinct specificity in the recognition of phosphoinositides by the pleckstrin homology domains of dynamin and Bruton's tyrosine kinase.* Embo J, 1996. **15**(22): p. 6241-50.
144. Hampton, M.B., A.J. Kettle, and C.C. Winterbourn, *Inside the neutrophil phagosome: oxidants, myeloperoxidase, and bacterial killing.* Blood, 1998. **92**(9): p. 3007-17.
145. Rameh, L.E., et al., *A comparative analysis of the phosphoinositide binding specificity of pleckstrin homology domains.* J Biol Chem, 1997. **272**(35): p. 22059-66.
146. Myers, M.P., et al., *The lipid phosphatase activity of PTEN is critical for its tumor supressor function.* Proc Natl Acad Sci U S A, 1998. **95**(23): p. 13513-8.
147. Kimber, W.A., et al., *Evidence that the tandem-pleckstrin-homology-domain-containing protein TAPP1 interacts with Ptd(3,4)P2 and the multi-PDZ-domain-containing protein MUPP1 in vivo.* Biochem J, 2002. **361**(Pt 3): p. 525-36.
148. Vanhaesebroeck, B., et al., *Synthesis and function of 3-phosphorylated inositol lipids.* Annu Rev Biochem, 2001. **70**: p. 535-602.
149. Freeburn, R.W., et al., *Evidence that SHIP-1 contributes to phosphatidylinositol 3,4,5-trisphosphate metabolism in T lymphocytes and can regulate novel phosphoinositide 3-kinase effectors.* J Immunol, 2002. **169**(10): p. 5441-50.
150. Lee, S.R., et al., *Reversible inactivation of the tumor suppressor PTEN by H2O2.* J Biol Chem, 2002. **277**(23): p. 20336-42.
151. Ivetac, I., et al., *The type Ialpha inositol polyphosphate 4-phosphatase generates and terminates phosphoinositide 3-kinase signals on endosomes and the plasma membrane.* Mol Biol Cell, 2005. **16**(5): p. 2218-33.

152. Norris, F.A. and P.W. Majerus, *Hydrolysis of phosphatidylinositol 3,4-bisphosphate by inositol polyphosphate 4-phosphatase isolated by affinity elution chromatography.* J Biol Chem, 1994. **269**(12): p. 8716-20.
153. Cully, M., et al., *Beyond PTEN mutations: the PI3K pathway as an integrator of multiple inputs during tumorigenesis.* Nat Rev Cancer, 2006. **6**(3): p. 184-92.
154. Kimber, W.A., et al., *Interaction of the protein tyrosine phosphatase PTPL1 with the PtdIns(3,4)P2-binding adaptor protein TAPP1.* Biochem J, 2003. **376**(Pt 2): p. 525-35.
155. Hogan, A., et al., *The phosphoinositol 3,4-bisphosphate-binding protein TAPP1 interacts with syntrophins and regulates actin cytoskeletal organization.* J Biol Chem, 2004.
156. Keep, N.H., *Structural comparison of actin binding in utrophin and dystrophin.* Neurol Sci, 2000. **21**(5 Suppl): p. S929-37.
157. Graziani, A., et al., *Purification and characterization of human erythrocyte phosphatidylinositol 4-kinase. Phosphatidylinositol 4-kinase and phosphatidylinositol 3-monophosphate 4-kinase are distinct enzymes.* Biochem J, 1992. **284 (Pt 1)**: p. 39-45.
158. Ivetac, I., et al., *The Type I{alpha} Inositol Polyphosphate 4-Phosphatase Generates and Terminates Phosphoinositide 3-Kinase Signals on Endosomes and the Plasma Membrane.* Mol Biol Cell, 2005. **16**(5): p. 2218-33.
159. Barnache, S., et al., *Phosphatidylinositol 4-phosphatase type II is an erythropoietin-responsive gene.* Oncogene, 2006. **25**(9): p. 1420-3.
160. Haenggi, T. and J.M. Fritschy, *Role of dystrophin and utrophin for assembly and function of the dystrophin glycoprotein complex in non-muscle tissue.* Cell Mol Life Sci, 2006. **63**(14): p. 1614-31.
161. Miura, P. and B.J. Jasmin, *Utrophin upregulation for treating Duchenne or Becker muscular dystrophy: how close are we?* Trends Mol Med, 2006. **12**(3): p. 122-9.
162. James, M., et al., *Adhesion-dependent tyrosine phosphorylation of (beta)-dystroglycan regulates its interaction with utrophin.* J Cell Sci, 2000. **113 (Pt 10)**: p. 1717-26.
163. Cerecedo, D., et al., *Role of dystrophins and utrophins in platelet adhesion process.* Br J Haematol, 2006. **134**(1): p. 83-91.
164. Chakkalakal, J.V., et al., *Expression of utrophin A mRNA correlates with the oxidative capacity of skeletal muscle fiber types and is regulated by calcineurin/NFAT signaling.* Proc Natl Acad Sci U S A, 2003. **100**(13): p. 7791-6.
165. Khurana, T.S., et al., *Activation of utrophin promoter by heregulin via the ets-related transcription factor complex GA-binding protein alpha/beta.* Mol Biol Cell, 1999. **10**(6): p. 2075-86.
166. Gramolini, A.O., et al., *Induction of utrophin gene expression by heregulin in skeletal muscle cells: role of the N-box motif and GA binding protein.* Proc Natl Acad Sci U S A, 1999. **96**(6): p. 3223-7.
167. Chaubourt, E., et al., *Nitric oxide and l-arginine cause an accumulation of utrophin at the sarcolemma: a possible compensation for dystrophin loss in Duchenne muscular dystrophy.* Neurobiol Dis, 1999. **6**(6): p. 499-507.

168. Fujimori, K., et al., *Interleukin 6 induces overexpression of the sarcolemmal utrophin in neonatal mdx skeletal muscle.* Hum Gene Ther, 2002. **13**(4): p. 509-18.
169. Bonet-Kerrache, A., et al., *The GTPase RhoA increases utrophin expression and stability, as well as its localization at the plasma membrane.* Biochem J, 2005. **391**(Pt 2): p. 261-8.
170. Banfic, H., et al., *A novel integrin-activated pathway forms PKB/Akt-stimulatory phosphatidylinositol 3,4-bisphosphate via phosphatidylinositol 3-phosphate in platelets.* J Biol Chem, 1998. **273**(1): p. 13-6.
171. Matheny, H.E., T.L. Deem, and J.M. Cook-Mills, *Lymphocyte migration through monolayers of endothelial cell lines involves VCAM-1 signaling via endothelial cell NADPH oxidase.* J Immunol, 2000. **164**(12): p. 6550-9.
172. Trautmann, A. and S. Valitutti, *The diversity of immunological synapses.* Curr Opin Immunol, 2003. **15**(3): p. 249-54.
173. Harriague, J. and G. Bismuth, *Imaging antigen-induced PI3K activation in T cells.* Nat Immunol, 2002. **3**(11): p. 1090-6.